Utrecht University, Faculty of Geosciences
Department of Physical Geography

FINE FUEL MOISTURE CODE: CREATING A PREDICATIVE REGIONAL FIRE WEATHER MODEL FOR THE MEDITERRANEAN AREA LA PEYNE, FRANCE

Master of Science Thesis

Niek Meijer
3259536
February 2014

Supervisor: Steven M. de Jong
2nd Supervisor: Elisabeth A. Addink

PREFACE

This thesis is the result of the implementation of the Fine Fuel Moisture Code and BEHAVE fire behavior prediction model in a tempo-spatial model. The model was calibrated, validated and analyzed with data from a field work campaign performed from the end of August 2013 to mid September 2013 in southern France.

I would like to thank Steven de Jong and Elisabeth Addink for their supervision and assistance during the work on this research and fieldwork preparation. I would also like to thank Chris Roosendaal for his help in providing the necessary equipment and explaining how it should be used. Additional thanks go out to Sterre Verdonck for his company during the last days in France and I would also like to thank my parents, not only for borrowing their car, but also for their unconditional support. Specials thanks go out to Marijn Boll, for her indispensable support during the fieldwork.

This thesis is dedicated to the memory of my uncle Karel Dekkers and grandmother Annie Meijer.

ABSTRACT

Mediterranean Europe suffers from over 50,000 forest fires annually, the vast majority of which has an anthropogenic ignition source. Climatic change and related land use changes are likely to increase the problems related to forest fires. Models that provide land owners, fire fighters and authorities with daily information on potential fire behavior are therefore of high added value.

In this study a Canadian model is applied that relates meteorological indices to fine fuel moisture content, an important indicator for flammability of the fuel complex. This Fine Fuel Moisture Code (FFMC) is adapted from Canadian boreal vegetation to Mediterranean vegetation. Moreover a part of the BEHAVE fire behavior prediction model is added to quantify estimations on rate of spread, fireline intensity and flame length. These three parameters are crucial in crown fire ignition but also have a big influence on the possible way of firefighting.

A $14\ \mathrm{km}^2$ study area in Southern France was selected to collect fuel moisture content samples in 14 locations over a 10-day period. For each of the four dominant Mediterranean vegetation species a plot was selected that had an 11mm rainfall event simulated. The fuel moisture content data was used to calibrate and validate the FFMC model over the fieldwork period. After calibration the data was used to simulate the moisture content over the period from June 1 to September 6, 2013. This simulated moisture content was used to drive the BEHAVE model.

The results showed moderate fire behavior conditions for almost the complete period in all vegetation classes. Extended fire behavior was found on the steep slopes in the dense and middle matorral but the absence of high windspeeds suppressed excessive fire behavior. The accuracy of the BEHAVE model could not be tested, such being outside the scope of this study, but it was successfully evaluated for the Mediterranean in other studies. For the calibrated FFMC model the uncertainty was estimated by a 95% confidence interval, that averaged at 4.3%. The expected accuracy (FFMC + BEHAVE) is assumed highest in dry conditions.

It is concluded that this model spatially and temporally estimates summer moisture content and fire behavior with an accuracy good enough for practical use. However also several defects such as parameter generalization and the high dependency on good meteorological data are discussed in this study.

TABLE OF CONTENTS

LIST OF FIGURES

LIST OF TABLES

LIST OF SYMBOLS AND ACRONYMS

BUI	Buildup Index
CFFDRS	Canadian Forest Fire Danger Rating System
DC	Drought Code
DFMC	Dead Fine Fuel Moisture Content
DMC	Duff Moisture Code
EMC	Equilibrium Moisture Content
FBP	Fire Behavior Prediction
FFMC	Fine Fuel Moisture Code
FMC	Fuel moisture content
FWI	Fire Weather Index
LFMC	Live Fuel Moisture Content
NFDRS	National Fire-Danger Rating System
NFFL	Northern Forest Fire Laboratory
RAWS	Remote Automatic Weather Station
ROS	Rate Of Spread
WAF	Wind Adjustment Factor
H	Relative humidity [%] or vegetation height [m] in Equation 17
W	Wind speed [km/h]
k_d	log drying rate [-]
k_w	Log wetting rate [-]
T	Temperature [°C]
E	Equilibrium Moisture Content [%]
m	Present day moisture content [%]
m_0	Initial moisture content [%]
m_r	Moisture content after rain [%]
r_f	Net Rainfall [mm]
r_0	Rainfall [mm]
T_f	Fuel temperature [°C]
T_a	Air temperature [°C]
I	Solar radiation [$W\ m^{-2}$]
H_f	Relative humidity at fuel level [%]
H_a	Relative humidity of the air [%]
τ_n	Net cloud/tree transmittance [-]
τ_c	Transmittance of the cloud cover
τ_t	Transmittance of the forest canopy [-]
U_H/U_{20+H}	Ratio between the 20ft wind speed and the fuel level wind speed [-]
F	FFMC value

R	Rate of fire spread $[m\ min^{-1}]$
I_R	Rate of heat release $[(kJ\ min^{-1})\ m^{-2}]$
ξ	Propagating flux ratio [-]
ϕ_w	Wind factor [-]
ϕ_s	Slope factor [-]
ρ_b	Ovendry bulk density $[kg\ m^{-3}]$
ε	Effective heating number [-]
Q_{ig}	Heat of pre-ignition $[kJ\ kg^{-1}]$
Γ'	Optimum reaction velocity $[min^{-1}]$
Γ'_{max}	Maximum reaction velocity $[min^{-1}]$
w_n	Net fuel loading $[kg\ m^{-2}]$
h	Fuel heat content $[kJ\ kg^{-1}]$
n_M	Moisture damping coefficient [-]
η_s	Mineral damping coefficient [-]
(β/β_{op})	Relative packing ratio [-]
σ	Surface-area: volume ratio [-]
w_O	Oven dry load $[kg\ m^{-2}]$
δ	Fuel bed depth [m]
ρ_b	Fuel particle density $[kg\ m^{-3}]$
S_T	Fuel mineral content [-]
M_f	Fuel moisture content [%]
M_x	Fuel moisture of extinction [%]
S_e	Effective mineral content [-]
β	Packing ratio [-]
U	Midflame wind speed $[m\ min^{-1}]$
$\tan(\phi)$	Vertical rise / horizontal run [-]
I_B	Byram's fireline intensity $[(kW\ m^{-1}]$
L_f	Flame length [m]
R_b	Geometric factor solar radiation [-]

1 INTRODUCTION

Globally and throughout history forest fires are known for their spectacular action and devastating effects (Marlon et al., 2012). Their occurrence is natural and forest fires fulfill an important role in the ecological dynamics of most ecosystems (Lloret et al., 2003). For humans, forest fires were mainly a rural hazard in the past but, increasingly, they break out in the urban outskirts and leisure areas with a potential to threaten dense populated areas (Smith, 2001). Apart from their potential to cause human losses, the socio-economic effects of forest fires include losses of crops, timber, houses and other human property but often also have a negative effect on tourism, air quality and soil quality.

The Mediterranean Basin is characterized by an unusual geographic and topographical variability that can be related to the presence of a jagged coastline and many relatively young mountain ranges of reasonable height (Scarascia-Mugnozza et al., 2000). Geographically, the region stretches from the European Alps to the Sahara and from the Atlantic Ocean to the Caspian Sea. It encompasses a total of 25 countries of which France, Italy, Portugal and Spain are grouped in Southwestern Europe (FAO, 1999). Together with Greece these countries form the European Mediterranean. The countries around the Mediterranean Basin are all in the same climatic zone, the Mediterranean climate (Peel et al., 2007).

This Mediterranean climate is known for its climatic bi-seasonality with dry and hot summers and cool and moist autumns and winters. Precipitation can be torrential with a large year-to-year variability in total rainfall and frequent strong and dry winds (Scarascia-Mugnozza et al., 2000). This climate in combination with the long intense human impact influence the role of fire in the Mediterranean Basin and most of the features that make the landscapes of the Mediterranean Basin different from those of the rest of Europe are related to these three factors. The human impact has been so strong that it is not possible to understand current vegetation patterns without taking into account past anthropogenic activities and land-uses (Pausas and Vallejo, 1999). The combination of a dry and warm summer climate and the vegetation that adapted to this climate makes the Mediterranean prone to forest fires. The European Union estimated that in the period 1980-2010 a yearly average of 465.314 hectares vegetation burned in these southern members of the European Union. This number includes all fires over 0.5 hectare in 50,000 events (Schmuck et al., 2011).

1.1 FOREST FIRES AND FOREST FIRE MODELS

Despite difficult modelling (Chuvieco et al., 2004), the principle behind forest fires is easy to understand. Provided sufficient oxygen, only combustible fuel and an ignition source are needed to start a forest fire. Statistics on the causes of forest fires in the Mediterranean Basin are not complete, but anthropogenic ignition is by far the biggest cause (Pausas and Vallejo, 1999). In addition to an ignition source a forest fire needs fuel to both start and spread. This fuel load is a crucial parameter in forest fires and includes both vegetation and vegetation residues such as litter layers and dead shrubs. Globally almost all

vegetation and organic residues can be considered as fuel when their moisture content is low enough to burn exothermic. The fuel moisture content is a critical parameter in forest fires since water acts as an determinant in fire ignition and fire propagation (Chuvieco et al., 2004). Moisture content is obviously highly influenced by weather conditions through various physical processes such as water vapor absorption, condensation, evaporation and desorption, in addition to direct contact with liquid water (Camia and Amatulli, 2009). As water interactions are very complex and difficult to generalize, estimation of the fuel moisture content is one of the most difficult problems in fire danger rating (Chuvieco et al., 2004) however this information is also essential for assessing overall fire hazard and risk (Stambaugh et al., 2011). Pausas (2004) found that weather conditions are also related to forest fire fuel by another mechanism; on a country scale summer rainfall can be correlated with the area burned in summer with a time lag of 2 years. This indicates that more rainfall increases the fuel loads that burn two years later.

Different vegetation means a different type of fuel and therefore a different fire regime. To illustrate the diversity: forests with a lot of fine surface fuel such as litter are prone to a propagating fire with a high fire intensity as there is a continuous surface fuel bed (Stambaugh et al., 2011). Forests with a high stem density have potential to produce a high-severity fire as there is a high fuel load (Van de Water and North, 2011). Mediterranean forests can contain species such as the Allepo Pine that contain a very high content of resin or oils that make them extremely inflammable (FAO, 2007). Due to this high variability in fuel loads, the data collected in different study areas cannot be used to estimate fuel loading in another (Stambaugh et al., 2011) and fuel loads for a detailed study or model have to be site specific.

In the 1980's introduction of the computer allowed the use of software packages with mathematical forest fire models. These models were mainly built and tested in the United States, Canada and Australia. The United States Department of Agriculture, Forest Service started with the BEHAVE program in 1984. The BEHAVE model calculates the potential surface fire rate of spread and fireline intensity mainly by the use of meteorological and fuel data, all based on Rothermel studies (Rothermel, 1972). A possible BEHAVE sub-model used for estimating the fuel moisture content out of meteorological inputs is a direct derivation of a sub-index in the Canadian Fire Weather Index; the Fine Fuel Moisture Code (FFMC). The FFMC estimates the water content of litter and fine dead fuels as this indicates the relative ease of ignition and flammability of fine dead fuels (Camia and Bovio, 2000). The moisture content of these fuels is of high importance for the rate of spread and the sustainability of fire and models like the BEHAVE model rely on these estimates to predict both the fire spread rate and the consumption of fuels (Wotton and Beverly, 2007).

In addition to a fuel moisture estimator, the BEHAVE model is mainly a fire behavior prediction system. It relates dead fuel moisture content to vegetation type on depending fire characteristics like fire intensity and flame length. As the BEHAVE model was created by the U.S Forestry Service with the intention to be used under field conditions the fuels are classified in fuel models according to flammability parameters like height, pine/deciduous and understory to allow quick assessments. Both the FFMC and the BEHAVE model were used in this study.

1.2 AIM

This study focuses on the deterministic Fine Fuel Moisture Code (FFMC) and its adaptation to the regional-scale of the Mediterranean area of La Peyne, Languedoc-Roussillon, southern France. Furthermore, the BEHAVE model will be applied to this spatial fuel moisture content map in order to create a fire behavior model and fire hazard map of the area. This map can aid land owners and firefighters in forest fire management. The fire behavior model and fire hazard map will be made by combining existing literature with a small field experiment to calibrate and validate the fine fuel moisture model and obtain information about the prevalent fuel types.

The main objective is:

- *To create a fire behavior model and fire hazard map based on the Fine Fuel Moisture Code and the BEHAVE Fire Behavior Prediction model for the Peyne study area in Mediterranean France.*

The main research questions are:

- *What is the spatial and temporal fuel moisture content distribution in the La Peyne area of southern France?*

- *Which areas have the highest fire danger risk in terms of flammability, rate of spread and fire intensity?*

- *What is the accuracy of the model inputs and what is their effect on the model output uncertainty*?

1.3 THE CONTENT

The structure of this thesis is as follows: First, chapter 2 will discuss the academic background of forest fires, their effects, factors of influence and an introduction on forest fire modeling. Then chapter 3 will provide an introduction on the study area. Chapter 4 will explain the methods used for model building, data collection and calibration and validation of the results. Additionally, chapter 5 will provide the results of the data collection and the FFMC and BEHAVE model, followed by chapter 6 where these results and the general process will be discussed. Finally, in chapter 7, the final conclusion will be drawn and recommendations for following research will be made.

2 THEORETICAL BACKGROUND

This chapter presents the academic background of the main topics of this research, starting with a general introduction on forest fires and their different appearances, followed by an overview of factors that influence forest fires and the relation with climate change.

2.1 FOREST FIRES AND THEIR EFFECTS

International law and legal definitions of the term 'forest fire' mutually agree with a *forest fire* meaning 'any fire burning uncontrolled on any lands partially or wholly covered by timber, brush, grass, grain or other inflammable vegetation' (State of California, 2013). So the term *forest* does not imply that an actual forest is burning as it could be any vegetation cover or mixture. In literature also *wildland fire, wildfire, bushfires, brushfires, vegetation fires* and *natural fires* are used but in general they all refer to a fire that consumes vegetation. In North America the term *wildfire* is also used to indicate forest fires that rage out of control. Within a forest fire a distinction can be made between a ground, surface or crown fire. The distinction is made on the fuel category, but often has direct consequences for the intensity, rate of spread, related risks and damage.

2.1.1 TYPES OF FOREST FIRES

The behavior of a forest fire is determined by the type of fuel that is combusted which can either be in the ground, on the surface or in the tree canopy, resulting in ground, surface or crown-fires respectively. Often one of these types dominates the general fire behavior, but a combination of two or all three types of fire can contribute to a single fire event (Office of Environment and Heritage NSW, 2011). Depending on conditions there are several different paths possible between ignition and extinction (Figure 2-1).

Ground fires smolder or creep slowly through the litter and humus layers, consuming all or most of the organic cover (Figure 2-2 top left). These fires are often found in loose soils with a high content of peat, coal, tree roots and deep humus layers. The entire soil has to be sufficiently dry for the fire to sustain. Ground fires can burn for weeks or months until precipitation extinguishes the fire or it runs out of fuel. They destroy many small organisms and fungi but also the roots and thereby the vegetation on the surface, including big trees. The removal of soil and vegetation exposes the rock or mineral soil and thereby increases the chance of erosion (Forest Encyclopedia, 1996). Ground fires can evolve from a smoldering phase to a surface fire (Office of Environment and Heritage, NSW 2011).

Surface fires are low to high intensity fires that burn on the surface of the ground but under the canopy. A surface fire combusts needles, leaves, grass, dead and down branch wood and logs, shrubs, low brush and short trees (Scott & Reinhardt, 2001), the so called understory. These fires move rapidly and do not

consume the entire organic layer as the moisture in the organic humus layers often is too high. As the heat pulse does not persist long enough, surface fires neither damage the roots and organisms in the humus layers nor the thick bark of large trees. However, they do reduce small-diameter branches, trees and other fine surface fuels. As a result of surface fires the tree canopy may be scorched but does not get burned (Office of Environment and Heritage, NSW 2011; Forest Encyclopedia, 1996) (top right picture in Figure 2-2). Although the behavior of surface fires is widely varying on the fuels it consumes their behavior is reasonable predictable due to the moderate intensity and speed. The first modeling of forest fire behavior was aimed at this fire type (Scott and Reinhardt, 2001). If conditions allow, also these fires can evolve to a more severe type: the crown fire.

Crown fires burns the elevated canopy fuels, but in general the whole vertical fuel complex is on fire (bottom left image of Figure 2-2). Crown fires are the most severe type of forest fires in terms of intensity, rate of spread, spotting, i.e. the start of a new fire downwind by aerial embers, radiation and control. There are three types of crown fires: passive, active and independent. Both passive and active crown fires depend on the heat generated by the surface fire below, whereas independent crown fires are completely standalone and initially only burn the tree canopies. Independent crown fires are the most dangerous due to their extreme intensity. Independent crown fires are very rare and short lived, so in this study the term crown fire will be used to indicate the dependent, passive and active, crown fires. Active crown fires are sometimes also called continuous crown fires because of their continuous behavior in spreading, so that despite their dependency on surface fires, the fire spreads at a certain constant rate. Passive crown fires, however, are fires that grow locally from a surface fire into a crown fire but this new fire is not consistently maintained throughout the canopy (Figure 2-2 bottom right). Despite the fact that a passive crown fire is not a complete crown fire it does raise the fire spread rate and dramatically enhances spotting, so the overall rate of fire growth increases (Scott and Reinhardt, 2001).

Mostly coniferous forests are subject to crown fires as the fire intensity in these species is often high. Canopy fuels normally consumed by crown fires consist of living and dead foliage, lichen and fine living and dead branchwood of which the moisture content is often higher than that of the surface fuels (Scott and Reinhardt, 2001) due to the fact that they are more often live fuels. The bulk density of these fuels is much lower and in combination with the easy supply of oxygen due to their elevated position the rate of spread can increase two to three times when a fire reaches the crown phase, resulting in a four to nine times larger burned area in the same time (Dimitrakopoulos et al., 2007). The increased rate of spread and intensity in combination with long range spotting make crown fires particularly dangerous and difficult to confront. The heat generated can be so tremendous that extinguishing becomes impossible until weather conditions change. Therefore, the focus is often on prevention rather than on suppression of crown fires and assessing the risk of crown fire initiation is an important element of fire prevention (Scott and Reinhardt, 2001).

A crown fire needs a coniferous forest of considerable height in order to generate enough heat to sustain. One type of pine found in over 2,500,000 ha in the Mediterranean Basin that is capable of generating active crown fires is the Aleppo pine or *Pinus halepensis* and one third of the total burned

area in the Mediterranean Basin can be related to this species. In these pine forests the probability of crown fires initiation is high even under moderate burning conditions. This is mainly the result of the low canopy base height and the heavy surface fuel load that can often be found in these forests. Passive crown fires are often seen in Mediterranean forests with uneven aged stands, while even aged stands often result in high intensity active crown fires. Therefore, assessment of fuel characteristics and potential crown fire behavior can be useful in fire and fuel management (Mitsopoulos and Dimitrakopoulos, 2007).

The forests in the study area are mostly dominated by evergreen species such as the *Quercus ilex* and the *Arbutus unedo* (Nijland, 2011) which are both broadleaved trees. Therefore it is unlikely that crown fires will play a significant role in the forest fire regime in the majority of this area, except for the patches covered with conifer species (Dimitrakopoulos et al., 2007).

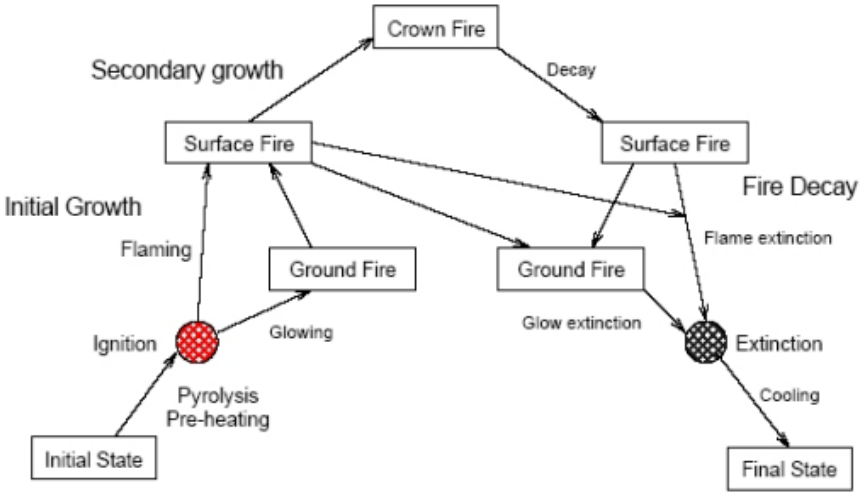

Figure 2-1. A flow chart showing the possible development and decay of a forest fire from ignition to extinction (Viegas, 2002) by (JRC, 2008).

Figure 2-2. Top left: An example of a ground fire, burning underground. Often smoke and heat are the only indicators of these fires (The Guardian 2009). Top right: A surface fire burns litter and small vegetation on the forest floor, while the canopy is preserved (Scott and Reinhardt 2001). Bottom left: An active crown fire consumes the whole fuel complex at once in a high intensity fire (Scott and Reinhardt 2001). Bottom right: An example of a passive crown fire consuming an individual small group of trees (Scott and Reinhardt 2001).

2.2 Factors that Influence Forest Fires

There are numerous physical factors that influence the start, behavior and extinction of forest fires (Figure 2-3) (Chuvieco et al., 2004). These factors include meteorological variables like temperature, wind speed, relative humidity and rain but also topographical and vegetation related variables such as fuel (vegetation) types, fine fuel moisture, elevation and aspect. The meteorological variables determine the short-term fire conditions, whereas the topographical and vegetation related variables change over a larger time-scale. In addition human activities and socioeconomic impacts have substantial influence on especially the ignition sources and fuel load, this includes factors such as time of the year and proximity of power lines, urban areas, roads and recreation areas (Vasilakos et al., 2008). Often the meteorological, topographical and vegetation variables are highly correlated and it can be very difficult to study the effect of one factor separately. In this chapter the most important factors are presented and discussed.

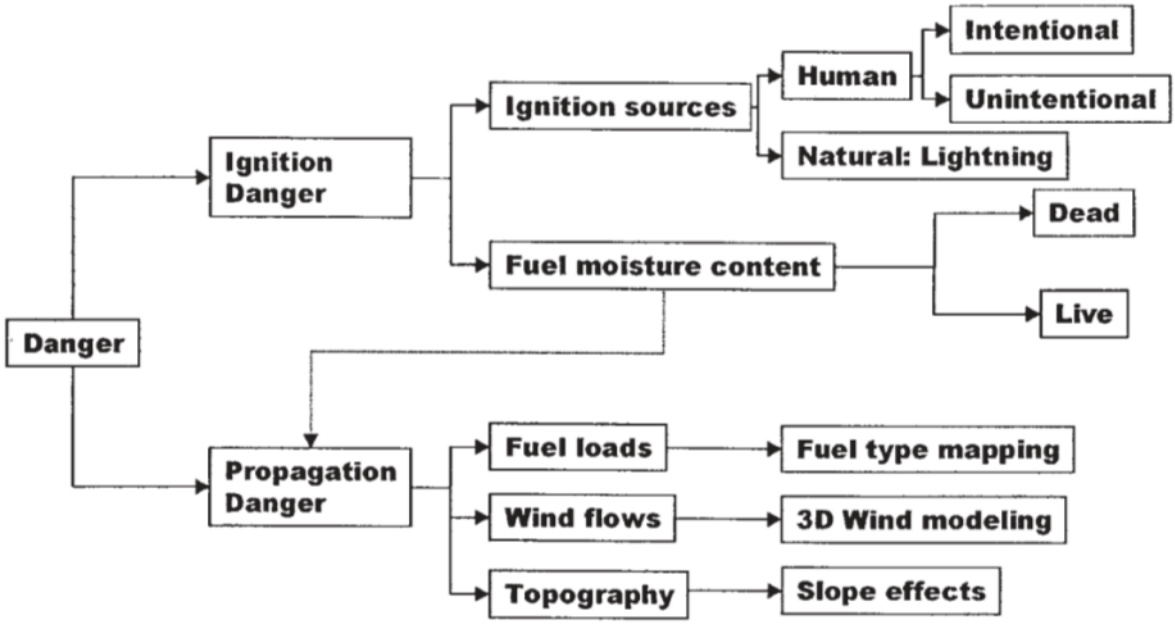

Figure 2-3. This framework shows all factors that contribute to the fire danger (Chuvieco et al., 2004).

2.2.1 Forest Fire Fuel and Moisture

In forest fire hazard research almost all effort is put in studying and mapping forest fire fuels. Forest fire fuel is not simply the same as the vegetation because it includes all inflammable natural (live and dead) vegetation, crops and residues. The different physiological properties among these fuels result in different flammability, where the term flammability refers to a fuels ability to ignite and sustain fire. The flammability of natural fuels itself is a very complex phenomenon that is influenced by many variable environmental factors (Dimitrakopoulos and Papaioannou, 2001) including the fuel load, bulk density, fuel particle size, heat content, moisture of extinction and vertical continuity (Scott and Burgan, 2005). These factors are largely variable, especially from one vegetation type to another. Therefore natural fuels are often classified in fuel types according to their expected flammability that can be related to the morphological, i.e. height, density, crown height, understory and litter, and physiological characteristics, i.e. moisture and resin, of the vegetation (Dimitrakopoulos and Papaioannou, 2001; Riano et al., 2002). Vegetation species are not necessarily relevant for fire management and research, because the same species may present completely different fire behavior if their fuel load, bulk density, vertical continuity, compactness or moisture, among others, change (Riano et al., 2002). The opposite, that different species may present almost equal fire behavior, can also be true as many species share the same physical properties.

Mapping of characterizing fuel types is considered to be an essential component of fuel hazard and fire risk assessment (Dimitrakopoulos and Papaioannou, 2001), but on a short term it is mainly the moisture content of the fuel type that determines the flammability. Fuel moisture content (FMC) is expressed as a percentage by the proportion water over the sample dry mass multiplied by a hundred and can be both live and dead. It is possible for live fuels to have moisture content well over 100% so that it contains more water than dry fuel weight. FMC is extremely important as it is inversely related to the probability of ignition as energy is needed to evaporate the excess water before the fire starts (Dimitrakopoulos and Papaioannou, 2001), decreasing its flammability. Through the same principle it also works as a determinant in fire propagation (Chuvieco et al., 2004).

FMC is highly influenced by weather conditions. For dead fuels, physical processes such as water vapor absorption, condensation, evaporation and desorption, in addition to direct contact with liquid water (Camia and Amatulli, 2009) all influence moisture content. These processes are all physically well understood and therefore reasonably easily modeled based on meteorological danger indices. Dead fuels lying on the forest floor are also the most dangerous because they are drier than live fuels and more dependent on rapid atmospheric changes (Chuvieco et al., 2004).

For live fuels the water interactions are very complex and difficult to generalize (Chuvieco et al., 2004) as most vegetation types have different physiological characteristics, phenology and adaptation to drought. Applying meteorological indices to live fuel moisture trends is therefore difficult as vegetation type depending mechanisms to extract water from the soil reserve and reductions in evapotranspiration have to be incorporated. Due to the relatively high moisture content, live fuel moisture content has a marginal role in fire ignition and is often not incorporated in fire danger ratings. Nevertheless, live fuel moisture content is a critical factor in fire propagation because water content is directly related to the

rate of spread. Despite the fact that researchers found strong non-linear relationships between long-term meteorological indices and live fuel moisture content it is not easy to incorporate them as the results were strongly species-dependent (Chuvieco et al., 2004).

There is an ongoing debate about the effect of forest fire suppression policies in the Mediterranean. One point of view holds that forest fires are fuel driven and systematic extinction of all reported wildfires allows fuel build up that leads to larger fires. The other point of view is that large fires are mostly wind/weather driven. Ferreira Leite (2011) found that for Portugal, areas that had been partially burned, i.e. only the litter, did not burn again until some years later, implying that large fires would be fuel driven (Ferreira Leite et al., 2011). Also Stambaugh et al. (2011) found that litter fuels can be effectively replenished within a few years during which potential fire spread rates and flame lengths rapidly increase, supporting the fuel driven theory. Nevertheless, others found that big fires in the Mediterranean shrub lands show a pattern more or less unrelated to the fire history (Keeley et al., 1999), but related to meteorological conditions. The processes of forest fires and the effect of fuel and moisture content on the fire size and abundance is not yet completely understood.

2.2.2 SLOPE AND WIND

In addition to the fuel moisture content, the rate of spread (ROS) of a fire largely depends on wind velocity and the slope of the ground surface. The ROS is very important in forest fire modeling and suppression; changes in spread rate have caused many fatal accidents throughout the world (Viegas et al., 2004). However, a complete understanding of the mechanisms related to wind and slope driven propagation is still lacking because it depends on many complex variables such as conduction, convection, radiation and fuel morphology (Viegas et al., 2004). The first modeling and research on the ROS was either empirical or statistical and many of the current operational systems that are used for fire danger and fire behavior predication are based on these non-linear equations that relate easily measured variables. After 40 years of research Rothermel (1972) was the first to complete a conceptual ROS model with an empirical basis (Rothermel, 1972) and most of the physical based research is still based on his work. Most of the research done to the effects of slope and wind velocity considered them separately (Weise and Biging, 1997) in laboratory conditions or by using controlled fires in real vegetation beds (Boboulos and Purvis, 2009).

The ROS of fire spreading aided by wind is often considered as a power or exponential function of the wind velocity (Anderson 1982; Rothermel 1972). Apart from an additional supply of air to the fire, wind increases the radiant heat transfer process by changing the angle of the flame relative to the fuel, so more energy is transported from the flame to the unburned fuel (Boboulos and Purvis, 2009). At the main front of the fire this increases the ROS, whereas at the tail end of the fire the spreading is slower because of the decreased angle of the flame and radiant heat transfer. The backfire characteristics are important as backfire is a fire suppression tool and used by prescribed fires. A forest fire can also generate its own wind due to the strong convection set up by the heat of the flames. Under calm conditions the flames will slightly lean inwards, towards the already burned area, at the edge of the fire as the air rising in the convection column needs to be replaced. In this case the fire will still spread outward but at the slow rate of a backfire. The indrawn wind can also interact with the prevailing wind. With a stronger prevailing wind the fire moves more quickly due to the increased radiant heat transfer. As a result the convection column moves more to the front of the fire (Figure 2-4). In this case the indrawn wind reduces the effect of the prevailing wind at the front of the fire but increases the wind speed behind the flaming zone (CSIRO, 2011), resulting in an increased ROS.

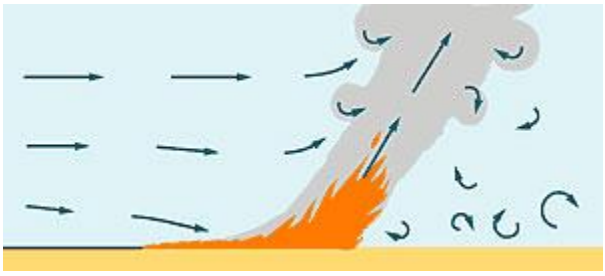

Figure 2-4. Headfire behavior on level ground with a prevailing wind (CSIRO, 2011)

The principle of the flame tilted towards the unburned fuel also holds for the effect of a slope and has a very similar and constant effect on the radiant heat transfer (Boboulos and Purvis, 2009); only in this case the ground is tilted towards the flames. On a slope, the indrawn wind can only reach the fire from underneath the convection column so that all air is sucked in from the down-slope direction (Figure 2-5). This further increases the total wind speed and ROS (CSIRO, 2011).

Figure 2-5. Headfire behavior travelling upslope with a prevailing wind (CSIRO, 2011)

On steeper slopes the energy released by the fire has important accelerating effects on the rate of spread, as the energy pre-heats all fuels upslope from the fire. This effect is called the chimney effect and creates extreme fire behavior (Viegas, 2002). One terrain configuration where the combination of prevailing wind and topography are particularly important is that of a ridge or canyon, where the effects of the often longitudinal wind direction, steep slopes and chimney effect are maximized (Viegas, 1998).

If a fuel load of a big forest fire is suddenly reduced the in drawn wind can push through the front of the fire and create extremely big flames, this is often seen when fires hit the edge of a forest, the top of a hill or a road. These big wind-blown flames carry many sparks and other flaming material and often create new (spotting) fires (CSIRO, 2011). Fire burning upslope aided by wind shows the highest rates of spread and thus the highest potential for damage, and highest difficulty to control (Weise and Biging, 1997). Despite the strong winds involved in the fire front, the prevailing wind (with topographical influences) will always determine the direction of the fire front (CSIRO, 2011).

2.2.3 IGNITION HAZARDS AND RISKS

With favorable fire weather conditions only an ignition source is needed to start a forest fire, often these are grouped in natural and anthropogenic sources. Without human intervention forest fires can start by four different mechanisms: a lightning strike, volcanic activity, sparks from rock falls and spontaneous combustion (Scott, 2000). European forest fires seldom have a natural ignition cause and are most often ignited by human intervention (FAO, 2007). In the whole Mediterranean basin one of the most important anthropogenic sources are shepherds and farmers who ignite forests and grassland to promote new flushes for their grazing animals or burn crop residues. Other sources include urban dwellers, agricultural expansion, solid waste burning and - especially in the western European Mediterranean - arson (FAO, 2007). In Spain during the period 1974 - 1994 only 5% of the forest fires started with a natural cause (lightning); 68% was lit intentional, 23% by negligence and 4% due to pasture burning (Pausas and Vallejo, 1999).

The anthropogenic ignition share is also visible in the relation of fire ignitions with respect to population density, distance to roads, urban-rural interspersed areas and agricultural fields (Catry et al., 2009 in Moreira et al., 2010). A Fire Risk Index (FRI) sensitivity analysis and fire history records of the Greek island Lesbos showed agreement in the ranking of human impact variables. It was found that most fires started in August and September, which is the result of drier weather conditions but also due to more human presence in forested areas. This is followed by the proximity to urban areas and main roads, because demographics and urban growth lead to pressures on rural areas and result in more ignition sources. The human presence on or close to roads causes more ignitions by accident or negligence. In this study, recreational areas such as beaches and places of religious and archeological attraction are ranked last as visitors tend not to cause fire ignitions. Generally speaking for the Mediterranean basin it can be concluded that the areas in the rural and urban interface seem to have a higher potential of ignition compared to rural areas (Vasilakos et al., 2008).

Natural ignition by lighting is often not incorporated in danger maps as it is quite random and only contributes to a small amount of forest fires. As to anthropogenic ignition sources it is possible to create a map that indicates the spatial variability and can assist forest and landscape authorities in developing better fire management plans (Conedera et al., 2011), reductions of fire ignitions and the mitigation of damages and victims (Vasilakos et al., 2008).

2.2.4 CLIMATE

The link between meteorological conditions and forest fire occurrence is obvious and well known, see chapter 2.2.1 and chapter 2.2.1. Forest fire occurrence tends to concentrate in the summer months when the temperature is high and both the air humidity and fuel moisture content are low. In this century there has been an increase in mean temperature at a global scale, especially noticeable since the 1970's (IPCC, 2007). For areas in Spain it was found that the increase of temperature was due to an increase in maximum but not minimum (1910-1994) or both maximum and minimum (1968-1994) temperatures. This is in contrast with global findings, in which the minimum temperatures increase at a higher rate than maximum values. In Spain the diurnal temperature range has increased (Pinol et al., 1998). Regarding mean temperatures, an increase of 0.05 – 0.35 ^{o} C per decade has been found for the western Mediterranean basin (Pausas, 2004; Pinol et al., 1998). In addition to this increase in temperature, the other important meteorological condition, summer rainfall, showed a slight decrease (Pausas 2004; IPCC 2007). So in summary the potential evaporation has increased due to a decrease in annual rainfall, increase of mean temperature and diurnal temperature range. These changes imply a decrease in fuel moisture and increase the fire hazard as a consequence (Pinol et al., 1998).

Forest fire occurrence has not been stable for the last decades and despite the fact that the number of events differs between different researchers and the high annual variability, they all show a dramatic increase in the number of forest fires in the Mediterranean basin (Schmuck et al., 2011; Pinol et al., 1998) and also Europe-wide (Figure 2-6) (Pausas, 2004). This increase persists when these historical numbers are corrected for the improved monitoring results by overestimating them with 25 to 50% (Pausas, 2004).

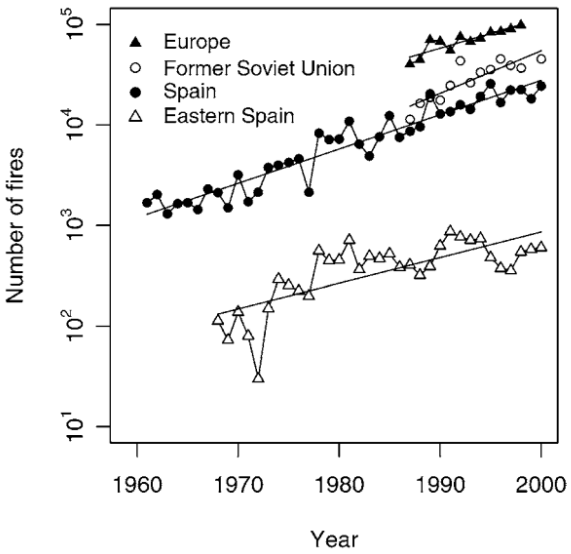

Figure 2-6. Comparison of trends in number of fires in Spain, Eastern Spain, Former Soviet Union and Europe. The uncertainty for the Former Sovjet union and prior to 1980 is quite high (Pausas, 2004). (Note the log scale of the y-axis)

Despite this increase in forest fire numbers the total burned area did not always show a clear trend in the Mediterranean (Schmuck et al., 2011) and it is important to understand that meteorological factors are only a part of the many factors that determine forest fire occurrence. For example, in many of the investigated areas the urban-wildlands interface has increased over time, something that favors ignition, but in contrary also the suppression and prevention methods have improved (Pausas, 2004). Nevertheless, a significant relationship between the modeled number of 'very high' fire risk days and the number and area of wildfires has been found (Pinol et al., 1998) and meteorological conditions remain to be an important factor in fire occurrence.

For the next century the IPCC has projected that European annual mean temperatures are likely to increase, for the Mediterranean especially during summer. Furthermore the annual precipitation and amount of precipitations days are very likely to decrease and especially decreasing rainfall trends in summer. Also extreme high temperatures are becoming more frequent and last longer with an increased risk of summer drought (IPCC, 2007). In a warmer climate, the conditions for forest fires will be more severe and the fire-prone area and the fire season are likely to expand, so that the number of fires and the total area burned is likely to increase (Pinol et al., 1998). As this rise in fire hazard seems unavoidable (Pausas, 2004), it is important to further improve fuel and landscape management together with prevention and suppression techniques.

2.3 Forest Fire Modeling

This study focuses on two different types of forest fire models, a fire danger rating model and a fire behavior prediction model. The difference between fire danger rating and fire behavior prediction models is that a fire danger model provides an index for measuring the fire potential rather than modeling how an actual fire behaves as is done in a fire behavior system. However, most fire danger models are so advanced that they need information about the slope, vegetation, wind conditions and fuel moisture content in order to provide a good estimate of the potential rate of spread and intensity. Worldwide, almost all fire danger and fire propagation models are based on three different modeling approaches. The two most applied models are the Canadian Forest Fire Danger Rating System, CFFDRS) and the United States National Fire-Danger Rating System (NFDRS). The third is an approach made by McArthur (1966) but this model is mainly based on the work done in Canada (Weise and Biging, 1997) and will no further be discussed.

The Canadian CFFDRS model is empirical and started in the 1920's by measuring forest fire behavior at field scale in several fuel types. The nonlinear equations derived from this research related the rate of spread to easily measured variables such as wind speed, slope, temperature and relative humidity and were used to create an operational system that is used for fire danger and fire behavior. It is composed of two major subsystems: the Canadian Forest Fire Weather Index (FWI) system and the Canadian Forest Fire Behavior Predication (FBP) system that model fire danger and fire behavior respectively (Van Wagner et al., 1992). This model layout with two subsystems is also used in the United States NFDRS model, where the respective subsystems are called FUEL and BURN, however the NFDRS model is totally different as it has a deterministic basis. Research for this model started in the 1930's by Rothermel and aimed at the physical factors that influence forest fires in order to combine this knowledge with a mathematical model that included heat transfer terms for conduction, convection and radiation (Andrews, 1986).

Both the FUEL and FWI model use meteorological conditions to estimate the fire weather conditions, i.e. litter and forest surface moisture content, in a standardized forest type, but again they use a different approach. The FUEL model is based on the semi-empirical Rothermels 10-h fuel stick moisture content model, where the dead fuels are categorized according to their timelag that is based on the length of time required for a fuel particle to change moisture by a specified amount when subjected to changes in its environment (Andrews, 1986). The minimum time lag is 1 hour so this model requires a lot of calculations to model extend periods of time and fuel classification is cumbersome. The empirical Canadian fuel module (FWI), explained in chapter 2.3.1 is more versatile and uses daily observations and calculations. The FWI methodology was therefore also incorporated by the United States Forest Service in 1986 as an option. This was done in the first computer implementation of a non-spatial forest fire behavior model, called BEHAVE (Rothermel et al., 1986). Since then almost all fuel modeling by meteorological conditions globally is based on the work of Wagner (Van Wagner et al., 1992 in Pastor et al., 2003). Both models were initiated as non-spatial models, with a daily and hourly temporal resolution for the FWI and FUEL model respectively (Andrews 1986; Van Wagner et al., 1992).

In this research it was chosen to use the FWI model for fuel moisture content modelling on account of its more practical design with similar results. For fire behavior prediction modelling the BEHAVE model is used as it already incorporates some Mediterranean vegetation species and it therefore has obvious advantages over the Canadian FBP model. Both models are discussed in this chapter.

2.3.1 The Canadian Fire Weather Index

The Canadian fire weather index (FWI) is developed and described by Van Wagner et al., (1992). The model estimates the moisture content in dead fine surface fuels based on meteorological conditions. This fine dead fuel moisture content is of great importance for the rate of spread, the ignitibility, sustainability and intensity of fire. As explained in chapter 2.3 operational models for fire behavior predictions mostly rely on the Canadian Fire Weather Index. This FWI uses daily observations of air temperature, relative humidity and wind speed, taken at solar-noon, and 24hour accumulated rainfall to estimate moisture contents in three layers of the forest floor (Wotton, 2009). The fine surface fuels are represented by the Fine Fuel Moisture Code (FFMC), the upper organic layer is represented by the Duff Moisture Code and the deeper organic layers are represented by the Drought Code. These three moisture codes are generated from simple moisture exchange and each fuel is considered to dry exponentially, so that its drying rate is proportional to its current free moisture content (Van Wagner et al., 1992). The three moisture codes carry different information: the FFMC is an indicator for the ease of ignition and flammability of fine fuels, the DMC is an indicator of fuel consumption in medium-size woody materials and duff layers, whereas the DC indicates fuel consumption in large logs and smoldering in deep duff layers (Camia and Amatulli, 2009).

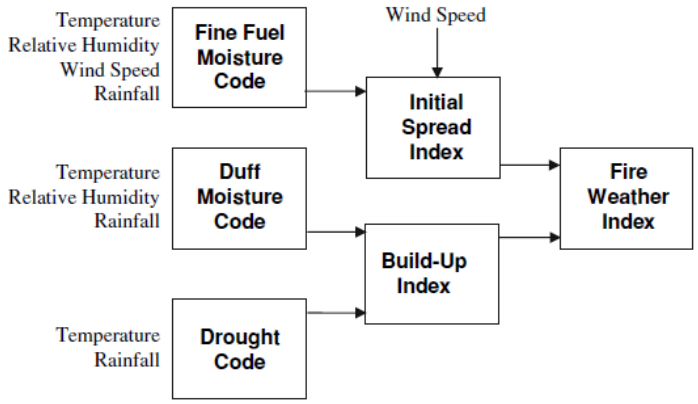

Figure 2-7. The structure of the Canadian Forest Fire Weather Index System (Wotton, 2009).

The three moisture codes are used as an input for three fire behavior indices, see Figure 2-7. The Initial Spread Index rates the expected rate of spread from the combination of FFMC and wind speed. The fuel that is available for combustion, the Build Up Index, is calculated from the Duff Moisture Code and the

Drought Code. Finally the FWI is the final index that combines the Initial Spread Index and Build-Up Index and rates the fire line intensity at the fire front (Wotton, 2009). All six indices are relative, so their value has no physical meaning; a higher value means a drier fuel, increased fuel load or fire intensity. As the FWI was made for Canada it is representative of the moisture content of fuels in mature, closed canopy pine stands. In addition it incorporates a lot of factors that are important for Canada's high latitude such as the two slow-reacting moisture codes, the DMC and the DC, that respond to changing day length in the season. However, it has proven to work in a wide variety of forest types and fire managers understand that a model outcome in one vegetation type can represent an actual different moisture content in another vegetation type (Van Wagner et al., 1992).

Each individual component of the FWI system is a sort of fire danger index with its own different aspect and information is lost by combining them in one single index. It is also important to realize that the FWI depends on weather observations alone. It does not consider differences in fuel types or topography, but provides a relative rating of fire danger through fuel moisture and fire behavior potential that is uniform over large areas (Van Wagner et al., 1992). However, as fuel moisture and wind are such important factors influencing the potential intensity and ROS of a fire and due to the fact that it is a relative index, the FWI is used by a lot of agencies worldwide. This includes the EFFIS program of the EU (Camia and Bovio, 2000), that produces and publishes daily large scale maps (20 x 20km pixel size) of the fire danger in Europe between March and October. The FWI is the most used fire danger model in the Mediterranean and is used both with and without adjustments to compensate for latitude, climate, day length and vegetation morphology, as the relative outcome is not always required to relate to a physical parameter. Furthermore a lot of studies have been done to calibrate the indices and these have shown that the FFMC correlates well with measured dead fuel moisture content values. The application of the DC moisture code in the Mediterranean is questionable however, as in the large majority of cases the soil deep organic layer is absent (Camia and Amatulli, 2009). All studies underline the importance of calibration to the most dominant fuel type (Wotton, 2009; Camia & Amatulli, 2009).

As was explained in the beginning of this chapter it was found that the FWI was a more versatile fuel moisture predictor than Rothermel's timelag method used in the NFDRS. Rothermel did successful research to use a modified version of the Fine Fuel Moisture Code (FFMC) in the BEHAVE model (Rothermel et al., 1986) as the additional value of both FWI's duff layers was insignificant. The modification was needed in the used solar angle, shading and sun/slope geometry (Camia and Bovio 2000), these solar input corrections adapted the FFMC to the lower United States latitude. In addition the original FFMC assumed 100% canopy coverage (i.e. total shading) and this is not always the case in forests found in the United States. By these corrections the adjusted FFMC model is better in expressing the air temperature and relative humidity and can be adapted to numerous different types of forests worldwide (Rothermel et al., 1986), including those of Mediterranean Europe (Dimitrakopoulos and Dritsa, 2003) where it was correlated with leaf litter moisture content with a root mean standard error of 5% (Aguado et al., 2007).

2.3.2 THE BEHAVE MODEL

The second model explained here is the fire behavior prediction model: BEHAVE. This model requires parameters related to the vegetation, slope, wind and the moisture content calculated by the FWI. The most important fire behavior parameters it outputs are the rate of spread, fireline intensity and flame length.

The BEHAVE model was made for surface fires with fuels less than 1.8m high but also supports crown and spotting fires in additional modules. The link between the fuel moisture predicator and the fire behavior prediction consist of tabular files or equations (Fuel Model File) that link the fuel moisture content to the fire behavior predictor. These fuel model files contain all information about the physical vegetation properties as described in Chapter 2.2.1. With information on the fuel, the fuel (moisture) condition, slope and wind speed the BEHAVE model is able to calculate the rate of spread and fire intensity (Andrews, 1986). In order to make a spatial fire danger assessment no actual fire behavior predication is required, an assessment on potential fire characteristics is sufficient, nevertheless it will be referred to as a (potential) fire behavior prediction in this study.

3 STUDY AREA

European forest fires mainly occur in the Mediterranean, with 90% of the total amount of fires taking place in Portugal, Spain, France, Italy and Greece (Schelhaas et al., 2003). This study focusses on these forests as the fuel types, and thereby the fuel mapping, are often very regionally specific. Additionally it is important to start with an introduction of the area so that it is clear why certain fire modeling aspects, e.g. fuel moisture under frozen conditions, melting snow, are not included in this review, while other such as solar radiation are included.

The selected research area is located around an artificial lake, Lac des Olivettes (43° 55'N, 3°21'E), in the La Peyne catchment, Languedoc-Roussillon, Southern France. The 70km^2 La Peyne catchment is found 60km west of Montpelier, see Figure 3-1, and is dominated by vine cultivation. The lower part of the catchment is representative for the French Mediterranean coastal plain with respect to climate, relief, geology, geomorphology, agricultural practices, vineyard management and vine species (Lagacherie et al., 2006). The upper part, that is the research area of 24km^2, is covered in large parts of scrubbed evergreen forest called *maquis* and shows more elevation with altitudes varying from 100 to 450meters (Sluiter, 2005). This site has been selected as it contains a meteo station and based on HyMap satellite imagery a detailed vegetation map exists (Sluiter, 2005), see Appendix A.

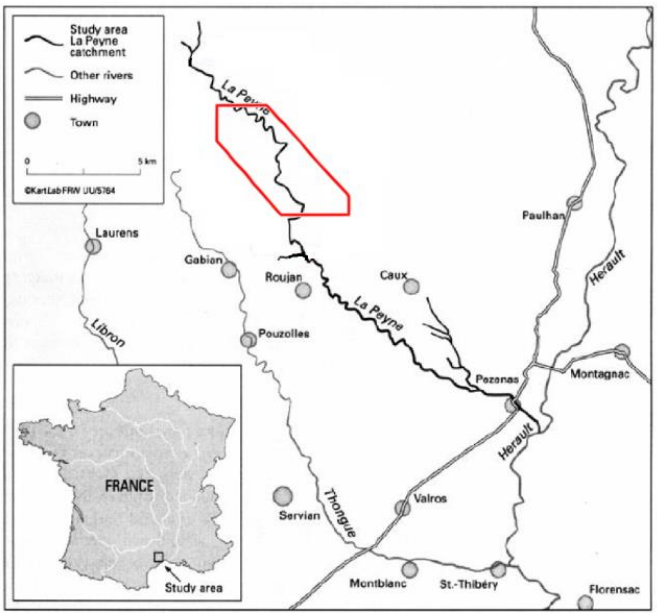

Figure 3-1. The La Peyne river catchment with the study area marked in red (Based on Sluiter (2005)).

Characterized by summer drought and heat while having cool winters, the research area is sub-humid Mediterranean. Average temperatures vary from 3°C to 11°C in January and from 18°C to 30°C in July. Nearby Montpellier has a yearly average of 2700 sun hours. The average annual precipitation is 600mm and the average annual evapotranspiration (PET) 1090mm. Spring and autumn show the most precipitation and the Peyne river discharges 60% of its total volume in spring (March, April, May) and only 1% in summer (June, July, August) ((Risson, 1995 in Sluiter, 2005)). This kind of bi-seasonality is unique to the Mediterranean climate and is important with respect to the summer fire hazard in the area.

Due to the prevailing Mediterranean climate with its long summer droughts large parts of the Mediterranean are covered in fire climax species (FAO, 2007). Although the diversity of plants and animal species in the Mediterranean is high with 25,000 plant species of which 50% is endemic and 200 species of terrestrial mammals (Scarascia-Mugnozza et al., 2000). The research area is mostly covered by low oak forest, natural scrub and agricultural areas (Sluiter, 2005). This vegetation mixture is partially the result of the depopulation that occurred throughout most of the 20th century causing farmlands to revert to shrub and woodlands ((Mather et al., 1999 in Sluiter, 2005)). Also logging practices had their influence on the vegetation as it caused many of the oaks to stool which created a dense forest.

4 METHODS

This chapter describes the methodology of this study. The methodology consists of three parts: model building, (field) data collection and model calibration and validation. The methodology will also be discussed in this order. Data acquired during the field campaign was used for calibration and validation of the model.

4.1 MODEL BUILDING

The main objective of this study is to compose a fire hazard map based on a fine dead fuel moisture content model that is used as input for a potential fire behavior model. Fine dead fuel moisture content was estimated by the Fine Fuel Moisture Code (FFMC) and potential fire behavior by the BEHAVE model. It is worth noting that the focus during the modeling and in this study as a whole has been on implementing and validating the FFMC model and that an outdated and simplified version of the BEHAVE model is used based on the original Rothermel equations (Rothermel, 1972). Creating a spatial model that incorporates all of the many factors that are being used in the most recent version of the BEHAVE model (BehavePlus 5.0.5, build 307) (Missoula Fire Sciences Laboratory, 2013) was outside the scope of this study.

The BEHAVE model is a based on the Rothermel surface fire spread model that allows fire behavior prediction in vegetation lower than 1.8 meters and therefore is not capable of predicting crown fire potential (Rothermel, 1972). Crown fires solely occur in coniferous forest and only 2.68% of the total land area in the study area is covered by coniferous vegetation. Although these Mediterranean pine forests are capable of creating intense crown fires even under moderate burning conditions (Mitsopoulos and Dimitrakopoulos, 2007), these effects require another approach and are therefore not included in this study. This results in the assumption that the main coniferous fire carrier is the high fuel loaded conifer litter.

In chapter 2.2 it is explained what factors influence forest fires and Figure 2-3 shows their interrelation. All except the ignition sources and live fuel moisture content are modeled in the study. Excluding the ignition sources will still allow forest services to use this model in case of an actual fire and in forest fire danger mapping, but only lacks statistical information on the likeliness that a fire will start in a certain place.

The model was implemented in PCRaster Python. PCRaster is a software utility for development and deployment of spatio-temporal environmental modeling made by the Department of Physical Geography, Faculty of Geosciences at Utrecht University (Wesseling et al., 1996). PCRaster is not developed to be a full-blown raster GIS (Utrecht University, 2013) but when used within the Python language environment it is well sufficient for this study. The model output data was further analyzed by using Microsoft Excel and when required prepared for publishing in ESRI's ArcMap.

The model structure is illustrated in Figure 4-1 with the two sub models (FFMC and BEHAVE) marked in blue. The FFMC uses fire weather observations and geographic parameters to calculate the fuel moisture content. The BEHAVE model uses fire weather observations (wind), geographic parameters and the calculated moisture content to predict the potential fire behavior. In the next few paragraphs of this chapter the theory behind both the sub models is explained in detail. The whole Pcraster Python script is provided in Appendix I. Due to the large number of equations described in Chapter 4, a detailed flowchart illustrating the relationships between the variables, constants and parameters of both models is provided as a foldout in Appendix J.

In this study the model was run from June 1, 2013 until September 6, 2013, covering the Mediterranean summer and the most important fire hazard season.

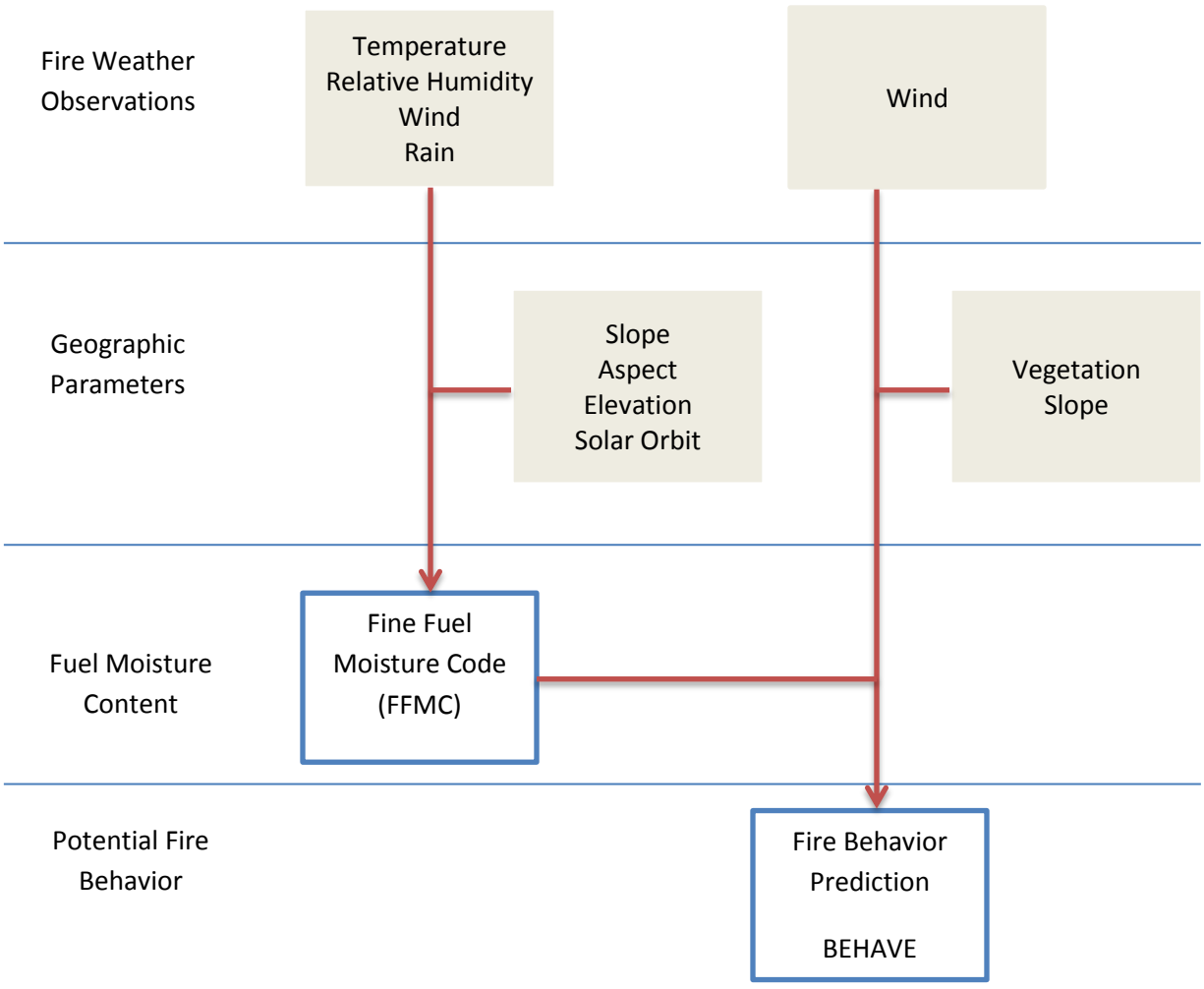

Figure 4-1. The model structure showing the input parameters and the two (FFMC and BEHAVE) major sub models used in this study.

4.1.1 THE STANDARD FFMC

Van Wagner (1987) presented the Fire Weather Index (FWI), based on work that had been done since 1938 by the Canadian forest fire service. The component of the FWI that is of interest for this research, the Fine Fuel Moisture Code (FFMC) is explained here, see also Appendix J.

The FFMC represents the moisture content of litter and other cured fine fuels in a forest stand, more specifically in the loose surface layer of the forest floor. It provides daily ratings of moisture content at the mid-afternoon (16:00) peak of fire danger that is calculated from yesterday's FFMC value in combination with today's (solar-noon) weather inputs. This fuel dries relatively fast, but still experiences a substantial time lag effect from its previous day value. This time lag is a measure of drying speed in which it is measured how much time is needed to lose 2/3 of the free moisture content above its equilibrium moisture content (EMC), which is the lowest moisture content that a fuel will reach for a given combination of weather conditions. Table 1 shows the physical properties of the FFMC as well those of the other two deeper duff layers for comparison.

Table 1. Physical properties of forest floor layers that are described within the moisture codes of the Canadian Forest Fire Weather Index (Lawson & Armitage, 2008).

Fuel moisture code	Forest floor layer	Nominal depth (cm)	Nominal load $(kg \cdot m^{-2})$	Bulk density $(g \cdot cm^{-3})$	Rain capacity (mm)	Saturated moisture content $(\%)$	Standard time-lag[a]
FFMC	Litter	1.2	0.25	0.021	0.62	250	2/3
DMC	Loosely compacted duff	7	5	0.071	15	300	15
DC	Deep compacted organic layer	18	25	0.139	100	400	53

[a] Time lags of the fuel moisture codes vary with weather conditions. Tabulated values represent standard drying conditions (temperature 21.1°C, relative humidity 45%, wind speed 13 km/h, July).

The daily FFMC index starts by calculating yesterday's moisture content out of yesterday's FFMC value. This is done by Equation 1:

$$m_0 = 147.2\,(101 - F)/(59.5 + F) \qquad \textbf{Equation 1}$$

where *F[-]* is yesterday's FFMC value and m_0 *[%]* is yesterday's moisture content.

This relates the relative FFMC scale length of 101 to that of *m* that ranges from 0 to 250, where 250 is equal to the maximum real moisture content percentage of pine litter. This scale is called the FF-scale.

After m_0 is calculated the FFMC discriminates two different phases in the moisture balance, drying and wetting. Drying occurs when the calculated moisture content is above the EMC, wetting occurs when the fuel contains less moisture than its equilibrium. This wetting does not include rain but is caused by an increase in relative humidity. For drying it is observed that exponential drying could be assumed and that, regardless of the actual moisture content, the rate of change from day to day can be described by the slope of the drying curve. This slope, called the log drying rate, is indicated at the normal temperature of 21.1 °C (70°F) by k_0 in Equation 2:

$$k_0 = 0.424\left[1-\left(\frac{H}{100}\right)^{1.7}\right] + 0.0694\,W^{0.5}\left[1-\left(\frac{H}{100}\right)^{8}\right] \qquad \textbf{Equation 2}$$

where *H [%]* is the relative humidity and *W [km/h]* the windspeed measured at 20ft (6m). Low relative humidity and high windspeeds result in a higher k_0 value and thus a high drying rate.

For wetting the drying rate equation (Equation 2) was reused by using 100-*H* instead of *H*:

$$k_1 = 0.424\left[1-\left(\frac{100-H}{100}\right)^{1.7}\right] + 0.0694\,W^{0.5}\left[1-\left(\frac{100-H}{100}\right)^{8}\right] \qquad \textbf{Equation 3}$$

where k_1 represents the log wetting rate at the normal temperature of 21.1 °C, *H [%]* the relative humidity and *W [km/h]* the windspeed measured at 20ft (6m).

In addition to wind speed and relative humidity, the temperature (T,[°C]) has a crucial role in both the rate of drying as wetting. Test on pine needles indicated a 50% increase in the drying rate during a temperature increase of 11 °C. The temperature effect is inserted by:

$$k_d = k_0 \cdot 0581\, e^{0.0365\,T}$$
$$k_w = k_1 \cdot 0581\, e^{0.0365\,T} \qquad \textbf{Equation 4}$$

for respectively drying and wetting with T [°C] as temperature. Here k_d and k_w are expressed in units of log moisture content per day ($\log_{10} m/day$).

To find out whether the drying or wetting rate should be applied the moisture content (m_0) is compared to the equilibrium moisture content (EMC, here *E* [%]. This is the moisture content at which the moisture content of the wood is in equilibrium to the relative humidity and temperature at that

moment. *E* in woody fuels is subjected to hysteresis, which means that for the same relative humidity and temperature different values are found when the initial state corresponded to higher or lower moisture contents. This also implies that their curves (called isotherms) are calculated in two different ways:

$$E_d = 0.9425H^{0.679} + 11e^{(H-100)/10} + 0.18(21.1 - T)(1 - e^{-0.115H}) \quad \textbf{Equation 5}$$

$$E_w = 0.618H^{0.753} + 10e^{(H-100)/10} + 0.18(21.1 - T)(1 - e^{-0.115H}) \quad \textbf{Equation 6}$$

where E_d is the equilibrium moisture content obtained by drying from 'above' and E_w is the equilibrium moisture content obtained by wetting from 'below' (Figure 4-2). The latter term is used to let both equations converge at zero when the relative humidity is zero and takes effect when H approaches zero.

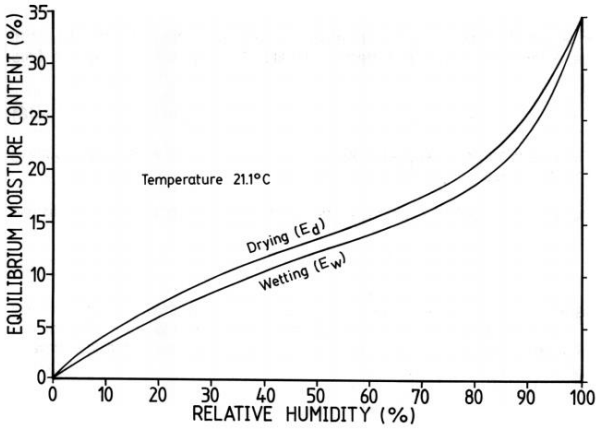

Figure 4-2. Isotherms of equilibrium moisture content *E* vs. relative humidity *H* at T=21.1 °C.

Next the value of E_d is compared to m_0 calculated with Equation 1. If m_0 turns out to be higher than E_d a drying regime prevails and the present day or todays moisture content (*m,* [%]) is found from Equation 7:

$$m = E_d + (m_0 - E_d) \cdot 10^{-k_d} \quad \textbf{Equation 7}$$

where k_d is the log drying rate obtained with Equation 4.

If m_0 turns out to be less than E_w a wetting regime prevails and *m* is found from Equation 8:

$$m = E_w - (E_w - m_0) \cdot 10^{-k_w} \quad \textbf{Equation 8}$$

where k_w is the log wetting rate obtained with Equation 4.

There also is a third case where m_0 is between both equilibrium curves ($E_d \geq m_0 \geq E_w$), see Figure 4-2. If this is the case neither drying nor wetting occurs and $m = m_0$.

Finally 'today's' FFMC value *F* is calculated from Equation 9:

$$F = 59.5(250 - m)/(147.2 + m) \quad \textbf{Equation 9}$$

where *m* [%] is 'today's' moisture content.

RAINFALL IN THE FFMC

Van Wagner (1987) created a separate term to include rainfall, where the accumulation of 24-h rainfall enters the FFMC by adjusting the initial moisture content of m_0. This means it is assumed to occur always before the current day's drying begins. It is only accounted for rainfall (r_0, [mm]) that is in excess of 0.5mm to compensate for the canopy interception; the so called net rainfall (r_f, [mm]) where:

$$r_f = r_0 - 0.5 \quad \textbf{Equation 10}$$

As explained in chapter 2.2.1 the moisture content m_0 is expressed as a percentage by the proportion of water over the sample dry mass multiplied by a hundred and can therefore be over 100%. For $m_0 \leq 150$ the rain corrected moisture content (m_r) is calculated by Equation 11.

$$m_r = m_0 + 42.5 \cdot r_f (e^{-\frac{100}{251 - m_0}})(1 - e^{-\frac{6.93}{r_f}}) \quad \textbf{Equation 11}$$

where r_f [mm] is the net rainfall, m_r [%] is the rain corrected moisture content and m_0[%] yesterday's moisture content.

The $m_0 \leq 150$ restraint is added because Equation 11 provides unwanted behavior for both high amounts of rainfall and high initial moisture contents.

For $m_0 > 150$ the factor $0.0015(m_0 - 150)^2 {r_f}^{0.5}$ is added:

$$m_r = m_0 + 42.5 \cdot r_f \left(e^{-\frac{100}{251-m_0}}\right)\left(1 - e^{-\frac{6.93}{r_f}}\right) + 0.0015(m_0 - 150)^2 \ {r_f}^{0.5} \qquad \textbf{Equation 12}$$

where r_f [mm] is the net rainfall, m_r [%] is the rain corrected moisture content and m_0[%] yesterday's moisture content.

In case of rainfall $r_0 < 0.5\ mm$ it holds that $m_0 = m_r$, assuming dry weather, and from there the standard FFMC procedure is followed.

4.1.2 Adjustments to the Standard FFMC

The standard FFMC was developed from data taken under a closed canopy of jack or pine trees, therefore it is not likely to perform well in vegetation with an open canopy. Drying of fuels exposed to direct sunlight is not something unique for the Mediterranean but occurs in fuels in large parts of the world, as a result several studies were conducted that focus on examining the effects of solar radiation on the drying rate (Byram and Jemison, 1943; Rothermel et al., 1986; Gibos, 2010). Solar radiation not only directly impacts the diffusivity at the fuel particle level but also affects the directly surrounding air temperature and relative humidity, the wind patterns in complicated sloped terrains and the composition of the fuel (vegetation) itself (Gibos, 2010). For this research the standard FFMC model is adjusted for ambient air temperature and relative humidity by means of incorporating the effects of solar radiation, shading and fuel-level windspeed.

Fuel Temperature

Byram and Jemison (1943) began with gathering field data to determine the effect of solar intensity and windspeed upon fuel temperature and moisture. Not all radiated heat will contribute to higher fuel temperatures because losses occur. According to Newton's law of cooling the rate of loss of heat is directly proportional to the temperature difference existing between the object and its receiver. In fuel temperature modeling this represents the fuel and its surroundings and includes free convection, conduction and radiation. They conclude that radiated losses of forest fuels are small and assume that all heat is lost by terms of convection and conduction.

A considerable amount of heat is lost by conduction through the fuel bed into the ground and is considered a constant part of the radiated input. The heat lost to convection however depends on the windspeed and is assumed to be directly proportional with the wind velocity. The following derivative of Netwon's law adequately fitted their experimental data (Byram and Jemison, 1943):

$$T_f - T_a = \frac{I}{aW + b} \qquad \textbf{Equation 13}$$

where (on a metric scale) $a = 42.5$ and $b = 32.7$, T_f is the fuel temperature [°C], T_a is the air temperature [°C] measured in the open, *W* is the windspeed at fuel level [km/h] and *I* is the solar radiation [$W\ m^{-2}$]. a and b are species-specific calibration parameters and it is emphasized that this research was done in hardwood litter and that fuel types that have higher or slower loss rates to both the air as the underlying ground are likely to have other values for constants a and b (Byram and Jemison, 1943). No other values for a and b were found in literature, however Rothermel et al. (1986) used the same values. Nonetheless with a pyranometer, anemometer, infrared thermometer and a normal thermometer a and b can be determined directly from this data. For this research the values $a = 42.5$ and $b = 32.7$ were used, but it is agreed that these factors should be investigated.

CORRECTED RELATIVE HUMIDITY

Byram and Jemison (1943) also described the relative humidity ambient to the solar heated fuel, they did so by using vapor pressure arguments concerning the temperature and relative humidity of the air. The correction for relative humidity as a function of the fuel temperature and air temperature is:

$$H_f = H_a \, e^{0.059(T_a - T_f)} \qquad \textbf{Equation 14}$$

where H_f is the relative humidity at fuel level [%], $H_a$is the relative humidity of the air [%], and T_a and T_f as previously defined (Byram & Jemison, 1943).

SHADING

The corrected fuel temperature and relative humidity from Equation 13 and Equation 14 both depend on the amount of solar radiation. In the standard FFMC total shading is assumed, which is not the case in most Mediterranean fuel types. The radiation in Equation 13 is the solar radiation that reaches the litter layers of the forest floor, however radiation in FFMC calculations is often calculated from the sun angle or measured in the open field. Therefore it is important that there is a correction factor that corrects the (calculated) radiation value for atmospheric transitivity and tree shading and thus compensates for the intercepted radiation. Rothermel (1986) used an equation that resulted net cloud/tree transmittance (τ_n, [-]):

$$\tau_n = \tau_c \cdot \tau_t \qquad \textbf{Equation 15}$$

where τ_c is the transmittance of the cloud cover and τ_t is the transmittance of the timber canopy. In this research a weather station is used and the measured radiance is automatically corrected for atmospheric transitivity. So Equation 15 can be simplified to:

$$\tau_n = \tau_t \qquad \textbf{Equation 16}$$

FUEL LEVEL WINDSPEED

Byram and Jemison's (1943) equation to calculate the fuel temperature (Equation 13) also requires a value for the wind speed at the fuel-level. Their data shows that despite the fact that the wind speed often decreases dramatically when measured close to the surface the cooling effect can be distinct (Rothermel et al., 1986). However, converting measured wind speed to fuel level wind speed is not straightforward. Firstly there are different standards heights in use for the wind measure instrument and because the measurement height/vegetation height ratio has an important influence on the measured roughness length it requires careful standardization. Secondly the amount of adjustment differs from one fuel type to another, the patchiness, the way it is orientated on a slope, the amount of overstory, etc (Rothermel et al., 1986). The influence of the vegetation is illustrated in Figure 4-3.

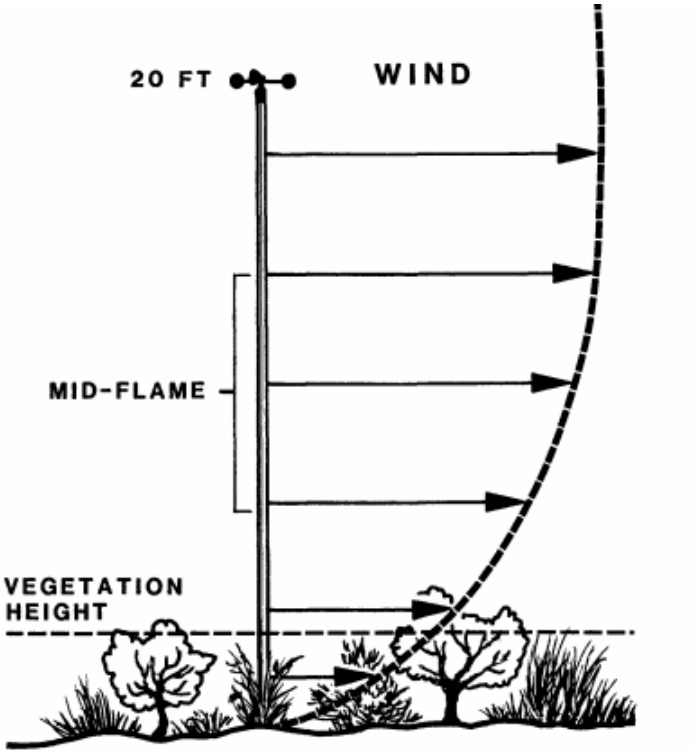

Figure 4-3. The near-surface wind profile showing the non-linear decrease due to the vegetation.

The meteo station (see chapter 4.2) in the study area measures at the Remote Automatic Weather Station (RAWS) standard of 20ft (6m). These wind speed values have to be converted proportionally to the degree of influence induced by the roughness and height of the vegetation cover. This is typically done by applying a universal dimensionless wind profile that can be applied to any vegetation, from short grass to tall trees. Hereby the 20ft wind speed is converted to a wind speed at the top of the

vegetation. Albini and Baughman (1979) found a relation between wind speed at 20ft and at the top of the vegetation, see Equation 17 (converted to metric).

$$\frac{U_H}{U_{20+H}} = \frac{1}{\ln\left(\frac{20 + 1.1811\ H)}{0.13\ 0.42651\ H)}\right)} \qquad \textbf{Equation 17}$$

where U_H/U_{20+H} is the ratio between the 20ft wind speed and the fuel level wind speed and H is the vegetation height in *[m]*.

However a preliminary calculation indicated that this equation provides unwanted results that do not relate to observations by the author; Equation 17 provides lower values for vegetation with a low vegetation height to account for lower wind speeds near the surface. However in the study area the effects of sheltered (overstory) and unsheltered (no overstory) fuels are considered to be larger, especially when the discrete vegetation types (Appendix A) used in this study are considered. These effects of dense and open forests and areas are studied by Scott (2007) and related to specific adjustment factors illustrated in Appendix B as well as the related U_H/U_{20+H} .

The wind speed discussed above is used in Equation 13 to calculate the fuel level temperature. Note that Equation 2 and Equation 3 are already calibrated to winds measured at the 20-ft (6m) RAWS standard and that conversion is not needed.

FFMC SCALE

Van Wagner (1987) has used several scales that relate the FFMC to fuel moisture content. The 'old scale' and F-scale were used in the first three editions of the FWI system and were replaced by the FF-scale for the fourth (and here described) edition of the FWI system (Van Wagner, 1987), that is still in use. As indicated before the FFMC was developed for closed canopy pine-forest in the high latitude regions of Canada, but Van Wagner made a scale that was adjusted for use in semi-arid and warm conditions. This scale named the FX-scale, as it is called, is a faster responding scale developed to improve the resolution of the FFMC at the dry end of the moisture range in hot and dry conditions. It is therefore likely to correlate better with moisture contents in open and exposed scrub fuels (Lawson et al., 1996). The FX-scale is defined as follows:

$$m_0 = 32.87\ (101 - F)/(13.28 + F) \qquad \textbf{Equation 18}$$

where *F* [-] is 'today's' FFMC value and m_0 [%] 'today's' moisture content.

When compared to the older scales its behavior in lower moisture contents is clearly visible from Figure 4-4. In dry areas a small decrease in already low moisture content causes a much bigger FFMC increase on the FX-scale than it does on the FF-scale. Behavior which can be expected when the moist boreal forest of Canada are compared to the already dry (and adapted to drought and heat) vegetation of the Mediterranean. Note that the FFMC scales are introduced to compare fire danger potential with other areas and vegetation types and it is therefore not further included in this study. It does not give additional information that can be used in the BEHAVE model and is therefore skipped in the calculations used for the BEHAVE model, i.e. the moisture values calculated by the FFMC are used directly.

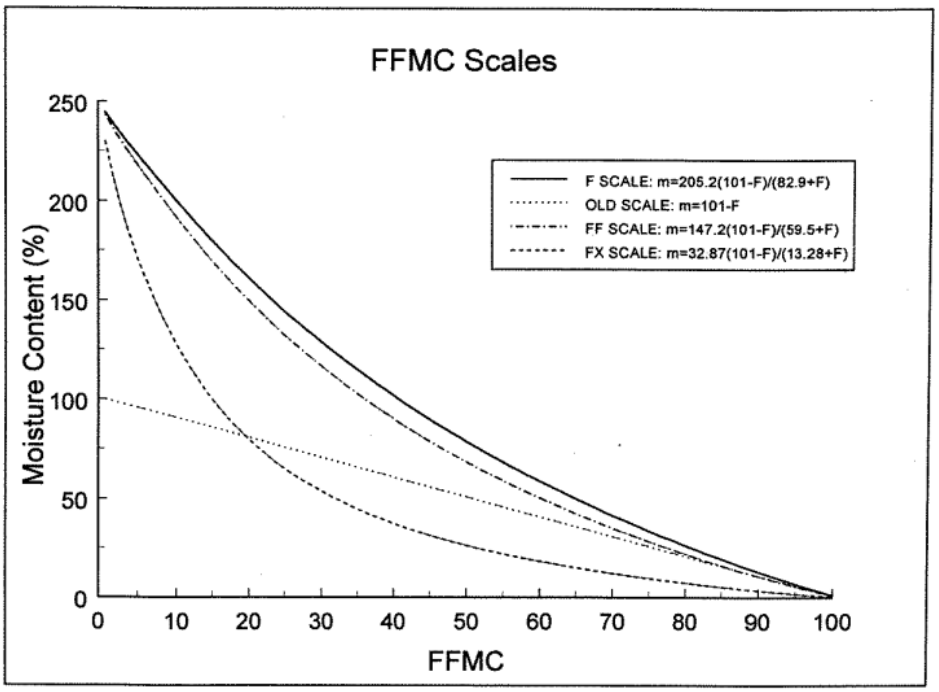

Figure 4-4. A graph of Fine Fuel Moisture Code scale equations that were used in various versions of the FWI system to link litter moisture content to FFMC (Lawson, et al., 1996).

4.1.3 THE BEHAVE SURFACE FIRE MODEL (ROTHERMEL, 1972)

The model used in this study is made of a set of equations and relationships by Rothermel (1972) that form the basis of the BEHAVE model. As explained before, the latest versions of the BEHAVE model are more extensive, as they for example include dynamic fire models that account for the drying of herbaceous fuels and calculate the related heat sink. However the BEHAVE model is originally a non-spatial model and converting more than the basis equations to a spatial model is outside the scope of this study. Therefore the original Rothermel equations with spatial and temporal varying input variables are used to predict fire behavior in this study.

Early work in fire spread research, mainly by Frandsen (1971), was primarily aimed at developing relationships between burning conditions and variables that were obvious to the forest service personnel. These variables, such as fuel moisture, fuel load, relative humidity, slope, etc, were studied and correlated to a fire behavior extend. Compared to the complexity and variability of the problem, these relationships performed well. Rothermel (1972) used these relationships as a basis, where the conservation of energy principle is applied to a fuel ahead of an advancing fire in a homogenous fuel bed (Frandsen, 1971; Rothermel, 1972). However, this equation was not analytically solvable at that moment and each term was examined separately by Rothermel who also determined experimental and analytical methods of evaluation. This resulted in Equation 19:

$$R = \frac{I_R \, \xi \, (1 + \phi_w + \phi_s)}{\rho_b \, \varepsilon \, Q_{ig}} \qquad \textbf{Equation 19}$$

where,

R = the rate (speed) of fire spread [$m\ min^{-1}$]

I_R = the rate of heat release per unit area at the front of the fire, also known as the fire reaction intensity [$(kJ\ min^{-1})\ m^{-2}$]

ξ = propagating flux ratio, which is the fraction of heat released by the flaming front and that of what is absorbed by unburned fuels ahead of the fire [-]

ϕ_w = wind factor, the effects of wind speed on the rate of fire spread

ϕ_s = slope factor, the effects of slope on the rate of fire spread

ρ_b = ovendry bulk density, or porosity of the fuel bed [$kg\ m^{-3}$]

ε = effective heating number, which is the fraction of the total fuel load that is heated to ignition temperature [-]

Q_{ig} = the heat of pre-ignition, heat required to bring a unit of fuel mass to its ignition temperature [$kJ\ kg^{-1}$]

The numerator in Equation 19 calculates the heat source by multiplying the reaction intensity with a combined factor that determines the propagation of energy. The denominator calculates the heat sink from the energy needed to ignite new fuels and the efficiency of heating those fuels. Equation 19 is a central model equation (Appendix J) and is worked out in detail in the following sections.

Reaction Intensity (I_R)

To solve Equation 19, the reaction intensity (I_R, $[(kJ\ min^{-1})\ m^{-2}]$) must be known:

$$I_R = \Gamma'\ w_n\ h\ n_M\ \eta_s \qquad \textbf{Equation 20}$$

where, Γ' is the optimum reaction velocity $[min^{-1}]$, w_n is the net fuel loading $[kg\ m^{-2}]$, h is the fuel heat content $[kJ\ kg^{-1}]$, n_M is the moisture damping coefficient [-] and η_s is the mineral damping coefficient [-]. The reaction intensity is the energy released by the fire front and is calculated by quantifying the rate in which solid organic matter is turned into a gas. Therefore it is a function of the parameters that influence this reaction speed, such as particle size, bulk density, moisture content and the chemical composition.

The optimum reaction velocity Γ' is calculated by:

$$\Gamma' = \Gamma'_{max} \left(\frac{\beta}{\beta_{op}}\ e^{(1-\frac{\beta}{\beta_{op}})} \right)^A \qquad \textbf{Equation 21}$$

where the relative packing ratio ((β/β_{op}), $[-]$) is a function of the surface-area: volume ratio (σ, $[cm^{-1}]$), oven dry load (w_O, $[kg\ m^{-2}]$), fuel bed depth (δ, $[m]$) and fuel particle density (ρ_b, $[kg\ m^{-3}]$, Equation 32) (Andrews et al., 2013) and also an arbitrary variable (A) and the maximum reaction velocity Γ'_{max} $[min^{-1}]$, that in turn is calculated from the surface-area: volume ratio.

Equation 21 predicts the reaction velocity for any combination of fuel particle size, surface-area: volume ratio and packing ratio. The relative packing ratio ((β/β_{op}), $[-]$) used in this equation is a ratio that describes how the fuel bed is packed relative to the optimum packing ratio. If the fuelbed is either too densely packed (higher than 1) or loosely packed (lower than 1) it will lower the reaction intensity. This however does not necessarily also mean a peak in spread rate and fire intensity as these factors are also depending on other variables.

The net fuel loading (w_n, $[kg\ m^{-2}]$) is calculated by:

$$w_n = w_O\ (1 - S_T)$$ **Equation 22**

where, w_O is again the oven-dry load $[kg\ m^{-2}]$ and S_T is the fuel mineral content.

The moisture damping coefficient n_M is a dimensionless fraction that accounts for the decrease in intensity caused by the combustion of fuels that contain moisture. This is done by using a ratio between the actual moisture content of the fuel and its moisture of extinction (i.e. the amount of moisture of which above a fire cannot sustain itself). The moisture damping coefficient (n_M, $[-]$ is calculated as follows:

$$n_M = 1 - 2.59\ \frac{M_f}{M_x} + 5.11\ \left(\frac{M_f}{M_x}\right)^2 - 3.52\left(\frac{M_f}{M_x}\right)^3$$ **Equation 23**

where M_f is the fraction fuel moisture content [-] and M_x is the fuel moisture of extinction [-]. In this study the value of M_f is derived from the FFMC, see Equation 12.

Not only moisture is capable of lowering the heat content, also non-combustible minerals will lower the intensity. This effect is captured in the mineral damping coefficient (η_s, $[-]$) which is a function of only the fuel effective mineral content (S_e, $[-]$) by:

$$\eta_s = 0.174\ {S_e}^{-0.19}$$ **Equation 24**

Finally when Equation 21-24 are used in Equation 20 the reaction intensity can be calculated.

Propagating Flux Ratio (ξ) and Propagating Flux ($1 + \phi_w + \phi_s$)

In Equation 19, the propagating flux is a ratio that relates the propagating flux ($1 + \phi_w + \phi_s$) to the reaction intensity (I_R). The propagating flux is needed in order to account for tilting flame effects as a result of slope and wind, as explained in Chapter 2.2.2. However the geometry of the fuel bed influences the efficiency of this heat transfer. This efficiency is captured in the propagating flux ratio by:

$$\xi = (192 + 7.9095\ \sigma)^{-1}\ e^{((0.792\ +\ 3.7597\ \sigma^{0.5})(\beta+0.1)}$$ **Equation 25**

where, σ is again the surface-area: volume ratio $[cm^{-1}]$ and β the packing ratio [-] (Wilson, 1980).

The wind factor ϕ_w and the slope factor ϕ_s represent the additional propagating flux produced by wind and slope. These coefficients are dimensionless and are functions of the wind speed, slope and fuel parameters. The metric formulation of the wind factor ϕ_w is given by Equation 26 (Wilson, 1980).

$$\phi_w\ = C(3.281\ U)^B\ (\beta/\beta_{op})^E$$ **Equation 26**

where, U is the midflame wind speed $[m\ min^{-1}]$ and β/β_{op} the relative packing ratio. C, B and E are calculated from the surface-area: volume ratio (σ) by:

$$C = 7.47\ e^{(-0.8711\ \sigma^{0.55})}$$ **Equation 27**

$$B = 0.15988\ \sigma^{0.54}$$ **Equation 28**

$$E = 0.715\ e^{-0.01094\ \sigma}$$ **Equation 29**

The midflame wind speed indicates the wind at the midpoint of the potential flame and affects the surface fire spread. This definition of height is considered difficult and it is often set to twice the fuelbed depth (Rothermel, 1972) (Albini and Baughman, 1979). To convert the 20ft wind speed to the midflame wind speed a table with Wind Adjustment Factors (WAF) can be used, see Appendix D.

The slope factor ϕ_s is easier to calculate:

$$\phi_s = 5.275\ \beta^{-0.3}\ tan(\phi)^2$$ **Equation 30**

where β [-] is the packing ratio and $\tan(\phi)$ ($vertical\ rise/horizontalrun$, $[-]$) represent the slope.

THE DENOMINATOR OF THE RATE OF SPREAD FORMULA

As explained the denominator of Equation 19 covers the factors that determine the heat sink, i.e. that have a negative effect on the spread rate. The spread rate of a fire highly depends on the ability of the adjacent fuel to burn. The amount of heat it requires to dry the adjacent fuels (heat of pre-ignition ($Q_{ig}, [kJkg^{-1}]$) is calculated by:

$$Q_{ig} = 581 + 2594\, M_f \qquad \textbf{Equation 31}$$

where M_f is the moisture content [%].

The amount of dry fuel has to be calculated in order to quantify the heat sink. This fuel particle density ($\rho_b,\ [kg\ m^{-3}]$) is calculated by:

$$\rho_b = \frac{w_O}{\delta} \qquad \textbf{Equation 32}$$

where w_O is the oven dry load $[kg\ m^{-2}]$ and δ the fuel bed depth ($\delta,\ [m]$).

Finally, it is necessary to known how efficient the heat transfer to the adjacent fuels is. The efficiency of this heating is captured in the effective heating number ε:

$$\varepsilon = e^{-4.528/\sigma} \qquad \textbf{Equation 33}$$

which is a function of the surface-area: volume ratio ($\sigma, [-]$) .

When the outcomes of Equation 20, 25, 26, 30, 32 and 33 are substituted in Equation 19, it is possible to calculate the spread rate of a fire in $[m\ min^{-1}]$. This spread rate is a very important factor in the danger an actual forest fire brings. It is important to realize that this model has been developed for predicting the rate of spread in a continuous stratum of fuel on the surface, which is not always the case in spatially varying vegetation. Therefore this spread rate value should be regarded as a mean value for the given conditions of wind and slope, rather than an exact figure. It also estimates the fire behavior parameters in a worst case scenario, i.e. a wind driven fire that travels upslope.

Another important factor in forest fire danger is the fire intensity, hence the fact that while a fire may spread quickly their fuel load and thus intensity can be low, e.g. grass land fires. In this case the related danger is relatively low.

This fire intensity (I_R, $[(kJ\ min^{-1})\ m^{-2}]$) calculated by Equation 20 is considered difficult to understand as it depends on both time and area. Therefore the Byram's fireline intensity (I_B, $[(kW\ m^{-1}]$) has been introduced.

$$I_B = \frac{1}{60}\ I_R\ R\ \frac{12.6}{\sigma}$$ **Equation 34**

This equation uses the reaction intensity (I_R), the rate of spread (R) and the surface-area: volume ratio (σ) to estimate the released energy per meter of fire front:

The third important parameter for fire behavior is the flame length. This is important for both the firefighting strategy as for crown fire initiation, as the distance between the height of the crown base and the length of the flames (measured from the ground) is a crucial criterion for the intensity in the forest canopy (Van Wagner, 1976). From the Byram's fireline intensity (I_B) the flame length ($L_f, [m]$) can easily by calculated:

$$L_f = 0.0775\ {I_B}^{0.46}$$ **Equation 35**

4.2 DATA COLLECTION

A database with a range of different parameters was needed for model input but also for calibrating and validating the model. This data is either acquired from literature, a meteostation in the area or a 10-day fieldwork period in the study area. The main goal of the fieldwork period was to obtain spatial and temporal varying data for calibration and validation of the model. The field data was acquired between the 27th of August and 8th of September in the La Peyne catchment, see chapter 3. This section first discusses the working methodology of the data that is acquired from literature and second the working methodology of the field and laboratory data.

4.2.1 DATA FROM LITERATURE AND METHODOLOGY

Most of the model inputs were selected from literature, already existing databases or the meteostation in the area. This chapter discusses how the data originating from literature was processed and used.

THE VEGETATION MODEL

Some of the fuel parameters are linked to a single vegetation type, this includes the fuel loading, fuelbed depth, moisture of extinction, packing ratio, etc. However, also the drying of the fuels described in the FFMC has a vegetation depending parameter in terms of shading. As explained in chapter 2.2.1 the focus during classification is mainly on factors that determine the intensity and rate of spread rather than on discriminating between single vegetation species. Moreover, the mapping of Mediterranean vegetation species by means of imaging spectroscopy or linear spectral unmixing is considered possible, but with large uncertainties of respectively 9-52% and 23-32% (Doelman, 2012). Therefore also in this study the vegetation is grouped, more specifically the vegetation is grouped on height and fuel loading.

For the study area a classified vegetation map is available in the form of an Ancillary Data Classification Model (ADCM) based on 2003 HyMap imagery made by Sluiter (2005). An ADCM aims at including non-spectral information in the classification process of earth observation image classification. This additional, so called ancillary, information may consists of elevation, aspect, soil type, topographical information, etc. Often relations exists between this ancillary data and the vegetation types. The classification model is therefore only able to compare the spectral data to classes that are likely to be present in an area with a certain environmental setting. Due to errors that arose from automatic classification and GPS accuracy the statistics calculated by Sluiter (2005) are relatively low at 51%. However visual interpretation of the results indicates that the ecological patterns are well resolved and that the accuracy results may in fact be much better that 51% (Sluiter, 2005). It was therefore chosen to also use this vegetation model in this study and reduce the 18 classes (14 vegetation, 4 land use) to 8 classes (4 vegetation, 4 land use), see Table 2.

This reclassification was done to reduce the large number of units present on the vegetation map. The reclassified vegetation map is included in Appendix A.

Reclassified vegetation model		ADCM (Sluiter, 2005)	
1	Dense matorral	**1**	Riparian vegetation
		2	Dense matorral
2	Coniferous forest	**3**	Coniferous forest
3	Middle matorral	**4**	Scattered Pinus species with conifers
		5	Scattered Quercus ilex with Cistus species
		6	Scattered Quercus ilex without dominant species
		7	Middle matorral dominated by Quercus coccifera
		8	Middle matorral dominated by Erica arborea
		9	Middle matorral dominated by pioneer species
		10	Middle matorral without dominating species
4	Low matorral	**11**	Low matorral dominated by Ulex parviflorus
		12	Low matorral dominated by grass and herbs
		13	Low matorral dominated by Cistus species
		14	Low matorral dominated by grass and herbs on erosive soils
5	Water	**15**	Water
6	Vineyards and other agricultural	**16**	Vineyards and other agricultural
7	Roads and tracks	**17**	Roads and tracks
8	Built-up	**18**	Built-up

Table 2. The ADCM map reclassification of the 18 classes by Sluiter (2005) to the 8 used in this study.

In Table 2 the dense matorral (tall matorral) corresponds to shrubs that grow between 2 and 5m high, with little undergrowth due to the closed canopy. The French name for these tall shrubs is *Maquis*. Due to the unfavorable (dry) climatic conditions in the area the organic decomposition in these shrubs is low and there is a lot of ground and standing litter (Doelman, 2012). This results in a very high fuel load which in case of a fire is difficult to reach on ground, see Figure 4-5. Dense matorral covers 41% of the total land area in the study area.

Coniferous forest is also present in the area as a timber plantation in the south east, but covers less than 3% of the total land area. These Mediterranean pine species are notorious for their crown fire risk and form a high danger for fire management (Dimitrakopoulos et al., 2007). In case of a crown fire the intensities and flame lengths can be so extreme that the turbulence complicates aerial approaches (Pollet and Brown, 2007). During the fieldwork it was found that the coniferous forest was thinned by cutting approximately a third of the stands, see Figure 4-6. This lowers the crown fire potential but the forestry activity (temporary) raised surface fire fuel loads as the branches and needles did not leave the area.

Figure 4-5. Dense matorral showing the ground and standing litter that is often abundantly present in this vegetation.

Figure 4-6. A thinned conifer forest as found within the study area. Approximately a third of the trees were removed.

Middle matorral is often a discontinued mixture of shrubs called *garrigue* in French and consists of shrubs between a 0.5 and 2m (Doelman, 2012). Their fuel load is considerable lower than that of dense matorral but there is also a lot of ground and standing litter present, see Figure 4-7. The scattered classes (13.4% of total land area) were added to middle matorral class as they form an intermediate fuel between dense matorral/ conifer forest and often low matorral. The total middle matorral class covers 32% of the total study area.

Low matorral is a very sparse vegetation that has many areas with (almost) bare rocks or soil, their French name is *Landes*. Its height is defined as less than 0.5m and it covers 7% of the total area. A typical sight is provided in Figure 4-8.

Figure 4-7. Middle matorral, in this photograph about 1.5m tall.

Figure 4-8. Low matorral, consisting mainly of grass and sparse shrubs.

The other classes are land use classes (water, vineyards and other agricultural, roads and tracks and built-up), for obvious reasons water, roads and tracks and built-up cannot be included in the FFMC nor in the BEHAVE model and are only included as an easy reference for the maps. This is a normal procedure in forest fire models (Scott and Burgan, 2005). Vineyards and other agricultural is a class that is also not included. Although it is possible that this class catches fire in some cases (olive trees, cereals and grass) there is often almost no dead fuel present or the land is kept in a non-combustible condition by irrigation. If for example cereals are allowed to cure before harvest a grass fuel model should be used but this would require the yearly mapping of crops in the area (Scott and Burgan, 2005). This is not within the scope of this study.

VEGETATION RELATED PARAMETERS

Scott and Burgan (2005) extended the original 13 fuel models of Rothermel by another 40 models. These 40 'new' models include several fuel models that are explicitly made for dry climate shrubs. During the fieldwork period each of the 4 vegetation classes as described in Table 2 will be assigned an unique fuel model.

Each fuel model has related parameters that are used as input for the BEHAVE model and can be found in the 53 models. These include the fuel load (w_O), surface-area: volume ratio (σ), fuel bed depth (δ), dead fuel moisture of extinction(M_x), packing ratio (β) and relative packing ratio (β/β_{op}) .

Technically a fuel model includes all fuel inputs of the Rothermel surface spread model, but several inputs are very constant between fuel types and/or have little influence. These constant inputs were quantified by Rothermel (1972) and Albini (1976) and reconfirmed by Scott and Burgan (2005). For all fuel models it holds that the total mineral content (S_T) is 5.55 percent, the effective (silica-free) mineral content (S_e) is 1.00 percent and the ovendry fuel particle density (ρ_b) is 513 $kg\ m^{-3}$.

4.2.2 Field and Laboratory Data and Methodology

To do quantitative evaluation of the model outputs, 14 plots were selected of which the relative humidity, fuel temperature, cloud-cover and moisture content were measured daily over a 10 day period. These plots are illustrated in Figure 4-9. These 14 plots were selected by their vegetation class (5 dense, 3 middle, 3 low matorral and 3 coniferous forest) and different land surface geometry (altitude, slope and aspect). Moreover, the plots needed to be relatively easy accessible as it is important to take samples around solar-noon. Without this limitation the total daily sampling time would be further removed from solar-noon and could include erroneous values. The Digital Elevation Model (DEM) (Figure 4-9) had the lowest resolution (25m) of all maps and therefore the model was run at this pixel size.

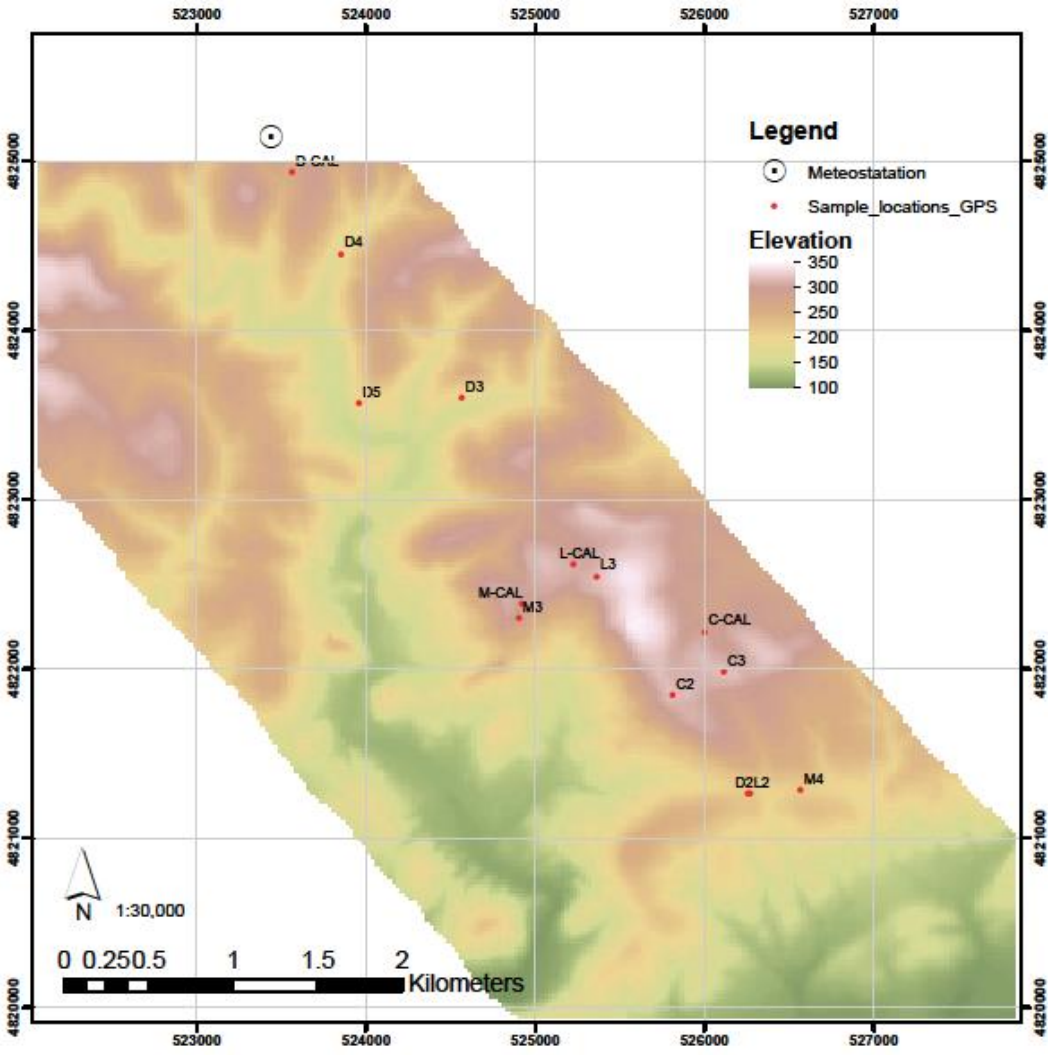

Figure 4-9. The digital elevation model (DEM) of the study area with the 14 sampling locations and the location of the meteo station in the north-west.

METEOROLOGICAL DATA

The meteo station owned by the Utrecht University is located in the neighborhood of Le Mas Castel (31T 0523440, 4825138) at an altitude of 282m, see Figure 4-9. This station was used to map the meteorological inputs of the FFMC model, namely the relative humidity (H), wind speed (W) or (U in the BEHAVE model), the temperature (T), solar radiation (R) and rainfall (r_0), the accuracy is listed in Table 3.

Sensor:	Device Type	Units	Accuracy
Temperature (T),	S-TMB-M006	°C	+/- 0.21°C from 0° to 50°C
Relative humidity (H)	S-THB-MOOx	%	+/- 2.5% from 10% to 90% RH
Wind speed (W)	S-WCA-M003	$m\ s^{-1}$	0.5 $m\ s^{-1}$
Solar Radiation (R)	S-LIB-M003	$w\ m^{-2}$	10 $w\ m^{-2}$
Rainfall (r_0)	-	$1.96\ mm\ count^{-1}$	-

Table 3. The different sensors of the Le Mas Castel meteo station, their units and their accuracy.

RAINFALL

The rainfall in this part of the Mediterranean is known to show large spatial differences and rain events often have a local nature. However there is only one meteostation available in the area and it is assumed that within a 5km radius with a maximal 180m vertical distance is small enough to assume equal values for rainfall throughout the area.

TEMPERATURE AND RELATIVE HUMIDITY

The altitude of the meteostation is 282m, while the elevation of the study area varies from 100 to 342m (see Figure 4-9). This height difference has influence on the (vertical) temperature and relative humidity distribution. A linear lapse rate for temperature is commonly used in hydrologic and terrestrial models and is therefore introduced into the model. The average environmental lapse rate was set to $-6.5\ C^{\circ}\ (1000m)^{-1}$ (Blandford, et al., 2008). A 2001 digital elevation model by the Institut National de l'Information Géographique et Forestière was available in the archive of Utrecht University.

A (linear) lapse rate for relative humidity does not exist and requires a more difficult approach. The definition of relative humidity (H) is as follows:

$$H = \frac{e_w}{e^*_w} \cdot 100\% \qquad \textbf{Equation 36}$$

where, e_w is the partial pressure of water vapor and e^*_w is the saturated vapor pressure of water at a given temperature. Partial vapor pressure (e_w), the amount of moisture that is in the air at a given temperature, is in relation with the dewpoint temperature $(T_d, [°C])$ by (NOAA, 2013):

$$e_w = 6.11 \cdot 10^{\frac{7.5\,T_d}{237.7+\,T_d}} \qquad \textbf{Equation 37}$$

The saturation vapor pressure e^*_w, the maximum amount of water vapor that air can hold at a given temperature relates only to that temperature $(T, [°C])$ by the same relation (NOAA, 2013):

$$e^*_w = 6.11 \cdot 10^{\frac{7.5\,T}{237.7+\,T}} \qquad \textbf{Equation 38}$$

Dewpoint temperature (T_d) is not measured at the meteostation but can be calculated (for the meteostation), with the know relative humidity and temperature, by Equation 39.

$$T_d = \frac{b\,\gamma(T,H)}{a - \gamma(T,H)} \qquad \textbf{Equation 39}$$

where,

$$\gamma(T,H) = \frac{a\,T}{b+T} + \ln\frac{H}{100} \qquad \textbf{Equation 40}$$

where the dewpoint temperature (at the meteostation) (T_d) and temperature (T) are in °C, relative humidity (H) in %, constant $a = 17.625$ and constant $b = 234.04$ °C. This relation is based on the August-Roche-Magnus approximation for the saturation vapor pressure of water in air as a function of temperature and is considered valid for the temperature range found in the study area (Blandford et al., 2008). A commonly used linear vertical distribution relation for the dewpoint temperature (T_d) is $-2.73\ C^{\circ}\ (1000m)^{-1}$, which allows the calculation of the elevation depended relative humidity (H) by Equation 36-40. Note that both the temperature as the relative humidity were also adjusted for solar radiation, see chapter 4.1.2.

The solar heating described in Chapter 4.1.2 is incorporated in the FFMC model by Equation 13 to account for the considerable solar heating of fuels by the sun. The required solar radiation I [$W\ m^{-2}$] was measured by a horizontal orientated pyranometer in the meteostation. However this solar radiation is also strongly depending on the slope and aspect for non-horizontally orientated surfaces (Rothermel et al., 1986), see Figure 4-10. A solution for this by Buffie and Beckman (2013) starts by calculating the ratio of beam radiation on a titled surface to that on a horizontal surface. This ratio or geometric factor R_b represents the ratio between the cosine of the angle of incidence θ, the angle between the solar radiation on a surface and the normal to that surface, and the cosine of the zenith angle θ_z, the angle between the vertical and the line to the sun:

$$R_b = \frac{\cos\theta}{\cos\theta_z} \qquad \textbf{Equation 41}$$

The calculations of the angle of incidence and the zenith angle are elaborate due to the geometric complexity of the problem and are only briefly described here.

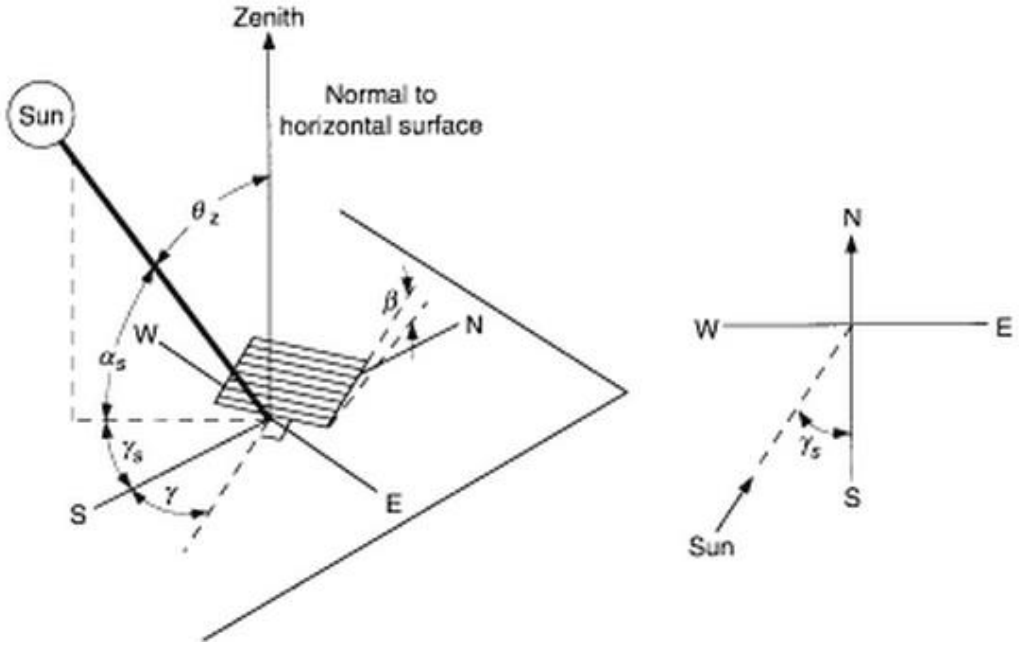

Figure 4-10. The image to the left shows the zenith angle, slope, surface azimuth angle and solar azimuth angle for a titled surface. The image to the right shows the solar azimuth angle (Duffie & Beckman, 2013).

The cosine of the angle of incidence is calculated by: (Duffie and Beckman, 2013)

$$\begin{aligned}\cos\theta = \ & \sin\delta\sin\phi\cos\beta \\ & -\sin\delta\cos\phi\sin\beta\cos\gamma \\ & +\cos\delta\cos\phi\cos\beta\cos\omega \\ & +\cos\delta\sin\phi\sin\beta\cos\gamma\cos\omega \\ & +\cos\delta\sin\beta\sin\gamma\sin\omega\end{aligned}$$

Equation 42

The zenith angle by:

$$\cos\theta_z = \cos(\phi-\beta)\cos\delta\cos\omega + \sin(\phi-\beta)\sin\delta$$

Equation 43

where δ is the declination angle (the angular position at solar noon with respect to the equator, depends on the time of the year), ϕ is the latitude (43.55° for the study area), β the angle of the slope, γ the surface azimuth angle (the deviation of the projection on a horizontal plane of the normal to the surface from the local meridian, where the south is zero) and ω the hour angle (the angular displacement of the sun due to the rotation of the earth), all in degrees. When the ratio R_b is multiplied by the measured horizontal plane radiation this results in an appropriate value for the solar radiation on a surface with a given slope, aspect and latitude at that moment of the day and year.

The use of R_b and measured radiance avoids the problem of estimating cloud cover as it is already included in the radiation measurements (assuming equal distribution). However vegetation shading/transmittance must still be accounted for, see chapter 4.1.2.

In tall multistory vegetation the canopy causes shading on the surface fuels. In this study this is the case in the conifer and dense matorral vegetation types. The amount of vegetation shading was estimated by using upward hemispherical photographs that were analyzed using the Gap Light Analyzer (GLA) developed by the Simon Fraser University, Institute of Ecosystem Studies. As only the total plant cover is of interest here the process is relatively easy and reports the shading caused by vegetation in that location. In the middle and low matorral classes there are no trees present and therefore the canopy cover is often set at zero in these single story vegetation types (Salis, 2007). Moreover, downward hemispherical photography under sunny illuminated conditions results in poor canopy cover estimates (Demarez et al., 2008). A canopy cover fraction of zero relates to the total amount of available solar radiation reaching the surface fuels.

The solar radiation corrected to the topography and shading of vegetation is used in Equation 13.

Figure 4-11. An example of hemispherical photograph used to estimate the vegetation cover (shading) before processing.

MOISTURE SAMPLING

From the different 1m^2 sampling plots for the calibration plots or a wider area for normal plots, a daily fuel sample was collected that contained a realistic representation of the fuels present. This included all litter, sticks and other dead material that was disconnected from the vegetation as described by the official fuel collecting method of the United States Forest Service (Pollet and Brown, 2007). The fine fuel samples taken from the plots were put into air tight plastic zipbags and weighed immediately on a scale with a precision of 0.01 grams. The standard deviation of the zipbags was smaller than the precision of the scale and the weight was therefore considered equal for each bag.

Before the oven drying the aluminum containers were weighed as there was significant difference in weight with a standard deviation of 0.03 grams. The samples were transferred from the zipbags to the aluminum containers and the zipbag was cleaned with a brush. The method by Pollet prescribes at least 24 hours of drying at 105 °C, however the fuel samples in this study needed 72 hours of drying at 105 °C to reach a stabilized weight. After the oven drying the samples were weighed again and the moisture content was calculated by:

$$\frac{\left(\begin{matrix}Wet\ weight\ of\ sample\\ -Weight\ ZipBag\end{matrix}\right)-\left(\begin{matrix}Dry\ weight\ of\ sample\\ -Weight\ Container\end{matrix}\right)}{(Dry\ weight\ of\ sample-Weight\ Container)}*100\%=percent\ moisture\ content \qquad \textbf{Equation 44}$$

These moisture content values were used to calibrate and validate the model.

4.3 Model Calibration and Validation

Numerous studies have indicated the importance of calibrating the FFMC model to the applied vegetation and also the BEHAVE model allows custom fuel models for vegetation types that are not included. This supports the necessity for calibration and an objective way of validating the results. The method that was used for calibration of the FFMC is discussed first. After that it is explained why calibration and validation of the BEHAVE model is not included within this study and how uncertainties in the FFMC propagate through the BEHAVE model.

4.3.1 FFMC Model

The standard FFMC model does not account for different vegetation types and also the adjustments described in chapter 4.1.2 only affect radiation parameters (Rothermel et al., 1986). However more differences can be expected due to processes related to the presence of a thicker (and thus wetter) organic layer under dense vegetation, different amounts of canopy interception, different wind influences like those described in the BEHAVE model or even almost complete sheltering from most winds by an overstory canopy. Wotton and Beverly (2007) also state that stand density, seasonality and forest type have influence on the relationship between the FFMC and observed litter moisture. To account for these different relationships they provide a list of models that relate the forest type, density, season and the calculated FFMC value to observed values. It must be noted that this method of adjusting the FFMC end-result to observed values is not differentiating between different drying and wetting rates nor does it allow for differences in wetting by rain or higher relative humidity.

It easy to incorporate the effects induced by different vegetation types by using the existing vegetation map. A calibration study was added that adjusts the way the FFMC was calculated for each of the four vegetation types. Calibration of the FFMC was done by either multiplying the log drying rate, the log wetting rate (both Equation 4), the equilibrium moisture content equations (Equation 5 and Equation 6) or the rain input (Equation 11), or a combination, by a factor to be determined from the observed moisture values. This way the FFMC model is calibrated with respect to non-equal changes in drying and wetting rates.

Calibration is only useful when there is contrast in the data (note that prediction of a value that is constant over time tells little about the overall model predictions), therefore a strong change in observed and modeled moisture contents is helpful. This can be achieved by natural fluctuations in relative humidity or a natural rainfall event, but as the Mediterranean is known for its summer-drought it was chosen to simulate a rainfall event.

For each vegetation type several representative $1m^2$ plots were selected based on their elevation and slope and carefully watered with 11L on day two of the fieldwork. The geometric requirements on this plot selection were used to reduce the chance of errors in the extrapolation of the meteo station data, so all of the calibration plots had a slope of less than 10° and a elevation within 20m of the meteo station elevation. By using these limitations the influence of aspect, slope and elevation accumulated in a maximal error of less than 1% modeled moisture content. To avoid specific local conditions (such as

shading) the multiple plots of one vegetation type were sampled together into one moisture content sample as described in the Fuel Moisture Sampling Guide (Pollet and Brown, 2007). For dense matorral this was done with three $1m^2$ plots and for conifer and middle matorral two plots were used. In the case of low matorral it was found to be impossible to collect enough fine fuels from multiple plots and a simulated rainfall event of that vegetation type is therefore not included. The locations of the calibration plots are illustrated in Figure 4-9 as D-CAL, C-CAL and M-CAL.

Figure 4-12. A 11mm rainfall event was simulated on a $1m^2$ meter plot of in this case the dense matorral forest floor.

FFMC model validation was done by calculating the 95%-confidence interval from the model and observed data and assuming a normal distribution in moisture content. The 95%-confidence interval provides a range of values which is likely to contain the observed moisture content. This means that if more samples (subsequent time steps) are taken on other occasions and interval estimates are made on each of these occasions the observed value is between these two values in 95% of the cases. An interval of 95% is the value most often used. It is calculated by calculating the absolute error between the observed data and the modeled data. From this data the mean and standard deviation is determined. Next the 95% confidence interval of the error can be calculated by:

$$\bar{x} \pm Z^* \left(\frac{\sigma}{\sqrt{n}}\right) = Confidence\ Interval \qquad \textbf{Equation 45}$$

where $\bar{x}$ is the sample mean, Z^* the critical value for the standard distribution (for CI 95% it is 1.96), σ the standard deviation and n the sample size. This returns two values, the upper and lower limit of the 95% confidence intervals of the error. This uncertainty is assumed constant and added to the model output. Note that a small confidence interval means that the model estimates the observed value well.

4.3.2 BEHAVE MODEL

For the BEHAVE model it is not possible to include a calibration or validation part within the scope of this study as this would require substantial analysis of the model parameters as discussed in chapter 4.1.3 and field experiments that simulate a forest fire. However the BEHAVE model has validated itself in numerous other studies (Rothermel et al., 1986; Pastor et al., 2003), including those carried out in arid regions (Grabner et al., 1997) and Mediterranean forests in Europe (Dimitrakopoulos and Dritsa, 2003). Moreover, it is in operational use by the US forest service and other agencies worldwide.

It is possible to calculate the effects of the uncertainties related to the FFMC model on the BEHAVE model using the 95%-confidence intervals described in chapter 4.3.1. Using the boundary values of the 95% confidence interval to calculate the effect of the propagating error on the range of BEHAVE parameters. This approach starts with the fine fuel moisture content entering the BEHAVE model in Equation 23 that in turn is used to calculate the reaction intensity (I_R). This reaction term is again used to calculate the three main forest fire danger parameters; rate of spread R, fireline intensity I_B and flame length L_f. This quantifies the effect on the fire behavior predictions due to the error in the FFMC estimations.

5 RESULTS

This section provides an overview of all the acquired data and model and model validation results. First, the model inputs and fieldwork results are presented. Next the FFMC and BEHAVE model outcomes are described and shown in both graph and map form. Furthermore the accuracy of the model data is accessed as well as the influence of that accuracy on the model results.

5.1 MODEL INPUTS AND FIELDWORK RESULTS

This section bullet-wise presents the results that were used as model inputs and for calibration and validation. This data originates from both fieldwork and literature.

- METEO STATION DATA

In the period between June 1, 2013 and September 8, 2013 the data-logger of the meteo station measured a mean temperature of 25.6 °C, mean relative humidity of 54 %, solar radiation averaged at 666 $W\ m^{-2}$ and a mean windspeed of 3 $m\ s^{-1}$. Only two rainfall events were recorded, one around June 8 and one on August 8. The fieldwork period was relatively warmer (26.5 °C) and drier (RH = 39%, no rain), with a slightly lower solar radiation (600 $W\ m^{-2}$) and windspeed (2.56 $m\ s^{-1}$). The complete meteorological results are graphically included in Appendix E.

- FUEL MOISTURE

In total, 140 fuel moisture samples were taken from 14 locations (see Figure 4-9 and Appendix H) during a 10 day period from August 27, 2013 and September 6, 2013. In Figure 5-1 the average fuel moisture contents per vegetation class are provided, this data will be used for validation. It is clearly visible that each vegetation class has its own specific fuel moisture content average. The almost completely shaded dead fuels found in the dense matorral contained the highest average amount of moisture (10.5%) while the exposed fuels found in the low matorral only contained half of that moisture content (5.5%).

The temporal differences in moisture contents show a high similarity with the relative humidity and temperature (Figure 5-1). This makes sense as the moisture content calculated with Equation 7 mainly depends on the relative humidity and fuel temperature. Moreover, during the fieldwork period, the relative humidity and temperature describe more or less identical (opposite) behavior while the wind speed was low, this results in very effective drying. The trends in moisture content starts and ends with relatively low temperatures and high relative humidity values and are therefore also higher than the warm and dry time in-between (Figure 5-1). The relative humidity data during the fieldwork period is provided in Figure 5-5.

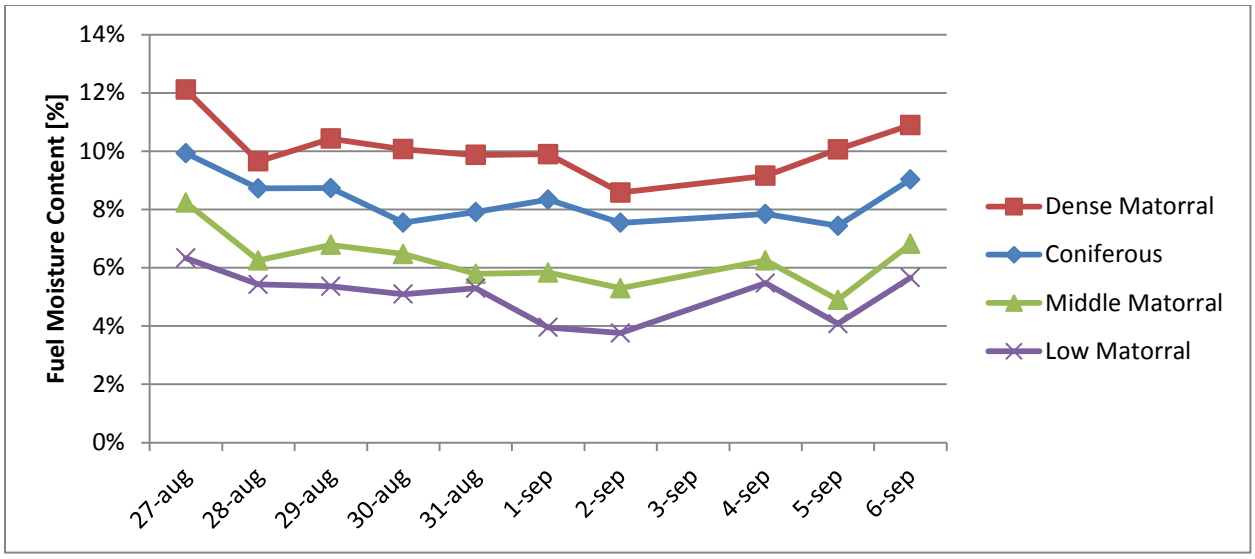

Figure 5-1. The average vegetation class fuel moisture content over time as measured in the study area (excluding the D-cal, C-Cal and M-Cal plots). It is clearly visible that each vegetation class fluctuates around a different average but that they show the same trends.

The simulated 11 mm rainfall event has a clear effect on the fuel moisture content (Figure 5-2). For L-CAL it was not possible to find enough fine dead fuels in $1m^2$ plots and therefore no rainfall event was simulated. The topography and shading of the D-Cal plot allowed only for limited drying and therefore a slow drying curve.

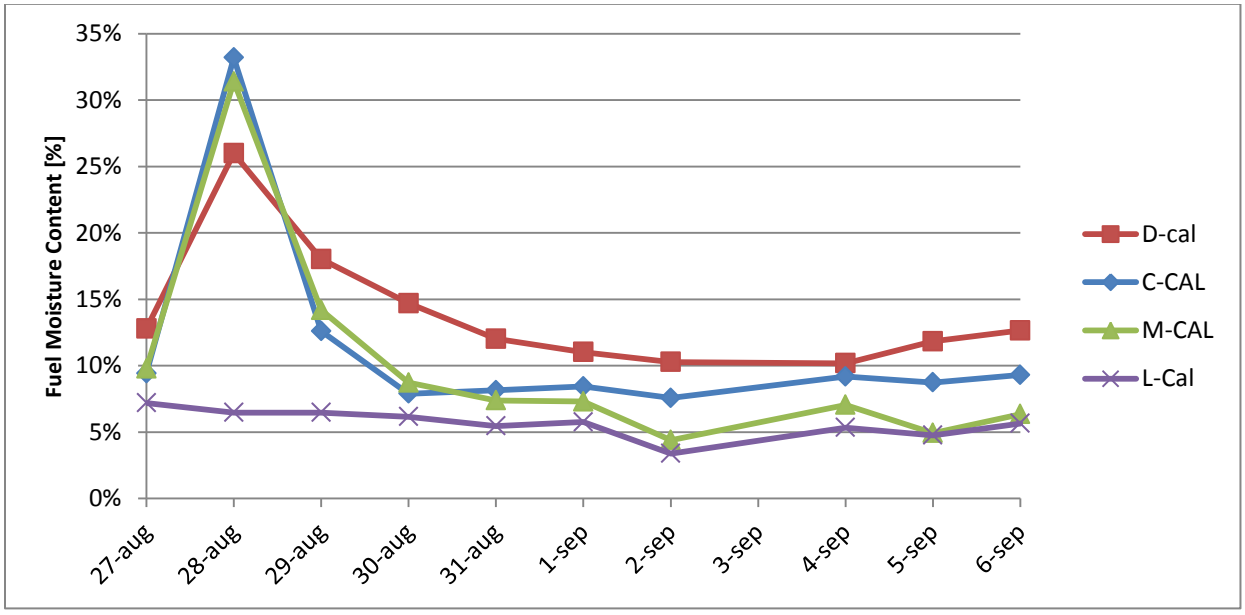

Figure 5-2. The fuel moisture content for the four calibration sites. The effect of the 11mm rainfall event on August 28 is clearly visible in the D-cal, C-cal and M-cal.

The warm and aerated coniferous and middle matorral plots only showed rainfall related effects for 2-3 days. This means that small and single summer rainfall events bring only short term relief to fire hazard. This is due to high surface to volume ratio of fine surface fuels which, with rapidly changing environmental conditions only reflect the weather conditions over the past three days (De Groot, 1987).

- FUEL MODELS

For each of the 14 plots the fuel model was determined and the four vegetation types were easily assigned to the same group of four fuel models without exceptions. In the table below, the related fuel model and description by Scott and Burgan (2005) of each vegetation type is provided. The matorral classes corresponded well to fuel models described here. The coniferous forest however was thinned by approximately a third of the trees, see Figure 4-6 and Figure 4-11. The litter that was caused by this forestry activity is several times more than what would be present on the surface of a normal coniferous forest. The coniferous forest is therefore classified as a so-called activity fuel model.

Vegetation type	Fuel Model
Dense Matorral	**SH7 – Very high load, dry climate shrub** The primary carrier of fire in SH7 is woody shrubs and shrub litter. Very heavy shrub load, fuelbed depth up to 1.8m. Spread rate is high and flame length is very high.
Middle Matorral	**SH2 – Moderate load, dry climate shrub** The primary carrier of fire in SH2 is woody shrubs and shrub litter. Moderate fuel load, fuelbed depth about 0.3m, no grass fuel present. Spread rate is low, flame length low.
Low Matorral	**SH1 – Low load, dry climate shrubs** The primary carrier of fire in SH1 is woody shrubs and shrub litter. Low shrub fuel load, fuelbed depth about 0.3m; some grass is present. Spread rate and flame length are both very low.
Coniferous	**SB3 – High load activity fuel or moderate load blowdown** The primary carrier of fire in SB3 is heavy dead and down activity fuel or moderate blowdown. Fine fuel load is 1.6 – 2.7 $kg\ m^{-2}$ and the fuel bed depth is more than 0.3m. Blowdown is moderate, trees compacted to near the ground. Spread rate and flame length are both high.

Table 4. The four vegetation types and related fuel models by Scott and Burgan (2005). For each fuel model the description is provided.

- SAMPLE TIME, INFRARED TEMPERATURE, RELATIVE HUMIDITY AND CLOUD COVER

The time, infrared temperature in sun and shade, relative humidity and cloud cover were noted for each sample. Appendix F provides all these results per sample plot and day. The results for the infrared temperature as measured in the sun were very high, up to 58 °C. These high values were all found in open areas that were shielded from the wind. There is no reason to assume that these values are erroneous.

- WIND ADJUSTMENT FACTOR, SHADING FACTOR AND FUEL DEPENDENT PARAMETERS

The fuel models of Scott and Burgan (2005) have related fuel dependent parameters that strongly relate to the type of vegetation. These are needed as input for the BEHAVE model. Additionally, for each of the four fuel models the wind adjustment factor was calculated, so that the measured wind speed by the meteostation is corrected for the amount of sheltering of the specific fuel type. By using hemispherical photographs and data from literature also the amount of shading is determined. All these values are presented per vegetation type in the table below.

Vegetation type	Fine fuel load [kg/m2]	SAV [cm-1]	Packing ratio [-]	Extinction moisture [%]	relative packing ratio [-]	heat content [kj/kg]	fuels depth [cm]	WAF [-]	Shade [-]
Dense Matorral	1.551	40.45	0.00344	15	0.350	18608	182.88	0.1	0.8
Coniferous	1.236	63.48	0.01345	25	1.974	18608	36.576	0.2	0.7
Middle Matorral	1.169	54.86	0.01198	15	1.560	18608	30.48	0.4	0.3
Low Matorral	0.382	54.92	0.00280	15	0.365	18608	30.48	0.5	0.1

Table 5. The vegetation types and the related vegetation dependent fuel model parameters.

5.2 Model Results

This chapter presents the results of the FFMC and BEHAVE model runs, furthermore the measure of uncertainty related to the FFMC model was determined.

5.2.1 FFMC Model Results

The fuel moisture content is subject to both spatial and temporal variations. The spatial variation is mainly influenced by slope, elevation, aspect and vegetation dependent parameters but are often relatively similar within one vegetation type. The FFMC model results are therefore analyzed for temporal variations within the 14 plots and next a spatial overview is provided.

When the uncalibrated FFMC model outputs are compared to the observed data the moisture content trend corresponds well. However the width of the 95% confidence interval (further referred to as CI 95%) varied substantially from one sample plot to another and even more between vegetation types, see Table 7. The uncalibrated model preformed best in the dense matorral with an average CI 95% of 4.9% while the results in low matorral plots were poor with CI 95% of 11.4%, with a respective average moisture content of 10.5% en 5.5%. This high error to value ratio for especially the lower vegetation types and the indications found in literature (see chapter 4.3) supports the need for calibration.

FFMC model calibration was performed by curve-fitting the model-outputs to the observed values. The required factors that were added (includes operations of addition and multiplication) are shown here:

	Log drying rate (Equation 4)	Log wetting rate (Equation 4)	EMC-drying (Equation 5)	EMC-wetting (Equation 6)	Rain input (Equation 11)
Arithmetic Operation:	x	x	+	+	x
D-Cal	0.45	-			0.29
C-Cal	1.1	-	-2.0	-2.0	1.2
M-Cal		-	-2.5	-2.5	
L-Cal	-	-	-5.0	-5.0	-

Table 6. The factors that were used for calibration of the FFMC model with their respective arithmetic operation.

Both in the coniferous and the dense matorral plots the log drying rate and rain input needed to be adjusted. In the dense matorral plot the standard FFMC model underestimated the log drying rate with a factor two and overestimated the effect of rain with a factor of three, while the opposed effects (although smaller) were found in the coniferous vegetation. The trend observed in M-cal was very similar to the modeled trend and needed no adjustments in the calculation of drying and wetting. However, like C-cal and L-Cal, M-cal showed an overestimation of the overall moisture content trend by

several percent. This overestimation cannot be attributed to wrong rates of drying or wetting nor to wrong estimations of rain input as this showed constant behavior. This overestimation was removed by lowering the equilibrium moisture contents by a constant factor. Due to the lack of a (simulated) rainfall event in the low matorral it was not possible to find a significant trend in order to adjust the log rates or input of rain to the observed values. Moreover, it was found impossible to adjust the log wetting rate as large differences in relative humidity and temperature were absent during the fieldwork period.

Sample Plot	Uncalibrated 95% Confidence Interval Width	Calibrated 95% Confidence Interval Width
D-Cal	7.9%	3.7%
D2	2.9%	3.2%
D3	5.3%	5.6%
D4	4.3%	4.7%
D5	4.3%	4.2%
C-Cal	6.4%	3.8%
C2	6.2%	4.0%
C3	7.8%	3.8%
M-Cal	7.3%	2.8%
M3	12.3%	7.3%
M4	8.4%	3.5%
L-Cal	11.2%	3.3%
L2	11.4%	4.9%
L3	11.7%	4.9%
Average:	7.7%	4.3%

Table 7. The uncalibrated 95% confidence interval width for each of the 14 sample plots. The simulated rainfall event is included in the model for D-Cal, C-Cal and M-Cal.

The effect of calibration on the CI 95% is distinct as illustrated in the four calibration plots shown in Figure 5-4 and the quantified percentages in Table 7. The average interval width is almost decreased by half (from 7.7% to 4.3%), where the biggest benefit is observed in the open vegetation types of low and middle matorral. Considering the D-Cal, C-Cal and L-Cal plots the correlation between the observed and calibrated FFMC data is especially good in the first 7 days and shows a CI 95% of respectively 1.1%, 3.3% and 2.8%. After 7 days the observed moisture increases and the model is not capable of imitating this increase (Figure 5-4). As this effect is local and the model does not follow this trend at all the problem is likely to be found in the model input. With the meteorological data collected with each sample it is possible to verify the meteostation data and its extrapolation. The temperature in both the sample data (wet bulb and IR temperatures) and the meteostation data (air temperature) shows a relatively similar trend with a slight increase in the first days of the fieldwork period and constant behavior over the remaining period.

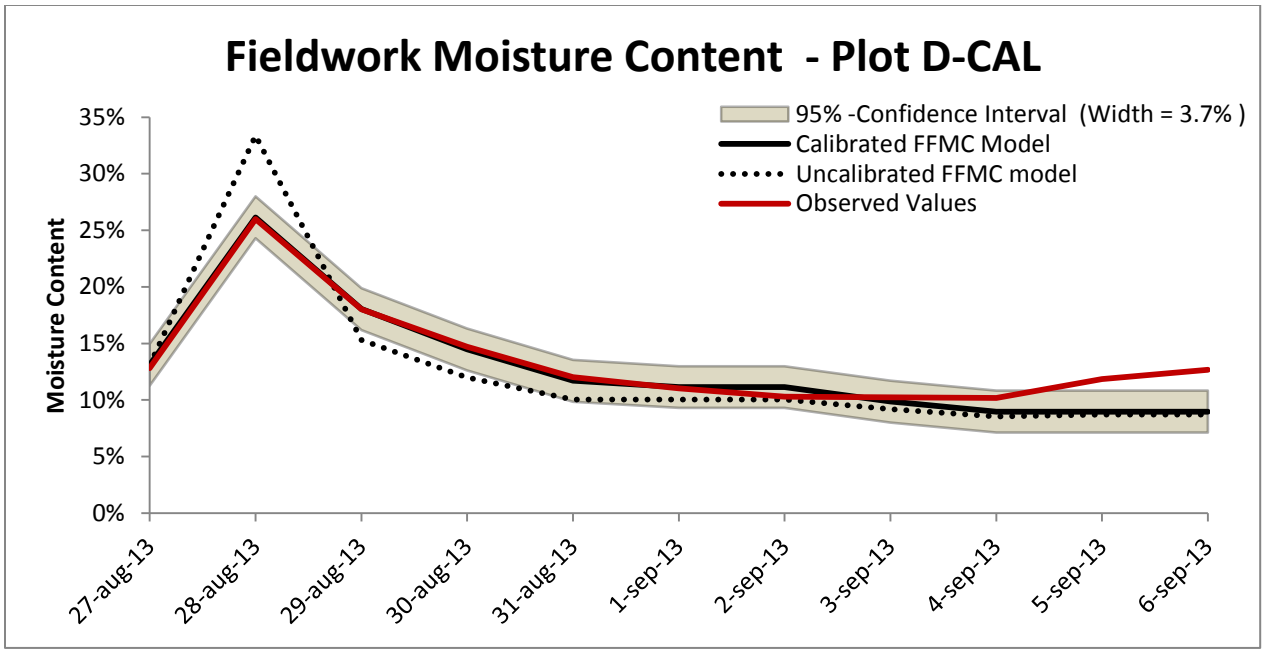

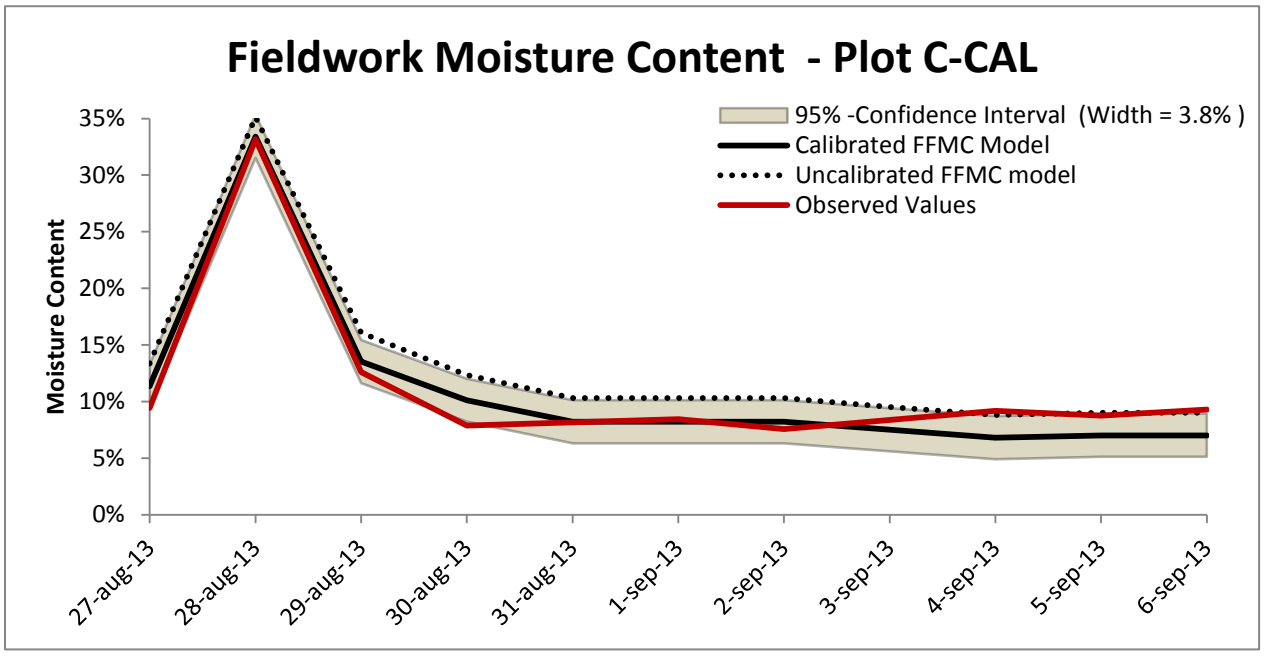

Figure 5-3. Four graphs showing the observed moisture content values in red. The results of the uncalibrated FFMC model as a dotted line. The calibrated FFMC model is shown as the black line and the related 95% confidence interval is incorporated as the gray bar. Also the constant width of the 95% confidence interval is included in the legend as a number.

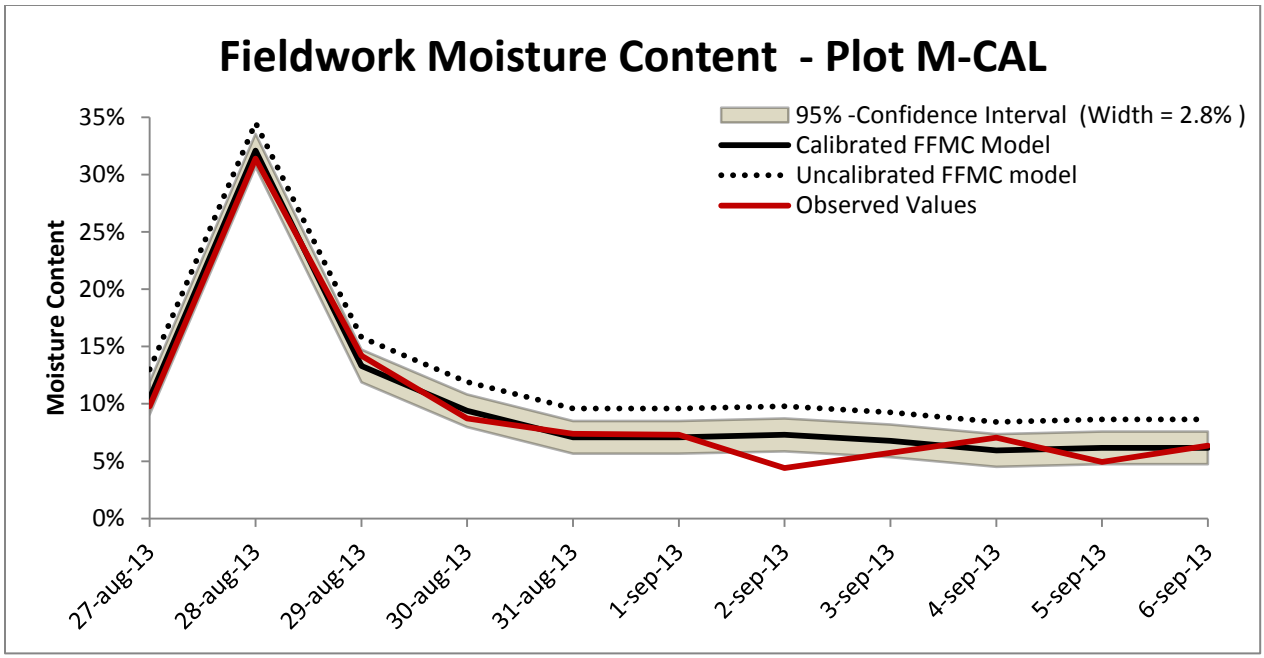

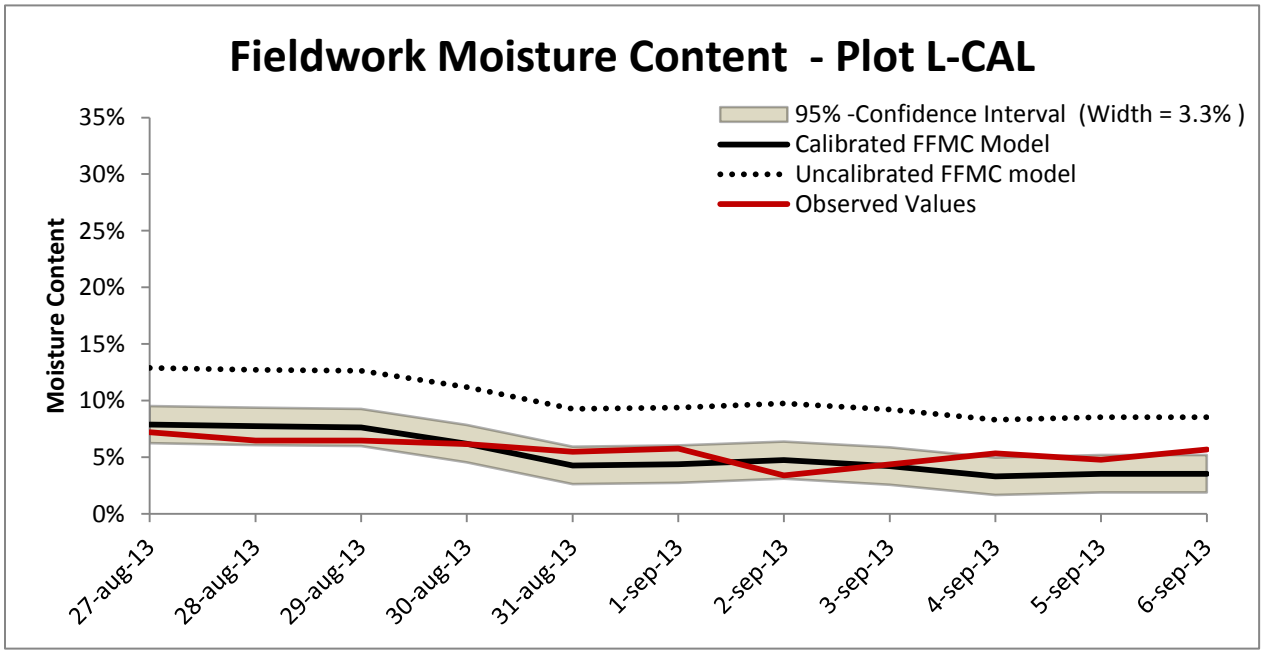

Figure 5-4. Four graphs showing the observed moisture content values in red. The results of the uncalibrated FFMC model as a dotted line. The calibrated FFMC model is shown as the black line and the related 95% confidence interval is incorporated as the gray bar. Also the constant width of the 95% confidence interval is included in the legend as a number.

the following week, see Appendix E. However when comparing the relative humidity data between field measurements and the meteo station data (Figure 5-5) it shows a very similar trend with a constant deviation for the first six days but from day six onwards that similarity disappears. Note that the field measurements of the relative humidity are averaged by vegetation class and that meteo station is represented by the unprocessed signal.

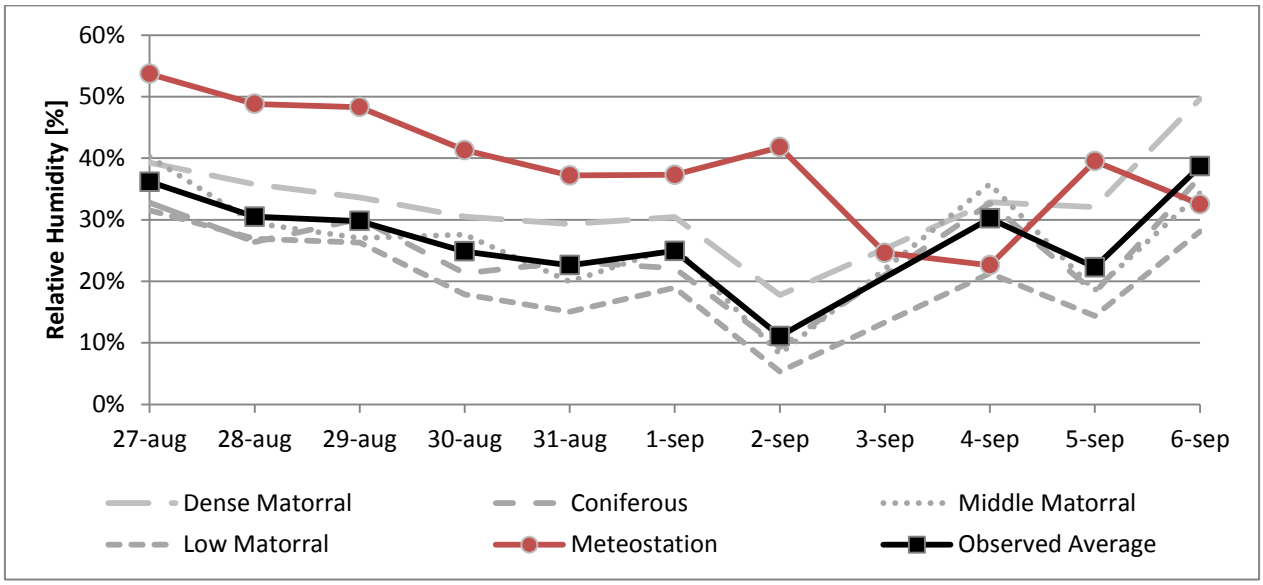

Figure 5-5. The relative humidity as measured by the meteo station in red. The relative humidity averaged over the 14 plots is provided by the black line. Note the divergence in trend after day 6 (September 1st). The meteo station data here does not use the corrected relative humidity as defined by Equation 14.

A similar effect is found with the fuel temperature (Equation 13), where the first 6 days correlate with measured IR temperature in the sun by $r^2 = 0.61$ for dense matorral and $r^2 = 0.52$ for the low matorral whereas overall correlations of respectively $r^2 = 0.28$ and $r^2 = 0.43$. Considering the importance of the relative humidity and fuel temperature on fuel sample moisture content and the time of divergence, an divergent relative humidity provided by the meteo station is the likely cause of the local temporally different moisture values. Moreover, while the fuel temperature correction was introduced to account for solar conditions it underestimates the fuel temperature in dense matorral by an average of 6 degrees and low matorral even by 14 degrees.

For the complete modeled period from June 1, 2013 to September 7, 2013 the summer moisture content of the D-Cal plot is illustrated in Figure 5-6. The effect of calibration on the three rain events is clearly visible as a strong decrease of modeled moisture content.

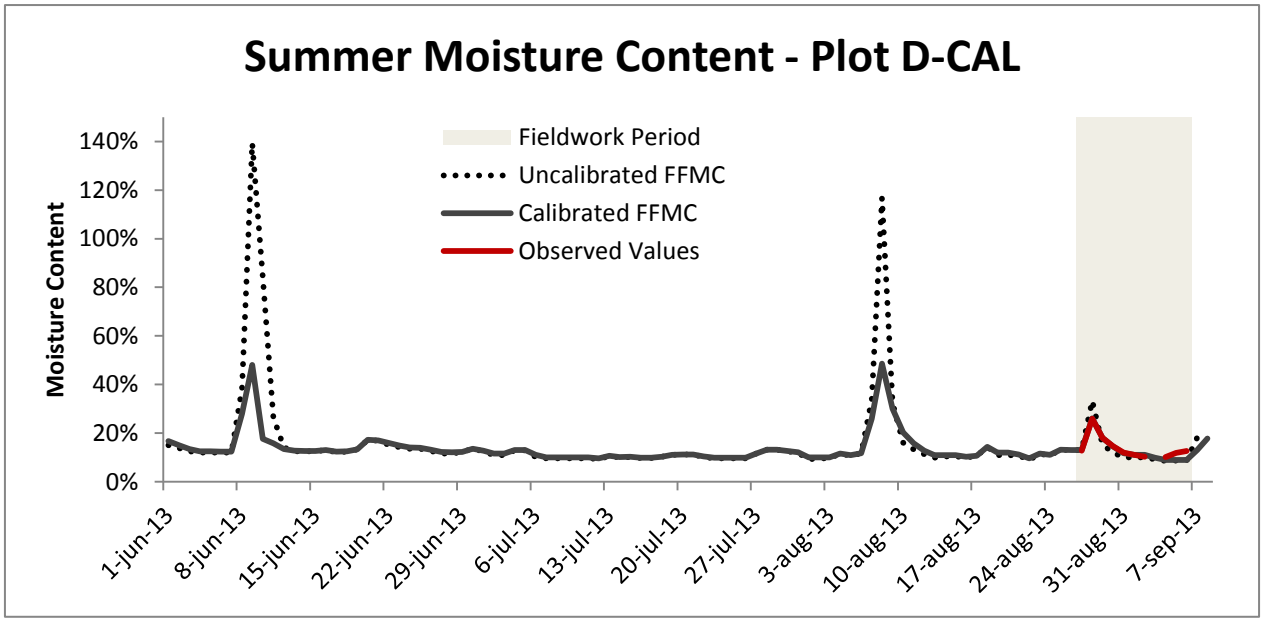

Figure 5-6. Summer moisture content for the D-CAL plot. The difference in wetting by rain between the calibrated and uncalibrated model is clearly visible in the three spikes in moisture content.

The spatial output of the calibrated FFMC model is displayed for three days in Figure 5-7. These three days were selected as they represent the three major events of rain (June 9), drying (June 12) and drought (July 12). Note that the classes of the landuse map (Appendix A) that do not burn or represent vegetation are transparent in this figure.

The map of June 9 shows the situation a day after a 29mm rainfall event and the differences in moisture content are substantial. The coniferous forest litter contains a maximum of 170% percent moisture and the dense matorral the lowest amount with a minimum of 46%. The low and middle matorral are also very moist and typically have a moisture content of above 100%. In accordance with the expectation that rain is equally distributed over the area, the geometry of the land surface is not visible and the moisture content is homogeneous throughout a vegetation type.

From June 9 to June 12 no additional rain occurred and the conditions were overall drying with climbing temperatures. This resulted in significant drer conditions on June 12 than modeled on June 9. The fuels under low and middle matorral have moisture contents under 12%. The coniferous forest fuels have a moisture content of about 13% and the dense matorral of 14%. The slower drying rate for dense

matorral matches the observations in Figure 5-2. The effect of the surface geometry is distinct with the southern orientated slopes about 0.8% drier than the northern (shaded) slopes.

After 33 days of drying, on July 12, the moisture content distribution has not changed. The overall moisture content has decreased further and follows the equilibrium moisture content trends. In areas with low solar radiation the lower temperature leads to a higher equilibrium moisture content and therefore the effect of land surface geometry is visible. Southern slopes have a typical 1% higher moisture content than the northern slopes.

The FFMC model predicts spatial differences of 2-3% within a vegetation type as a result of land surface geometry, so variation in that order would also be expected in the observations. However only small mutual differences were found: e.g. the four validation dense matorral plots had a mean fuel moisture content of 9.15 % with a standard deviation of 0.36 % (the elevation and aspect differences between the plots can be derived from Appendix H). Moreover, the number of sampling plots is considered too low to draw any significant conclusion about the spatial accuracy. So it was found impossible to spatially validate the FFMC due to a lack of data in combination with the small mutual differences.

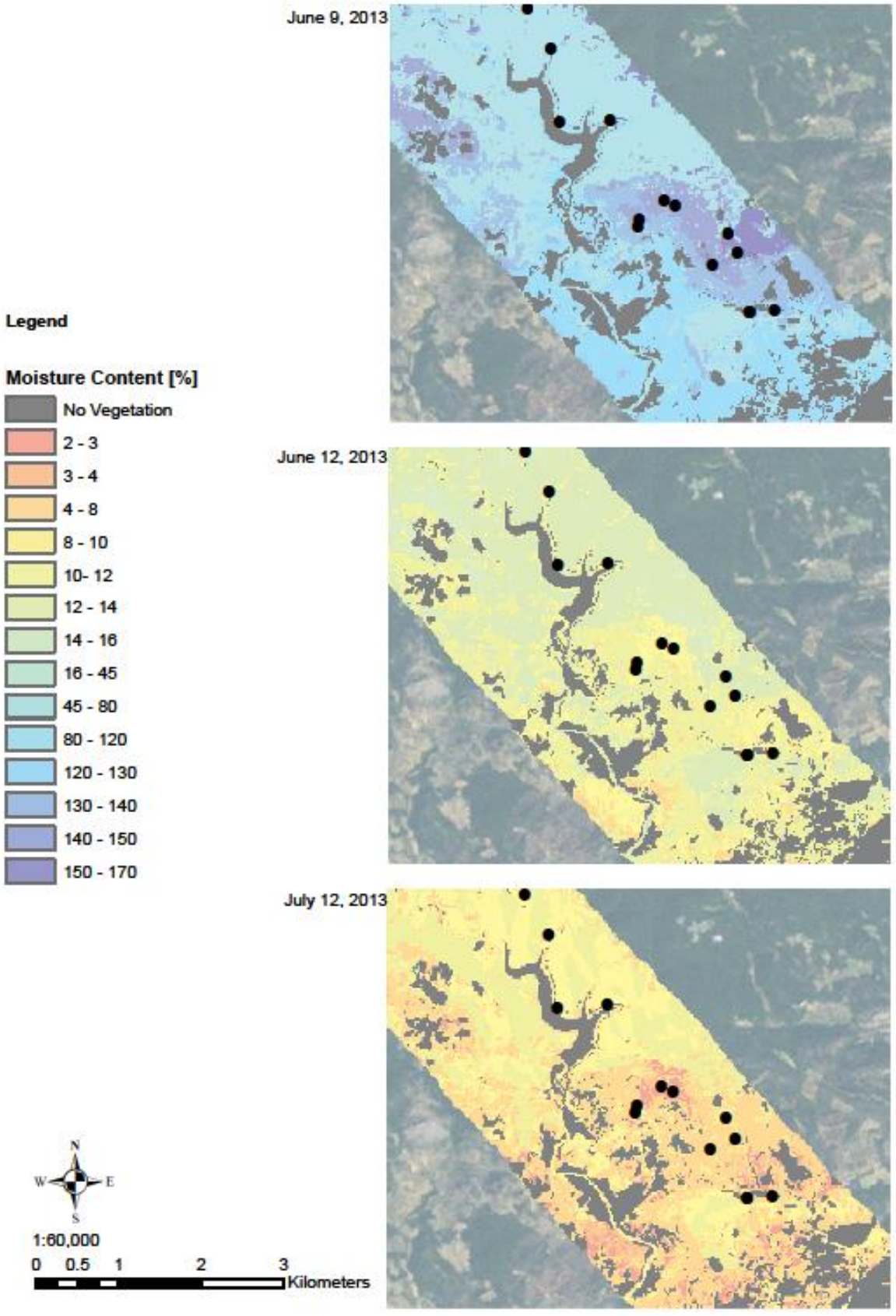

Figure 5-7. The FFMC output for three different days in summer; the day after a 29mm rain event (June 9), during the drying after that rain event (June 12) and after a month of drying (July 12). See Appendix E for the complete meteorological data. Note the (non-linear) scale!

5.2.2 BEHAVE MODEL RESULTS

The results of the BEHAVE model are also varying temporally and spatially. First the temporal variations are discussed with the aid of Figure 5-8. In this figure the behavior of the three major output components of the BEHAVE model (fireline intensity (I_B), flame length (L_f) and rate of spread (R)) relative to the Fine Fuel Moisture Content is shown.

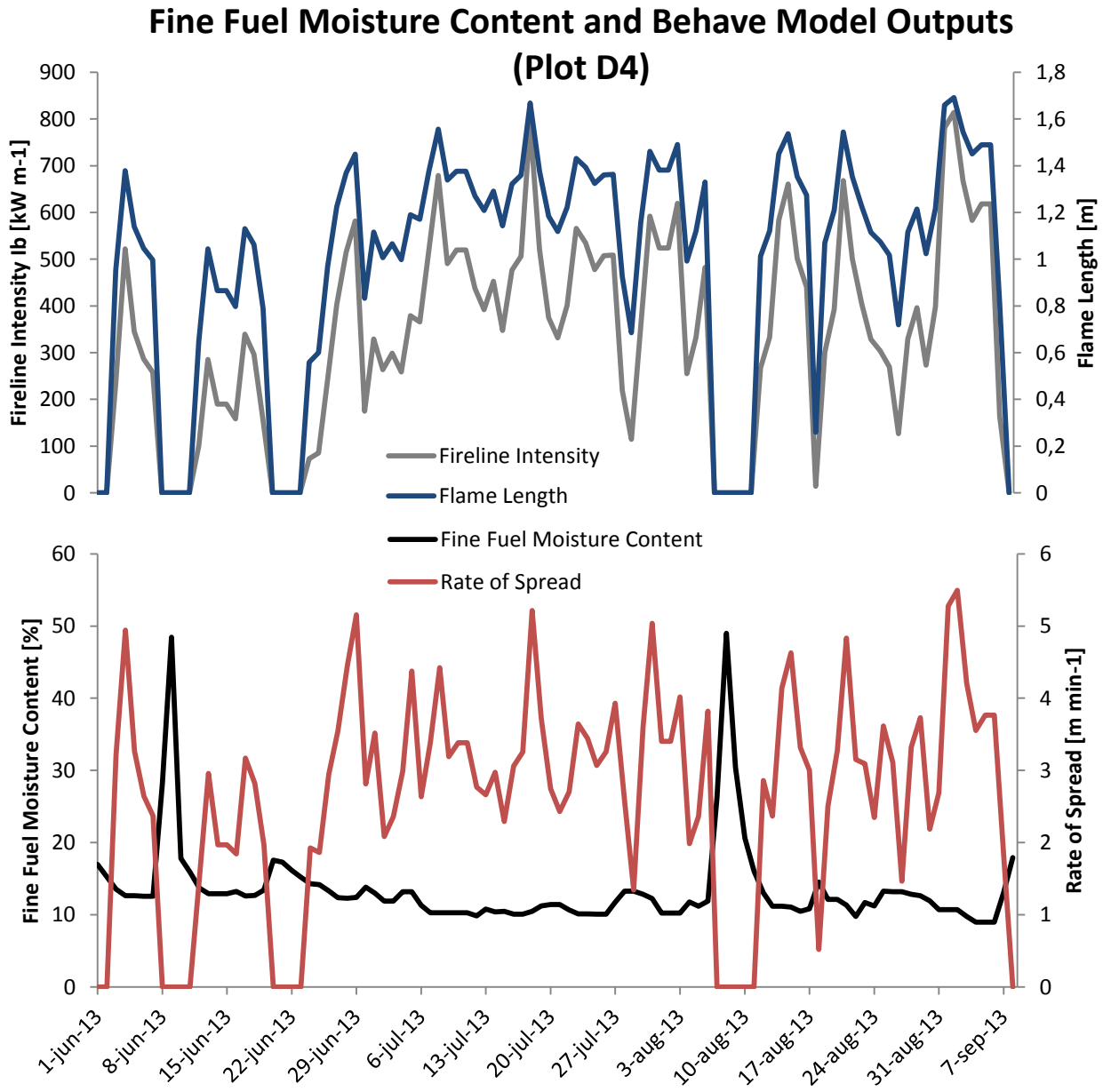

Figure 5-8. A comparison chart that shows the relation of fireline intensity, rate of spread, flame length to moisture content in the summer for plot D4. The three BEHAVE parameters show values of 0 when the fuel moisture content shows a peak.

An interesting observation in the D4 plot data is that the forest fire parameters reach values of zero with higher moisture contents at 5 times during the modeled period. This pattern is exactly the opposite of the modeled fuel moisture content that shows 5 peaks at the same timestep. This behavior corresponds to the ratio of fuel moisture content to moisture of extinction that must be lower than 1 (Equation 23). The two large peaks on June 8 and August 8 correspond to the two natural rain events. By the way the flame length is calculated (Equation 35) it shows a very similar trend to the fire line intensity and the model estimates maximal flame lengths of 1.7m with a fire line intensity of over 800 $kW\ m^{-1}$. The value of the flame length is relatively constant as it fluctuates between a more or less constant value and low values, whereas the fireline intensity shows a much spikier pattern with large fluctuations in addition to the 5 peaks mentioned. Both the flame length and the fireline intensity have typically lower values in June than in July and August. The pattern of the rate of spread fluctuates strongly around a more or less constant value and is high when the fireline intensity is high but also shows other peaks. These other peaks are induced by the wind velocity that is involved in the rate of spread calculation and have a big effect on its value. This agrees with literature and is considered a big uncertainty for fire managers.

Figure 5-10 shows the fireline intensity as calculated by Equation 34. After the rain event of June 8 there was no potential fire danger on June 9 so the fireline intensity, rate of spread and flame length were all zero. This corresponds to the high fuel moisture contents found throughout the study area on that day, see Figure 5-7. After three days of drying, on June 12 the fuel moisture content dropped below the moisture of extinction and the fire danger became present again. Southern slopes, especially those above the lake showed higher fireline intensity as a result of the lower moisture content modeled by the FFMC model . Maximal fireline intensity values were found up to 1000 $kW\ m^{-1}$ on steep slopes in both dense and middle matorral. The related flame length (Figure 5-11) shows maxima of about 1.8 meters on the same locations. Study site average fireline intensities and flame length were about 100-400 $kW\ m^{-1}$ and 0.3 - 1.2m respectively. On July 12 rain had been absent for 33 days and as shown in Figure 5-7 the conditions were drier. This long-term dry weather especially had its effect on the dense matorral with its slower drying rate, therefore also the fireline intensity and flame length showed the biggest changes there. As can easily be seen in Figure 5-10 and Figure 5-11 the north-western region shows the biggest fire danger on July 12 with fireline intensities up to 3000 $kW\ m^{-1}$ and flame lengths up to 3m. The rest of the study area also shows heightened fire danger where the average fireline intensity was 200-800 $kW\ m^{-1}$ and the average flame length 0.6 – 1.8m. The rate of spread shown in Figure 5-12 is low on June 12 with an average spread rate from 2 – 6 $m\ min^{-1}$. Its maxima are also found on steep slopes and double in the period to July 12. Again the dense and middle matorral show the highest values. It can be concluded that spatially and temporally the model predicts the highest fire danger in areas with steep slopes and on windy days. With relatively similar fire line intensities a much faster rate of spread is possible.

The effect of the uncertainties related to the FFMC model on these fire danger parameters can be calculated from the model. With a fixed moisture of extinction M_x (15% for dense, middle and low matorral) the relation (Equation 23) of the fine fuel moisture content to the moisture damping coefficient n_M is non-linear, see Figure 5-9.

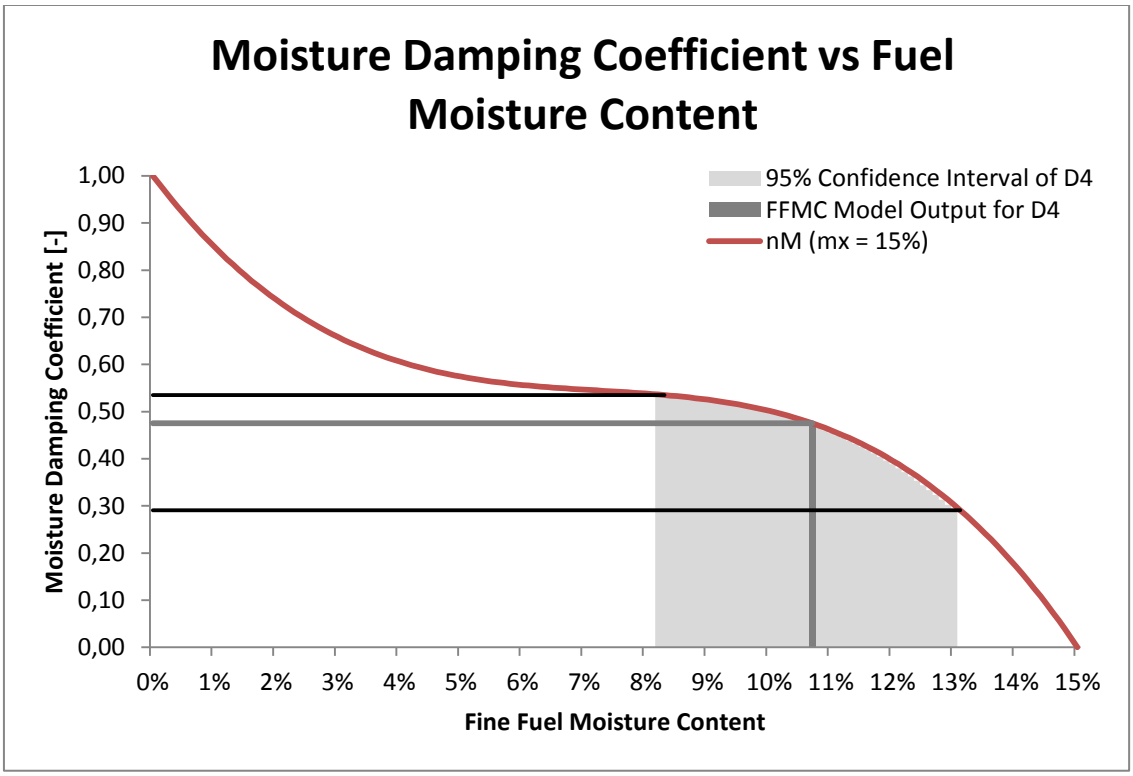

Figure 5-9. The non-linear effect of the uncertainty interval of fine fuel moisture content on the value of the moisture damping coefficient. The values used are for the D4 plot with a CI 95% of 4.7% wide (shaded grey area) on September 1st. The modeled moisture content is provided by the grey line (nm = 0.47). The range of nm is 0.29 – 0.54.

The calculated value of n_M with the moisture content provided by the FFMC model is 0.47, the range provided by the 95% confidence interval results in values of 0.29 to 0.54. When the reaction intensity (I_R) is calculated by Equation 20 with this range it results in I_R values (propagated error factors) 1.1 times higher in case of $n_M = 0.54$ or 0.6 times lower in case of $n_M = 0.29$. Due to the linear relation (Equation 19) of I_R with the rate of spread R this implies the same range for R. The propagated error factor is squared in the calculation of I_B (Equation 34) and this results in CI 95% boundary values that are a factor 1.21 and 0.36 different from the values calculated based on the model output. For the flame length L_f (Equation 35) this error factor is put to the power of 0.46 resulting in flame lengths of 1.1 and 0.6 times the normal model output.

D4 is a plot with an average CI 95% width and is therefore representative for the results of the other models. It must also be noted that the shape of the relation of n_M and the fine fuel moisture content (Figure 5-9) is such that derivative is 0.0 around a moisture content of 7.3%. The propagated error related to fine fuel moisture contents in the range of 5% to 10% will therefore be significantly smaller than those of moisture contents <5% and >10%. For example the widest CI 95% (7.3%) was found for M3. However, this plot had a modeled moisture content of 6.73% on September 1st. This resulted in a n_M that was a factor 1.2 bigger or 0.9 smaller than based on the FFMC output, which leads to smaller errors in fire behavior prediction than calculated for the D4 plot.

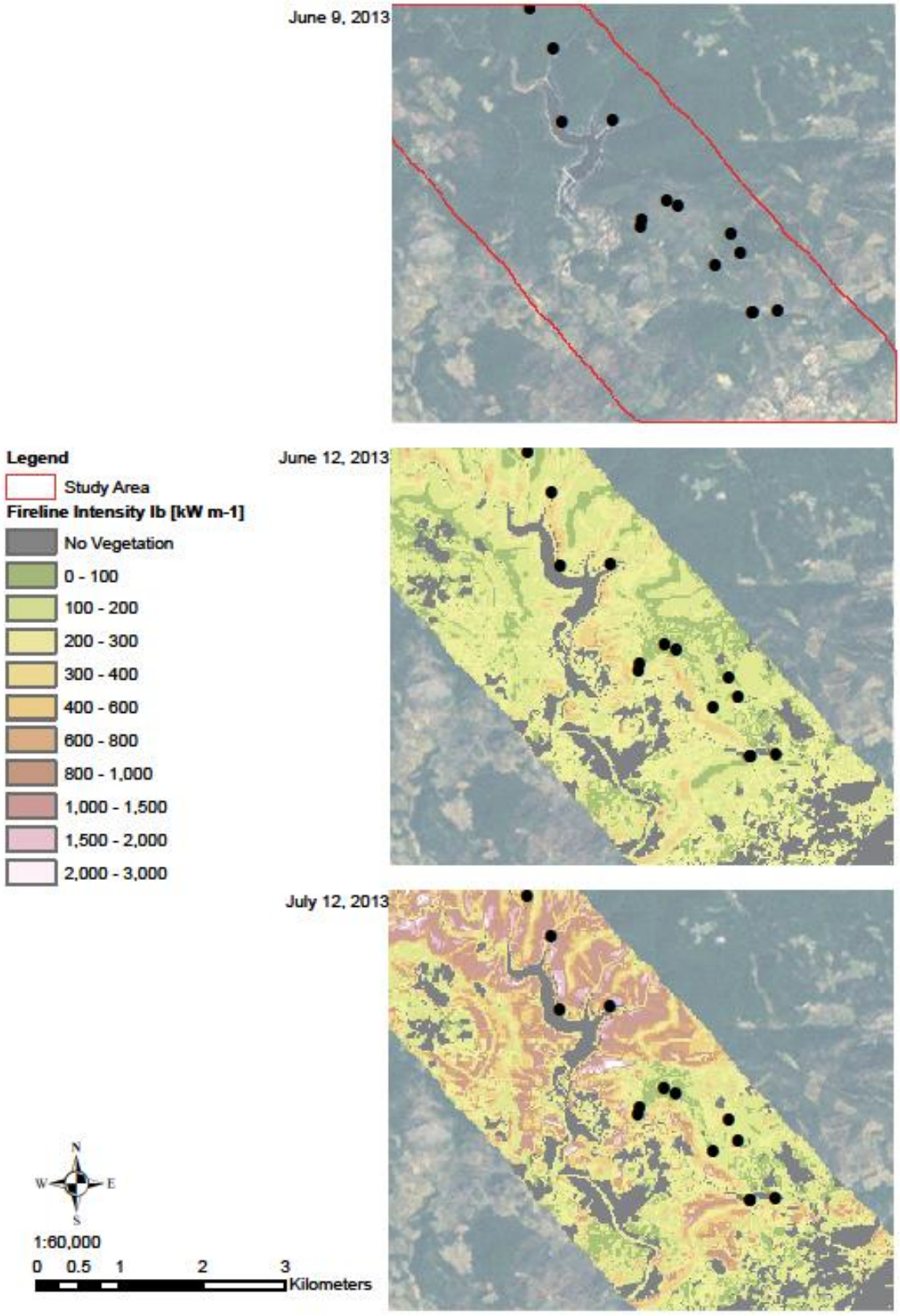

Figure 5-10. The Bryams fireline intensity spatially modeled for three days. On June 9 there was no potential fire danger. The high fire intensities concentrate in the dense matorral and especially on the steeper slopes. The scale is non-linear!

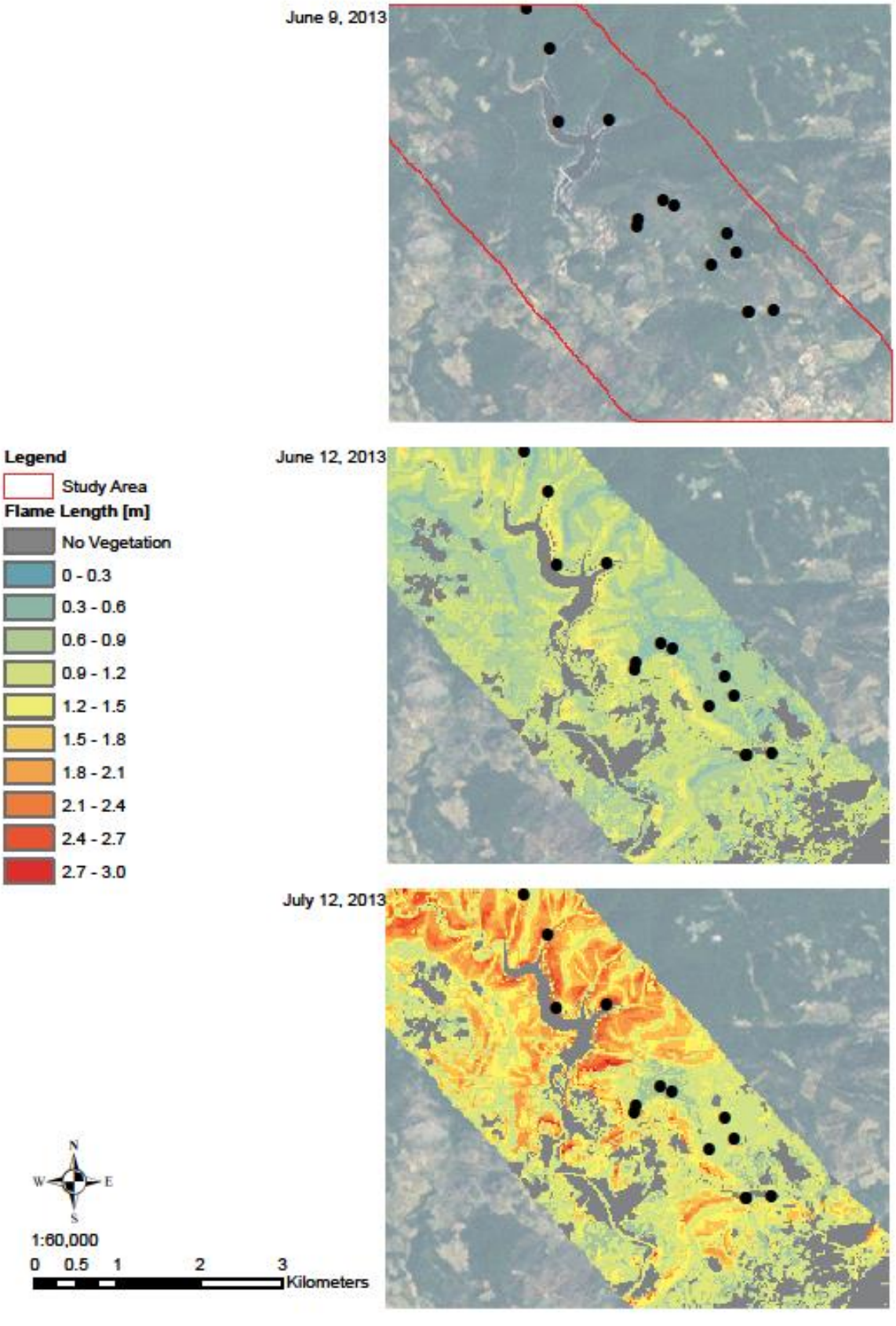

Figure 5-11. The flame length modeled for three days. On June 9 there was no potential fire danger. The biggest flame lengths are found in the dense matorral and especially on the steeper slopes.

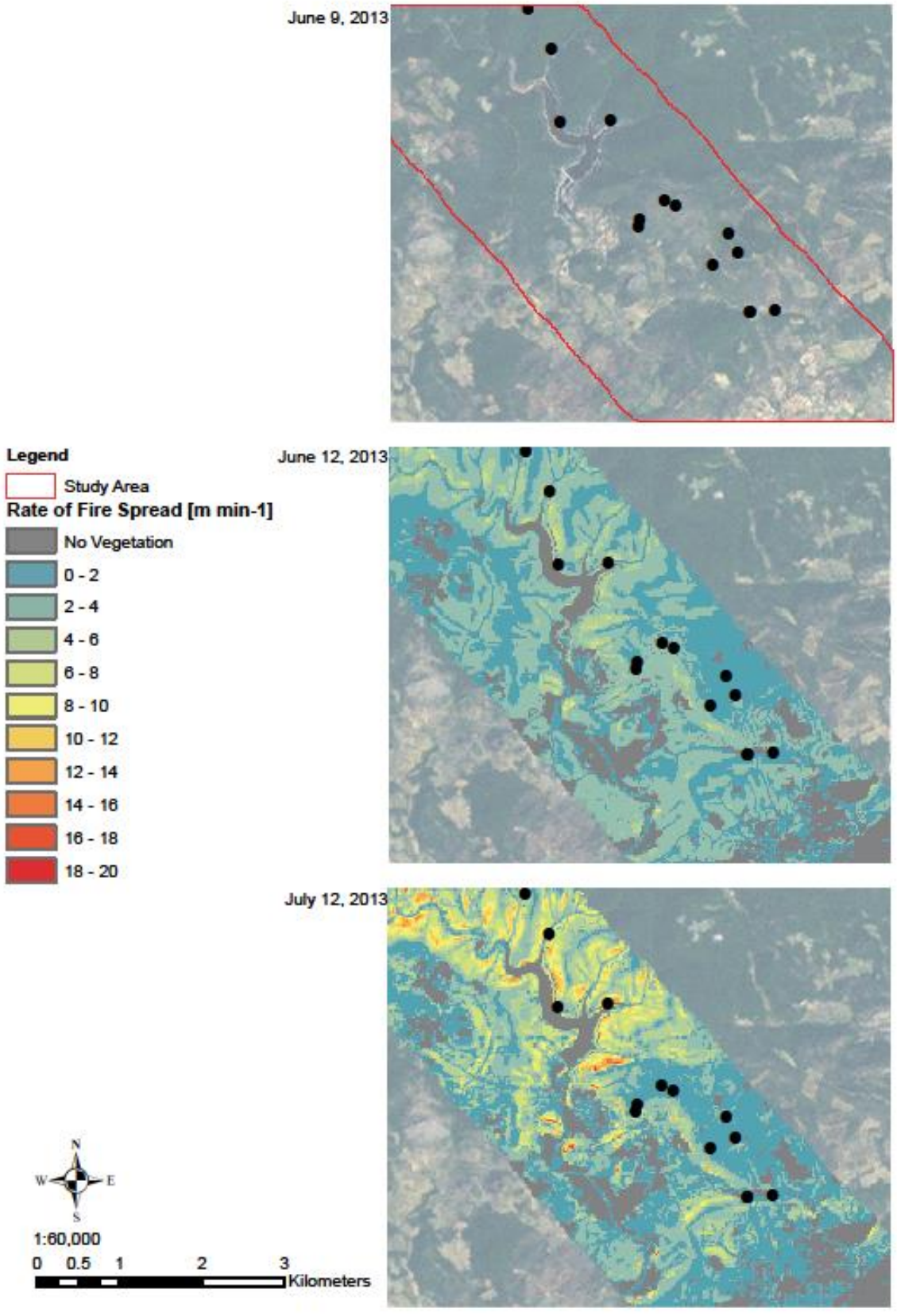

Figure 5-12. The rate of spread spatially modeled for three days. On June 9 there was no potential fire danger. The highest rate of spread is found on steep slopes within dense and middle matorral vegetation.

6 DISCUSSION

In this research Mediterranean fire danger potential was modeled for the summer of 2013. Fire behavior predictions were based on the BEHAVE model using the FFMC model to estimate the fine fuel moisture content. Here the data acquisition, the BEHAVE model, the FFMC model and its implementation are discussed with respect to the validation of the model predictions. Each part is discussed in detail, starting with the model build, followed by the data collection and data preparation and model performance.

6.1 MODEL BUILDING

The FFMC and BEHAVE models were built based on existing literature, mostly the original publications. The original FFMC model was made for Canadian boreal forest with a closed canopy. Despite of the fact that FFMC model was adjusted for the enlarged solar input, it is most likely that entrenched errors are present in the equations when used for the Mediterranean area. For example the Mediterranean summer drought and relatively warm temperatures at night prevent wetting by high relative humidity whereas this did have influence during the calibration of the model in Canada (Van Wagner, 1987). This problem could have been prevent by applying a model that uses (semi-)continuous meteorological data rather than a single solar-noon input. This would also reduce the risk of errors induced by a point measurement of meteorological variables, e.g. the measurement of solar radiation under a partially cloudy sky is likely to fluctuate strongly within short periods of time. The current model picks a single solar noon value of that fluctuating signal to model a full day and therefore has a chance to pick an outlining value. However, due to the large scale and pragmatic character of the FFMC model spatially continuous input is not yet included. Additionally, the adjustments made to the FFMC model were not made specifically for the European Mediterranean. The fuel temperature and corrected relative humidity were calculated based on a formula that was calibrated for hardwood litter, with the authors stating that it should be calibrated for each litter type (Byram and Jemison, 1943). Calibration of the discussed equations was outside the scope of this study and it is not easy to predict the effect for the Mediterranean litter types. Nevertheless, other studies proved that the FFMC model correlated fairly well with leaf litter in southern Europe (Aguado et al., 2007) and is assumed to be a good fuel fine fuel moisture content estimator for the Mediterranean (Camia and Amatulli, 2009; Dimitrakopoulos and Dritsa, 2003).

The BEHAVE model uses general deterministic equations that need vegetation specific variables so that it is better adapted to any specific type of vegetation. Problems with site specific calibration are therefore absent. However, for calculations on fuel level and midflame wind speeds, respectively used in the FFMC and BEHAVE model, large assumptions are made on the fuel bed roughness, patchiness and sheltering. The most important assumption is that these parameters are assumed equal within one vegetation type, which is not the case considering field observations and land surface geometry.

Especially in the BEHAVE model the effect of wind on the rate of spread is large and requires a more spatially accurate estimate in following studies.

6.2 Data Collection and Preparation

Data was collected from literature, a 10-day fieldwork period and a meteo station. For the FFMC model this included input data and calibration/validation data. As to the FFMC input data all but the shading was acquired from the meteo station and extrapolated over the study area. In spite of the effort put into a justifiable spatial extrapolation it includes some errors of which some can be quantified and others not. Rainfall is assumed to be equally spread throughout the area, despite the fact that a relation between precipitation amount and altitude has been found (see chapter 4.2.2). This simplification is best avoided by placing several meteo station throughout the area as this also improves the interpolation of other weather parameters. For the temperature and relative humidity the data from the meteo station was extrapolated using equations that respectively use the environmental and dewpoint lapse rates. As Figure 5-5 and the last part of chapter 5.2.1 clarify there is a difference, after fieldwork period day 6, in both the measured relative humidity and the temperature between the daily 16 field observations and the meteo station. This makes it questionable how valuable the data from the meteo station is outside the temporal range of the fieldwork period. An important difference between the field observations and the meteostation is the sheltering of the sensor (i.e. the meteo station is located in an open field, while the field observations were made with the sensor sheltered between the fuels). In general it is recommendable to place several meteo stations, or at least one in the center of the study area for follow-up studies. Although poor meteodata may influence the validation results it is not a problem that effects the model itself. Such cannot be concluded for the extrapolation of relative humidity and fuel temperature from the meteo station data as both seem to show a rather constant deviation from observed values. In this study these deviations are captured within the calibration part by adjusting the equilibrium moisture content as is also done in other studies (Dimitrakopoulos et al., 2011). Remarkably this adjustment of the EMC was not required for the only vegetation with a (almost) completely closed canopy (see Table 6, chapter 5.2.1) suggesting that this might be related to the Canadian full closed canopy conditions during the model calibration.

Despite of the fact that the vegetation map was 10 years old and based on 2003 HyMap imagery by Sluiter (2005) there were no irregularities found and the map corresponded to field observations, except the partial logging of the pine forest. These field observations also determined which of the fuel models by Scott and Burgan (2005) (Table 5, chapter 5.1) matched the vegetation classes by assigning them to each plot. Without exemptions within each vegetation class each plot was assigned the same fuel model. The 14 plots were selected based on vegetation class, land surface geometry but also based on their accessibility and mutual distance. This was needed in order to keep the mutual sampling time as small as possible and resulted in a 5km long area with the plots relatively close to each other, see Figure 4-9. More sampling plots and further spreading throughout the area would allow a spatial analysis of the model where fuel moisture contents show enough contrast to draw conclusions from. A prolonged sampling period with natural rain events is recommendable as the simulated rain events in this study do

not simulate the spatial differences that may be present in natural rain. Nevertheless, the simulated rain events was the only rain input for the FFMC and has proven to be crucial in order to calibrate the FFMC model during rain.

6.3 Model Performance

The uncalibrated FFMC model performed best in the dense matorral with an average CI 95% of 4.9%, much better than in the less sheltered fuels. Using 30 of the 140 fuel moisture samples the FFMC model was calibrated by curve fitting, requiring a different approach for each of the four vegetation types. As explained above, the general trend of the modeled dense matorral moisture content corresponded with the field observations in contrast to that of the middle and low matorral and the coniferous forests that had a constant overestimation. In the present study this deviation, caused by wrong equilibrium moisture values was compensated by lowering the EMC graph as a whole. The EMC was calculated from the temperature and the relative humidity and considering the problems existing with both these data inputs it is possible that this forms the cause of the problem. However, this does not explain why the model performs more accurately in the dense matorral, suggesting that the calculation of the EMC in the middle and low matorral and the coniferous forest is erroneous.

The log drying rate and rain input for the dense matorral and coniferous forest had to be changed in extend but more importantly with a different sign. With only one rain event available it was chosen to adjust these parameters by multiplication with a specific factor, it is however also possible that the error in the model was constant. No conclusion for this can be drawn from a single rain event and in further research several consecutive rainfall events should be considered. There are two likely explanations for the differences in the log drying rate and rain input. The first one is that there are big differences in soil horizons. The coniferous forest was littered with abundant forestry activity remnants so that much of the fuel layer was off the ground, while fuels were drying on the bare ground in the dense matorral. Rain in the coniferous forest is therefore more likely to be trapped in the fuel complex (especially in the thick layer of pine needles) than in the dense matorral where runoff water immediately drains to the soil. The other explanation is based on differences in plant morphology and characteristics; the surface to volume ratio of pine needles and branches with loose and scaly bark is higher than that of the leaves and branches collected form the dense matorral. This extra surface increases the absorption of water. Wetting by relative humidity could not be included in the calibration of the models and this is an important shortcoming of this study. The fluctuations in temperature and relative humidity that are used as input were too small to distinguish both trends and adapt the model to them.

The calibrated FFMC output has an average 95% confidence interval of 4.3%, 1.8 times smaller than the uncalibrated version. Especially the low and middle matorral correlated much better and provided results similar to the dense matorral and coniferous plots. This suggests again that the FFMC should be calibrated for use in the opener Mediterranean vegetation. The FFMC model in this study is fast drying and the effect of a 11 mm rainfall event on fine fuel moisture content is unnoticeable after 2 to 4 days. This behavior is typical for the FFMC model (Mantzavelas, 2006) and also means that the forest fire potential 4 days after a (11m) rain event is equal to the prolonged period of drought prior to the event.

Only two natural rain events occurred in the modeled summer as easily visible in Figure 5-6 and Figure 5-8, which correspond to the Mediterranean summer drought.

The BEHAVE model resulted in a prolonged period of possible fire-occurrence with only 5 short periods non-combustible conditions, emphasizing the fire danger related to the low moisture contents in the region. Fireline intensity and the related flame length reached maximum values up to 3000 $kW\ m^{-1}$ and 3m on the steepest slopes within the dense and middle matorral vegetation. These values are well within the values observed during the creation of the fuel model SH7 (Scott and Burgan, 2005) which in the most extreme cases consists of fires of 26000 $kW\ m^{-1}$ with flame lengths above 8 meters. Observations in the Mediterranean result in similar high values of 19000 $kW\ m^{-1}$ and flame lengths of 7.4 meters (Morandini et al., 2006). However, it is important to realize that the relationship between wind velocity and fire behavior shows high non-linear behavior and that the study by Morandini et al. (2006) measured wind velocities of over 8 $m\ s^{-1}$, while it peaked at 4 $m\ s^{-1}$ in this study. Additionally the vegetation used by Morandini et al. (2006) had a mean height between 2 and 3 meters and is therefore much higher than the maximum of 1.8m assumed in the BEHAVE fuel models. The rate of spread modeled by the BEHAVE model averaged at 8-10 $m\ min^{-1}$ with steep slope outliers of over 20 $m\ min^{-1}$ on the most severe days. Also this figure corresponds to both the observations used to create the fire model and Mediterranean observations that showed values of 60 $m\ min^{-1}$ (Scott and Burgan, 2005) and 6 to 24 $m\ min^{-1}$ respectively (Morandini et al., 2006). The output of the BEHAVE model is illustrated in Figure 5-9, Figure 5-10 and Figure 5-11 and when compared to the DEM in Figure 4-9 and the vegetation map in Appendix A it can easily be seen that the dense and middle matorral show the most extensive fire behavior as a result of the steep slopes, wind and fuel related parameters. All in all it can be concluded that at the driest point of summer the main fire behavior parameters of rate of spread, fireline intensity and flame length did exist but were low due to the mild wind conditions.

The accuracy of the BEHAVE model can no further be determined than stating its corresponds to other studies. However, by a detailed analysis of how the model works it is possible to determine the effect of the propagated uncertainty of the FFMC model (Figure 5-9). It was found that the effect of an error in the FFMC model was low on the BEHAVE model with moisture content values of about 7.4%. However, for both very low and high moisture contents the effect of 1% lower or higher moisture content resulted in 10% higher or lower fire behavior parameters. Similar behavior is described in literature (Harrington et al., 1983). It is therefore concluded that the model in this study performs best (known 95% CI of 4.3% for fuel moisture content and known effects on the BEHAVE model) in moderately dry moisture conditions of about 7.3%.

7 CONCLUSIONS AND RECOMMENDATIONS

The main objective of this research was to create a fuel moisture content model and a fire behavior prediction model for forest fires in the Mediterranean. The Canadian FFMC model was used to estimate moisture contents in the fine fuels from meteorological indices. This model was adapted from the Canadian boreal to Mediterranean vegetation, as especially the radiation budget on surface fuels is completely different. The BEHAVE model was used to provide straightforward estimations on rate of spread, fireline intensity and flame length based on the moisture content estimated by the FFMC model. Next the spatial and temporal fuel moisture content distribution for the La Peyne area of southern France was determined for the period from June 1 up to and including September 6, 2013. This resulted in daily maps that showed the areas with the highest fire potential and overall fire danger. Finally the accuracy of the FFMC model was determined with the aid of fuel moisture samples. The main conclusions are as follows:

- Fuel moisture contents in this study area varied between 2% and 170% where the lowest moisture contents related to low matorral vegetation after a prolonged period of drought. The highest moisture contents were found in the thick needle bed of the coniferous forest after one of the two rain events in the modeled period.
- The equilibrium moisture content of the four vegetation classes were significantly different and this supports the need for calibration as the average fuel moisture content for dense and low matorral differed 4%. Without vegetation class specific calibration this difference would be ignored and one single value was calculated for both classes.
- Although the FFMC model was developed for fully closed canopies in Canada it performs rather well after calibration and incorporation of solar radiation. On average the model had a 95% confidence interval width of 4.3%. It was however noticed that the first 7 days showed a relative much better accuracy which was caused by deviations in the meteorological input of unknown source.
- The BEHAVE model provided values on fire behavior prediction parameters that are within the range provided by literature. The rate of spread, fireline intensity and flame length were considered to be rather low due to the lack of wind. Maximum values were found on steep slopes of the dense and middle matorral.

For further research it is recommendable to study the effect of the constants used to calculate the fuel temperature (Equation 13), as the required conditions to use the standard values was not met. Furthermore the use of more than one meteo station would allow to verify the data and interpolate the meteorological values throughout the area. In addition would multiple rainfall events during the fieldwork allow for better calibration, including that of wetting. Finally the incorporation of sheltering and patchiness in the vegetation would allow more realistic fire behavior within the vegetation classes and - when combined with more sampling plots for fuel moisture- allow spatial validation.

8 BIBLIOGRAPHY

Aguado, I., Chuvieco, E., Boren, R., & Nieto, H. (2007). Estimation of dead fuel moisture content from meteorological data in Mediterranean areas. Applications in fire danger assessment. *International Journal of Wildland Fire, 16*, 390-397.

Albini, F. A. (1976). *Estimating Wildfire Behavior and Effects.* U.S. Department of Agriculture, Forest Service. Ogden, Utah: USDA Forest Service.

Albini, F., & Baughman, R. (1979). Estimating Windspeeds for Predicting Wildland Fire Behavior. *USDA Forest Service Research Paper*.

Anderson, H. E. (1982). *Aids to Determining Fuel Models For Estimating Fire Behavior.* General Technical Report, United States Department of Agriculture, Forest Service, Ogden.

Andrews, P. L. (1986). *BEHAVE: Fire Behavior Prediction and Fuel Modeling System.* Forest Service , United States Department of Agriculture. Odgen: Forest Service.

Andrews, P. L., Cruz, M. G., & Rothermel, R. C. (2013). Examination of the wind speed limit function in the Rothermel surface fire spread model. *International Journal of Wildland Fire*, E-K.

Blandford, T., Humes, K., Harshburger, B., Moore, B., & Walden, P. (2008). Seasonal and Synoptic Variations in Near-Surface Air Temperature Lapse Rates in a Mountainous Basin. *JOURNAL OF APPLIED METEOROLOGY AND CLIMATOLOGY*, 249 - 261.

Boboulos, M., & Purvis, M. R. (2009). Wind and Slope Effects on ROS during the fire propagation in East-Mediterranean pine forest litter. *Fire Saftey Journal*, 1-6.

Bonfils, P. (1993). *Carte Pédologicue de la France 1:100.000. .* Ardon .

Byram, G. F., & Jemison, G. M. (1943). Solar radiation and forest fuel moisture. *Journal of Agricultural Research, 67*(4), 149-176.

Camia, A., & Amatulli, G. (2009). Weather factors and fire danger in the Mediterranean. In E. Chuvieco, *Earth observation of wildland fires in Mediterranean ecosystems* (pp. 71-82). Berlin: Springer Verlag.

Camia, A., & Bovio, G. (2000). *Description of the indices implemented in EUDIC software for the European meteorological forest fire risk mapping.* European Commission, Joint Research Centre . Turin : EU.

Catry, F. X., Bacao, F., & Moreira, F. (2009). Modeling and mapping wildfire ignition risk in Portugal. *International Journal of Wildland Fire, 18*, 921-931.

Chuvieco, E., Aguado, I., & Dimitrakopoulos, A. P. (2004). Conversion of fuel moisture content values to ignition potential for integrated fire danger assessment. *Canadian Journal of Forest Research, 34*, 2284-2293.

Chuvieco, E., Cocero, D., Riano, D., Martin, P., Martinez-Vega, J., Riva, J. d., & Perez, F. (2004). Combining NDVI and surface temperature for the estimation of live fuel moisture content in forest fire danger rating. *Remote Sensing of Environment, 92*(3), 322-231.

Conedera, M., Torriani, D., Neff, C., Ricotta, C., Bajocco, S., & Pezzatti, G. B. (2011). Using Monte Carlo simulations to estimate relative fire ignition danger in a low-to-medium fire-prone region. *Forest Ecology and Management, 26*, 2179-2187.

CSIRO. (2011, October 14). *Fire-generated wind*. Retrieved June 3, 2013, from http://www.csiro.au/en/Outcomes/Safeguarding-Australia/FireGeneratedWind.aspx

De Groot, W. (1987). *Interpreting the Canadian Forest Fire Weather Index (FWI) System.* Prince Albert: Canadian Forestry Service.

Demarez, V., Duthoit, S., Baret, F., Weiss, M., & Dedieu, G. (2008). Estimation of leaf area and clumping indexes of crops with hemispherical photographs. *agricultural and forest meteorology, 148*, 644-655.

Dimitrakopoulos, A. P., & Dritsa, S. (2003). Novel nomographs for fire behaviour prediction in Mediterranean and submediterranean vegetation types. *Forestry, 76*(5), 479-490. Retrieved from http://forestry.oxfordjournals.org/content/76/5/479.full.pdf

Dimitrakopoulos, A. P., & Papaioannou, K. K. (2001). Flammability Assessment of Mediterranean Forest Fuels. *Fire Technology, 37*, 143-12.

Dimitrakopoulos, A. P., Mitsopoulos, I. D., & Raptis, D. I. (2007). Nomographs for predicting crown fire initiation in Aleppo pine (Pinus halepensis Mill.) forests. *European Journal on Forest Research* (126), 555-561.

Dimitrakopoulos, A., Bemmerzouk, A., & Mitsopoulos. (2011). Evaluation of the Canadian fire weather index system in an eastern Mediterranean envionment. *Meteorological Applications, 18*, 83-93.

Doelman, J. (2012). *Mapping Mediterranean natural vegetation species using heterogeneous endmember analysis of hyperspectral imagery.* Physical Geography. Utrecht: Utrecht University.

Duffie, J. A., & Beckman, W. A. (2013). *Solar Engineering of Thermal Processes.* Hoboken, New Jersey: John Wiley & Sons.

FAO. (1999). Mediterranean forests: ecological space and economic and community wealth. (O. M'Hirit, Ed.) *Mediterranean Forests*, 59. Retrieved February 2, 2013, from http://www.fao.org/docrep/x1880e/x1880e00.htm

FAO. (2007). *Fire Management Global Assessment 2006.* United Nations, Food and Agricultural Organization, Rome. Retrieved from ftp://ftp.fao.org/docrep/fao/009/A0969E/A0969E00.pdf

Ferreira Leite, F., Goncalves, A. B., & Vieira, A. (2011). The recurrence interval of forest fires in Cabec-o da Vaca (Cabreira Mountain—northwest of Portugal). *Environmental Research*, 215-221.

Forest Encyclopedia. (1996). *Forest Encyclopedia*. (Nyland, Editor) Retrieved March 21, 2013, from http://www.forestencyclopedia.net/p/p1464

Frandsen, W. H. (1971). Fire spread through porous fuels from the conservation of energy. *Combustion and Flame* , 9-16.

Gibos, K. (2010). *Solar Radiation Driven Differences in Fine Fuel Moisture Content on North and South Slopes.* MSc Thesis , University of Toronto , Forestry, Toronto .

Grabner, K., Dwyer, J., & Cutter, B. (1997). Validation of BEHAVE Fire Behavior Predicitions in Oak Savannas using Five Fuel Models. *Central Hardwood Forest Conference* (pp. 202-215). University of Missouri-Columbia.

Harrington, J. B., Flannigan, M. D., & Wagner, C. E. (1983). A study of the relation of components of the fire weather index to monthly provincial area burned by wildfire in Canada 1953-80. *Canadian Forestry Service* .

IPCC. (2007). *Climate Change 2007: The Physical Science Basis. Contribution of Working Group I to the Fourth Assessment Report of the Intergovernmental Panel on Climate Change.* Cambridge: Cambridge University Press.

JRC. (2008). *Assessment of Forest Fire Risk in European Mediterranean Region: Comparision of satellite-derived and meteorological indices.* European Commision, Joint Research Centre. Ispra: Office for Official Publications of the European Communities.

Keeley, J. E., Fotheringham, C. J., & Morais, M. (1999). Reexaming Fire Supression Impacts on Brushland Fire Regimes. *Science, 284*(5421), 1829-1832.

Lagacherie, P., McBratney, A., & Voltz, M. (December 2006). *Digital Soil Mapping: An Introductory Perspective.* Amsterdam: Elsevier.

Lawson, B. D., & Armitage, O. B. (2008). *Weather Guide for the Canadian Forest Fire Danger Rating System.* Weather Guide, Canadian Forest Service , Edmonton.

Lawson, B. D., Armitage, O. B., & Hoskins, W. D. (1996). *Diurnal Variation in the Fine Fuel Moisture Code: Tables and Computer Source Code* . Technical Report, Government of Canada , Forestry , Victoria.

Lloret, F., Pausas, J. G., & Vilà, M. (2003). Responses of Mediterranean Plant Species to different fire frequencies in Garraf Natural Park (Catalonia, Spain): field observations and modelling predictions. *Plant Ecology, 167*, 223–235.

Mantzavelas, A. (2006). Fire Paradox. *Project FP6-018505*.

Marlon, J. R., Bartlein, P. J., Gavin, D. G., Long, C. J., Anderson, R. S., Briles, C. E., . . . Colombaroli, D. (2012, February 14). Long-term perspective on wildfires in the western USA. *Environmental Sciences*, 535-543. Retrieved from www.pnas.org/cgi/doi/10.1073/pnas.1112839109

Mather, A., Fairbairn, J., & Needle, C. (1999). The course and drivers of the forest transition: the case of France. *Journal of Rural Studies , 15*, 65-90.

Missoula Fire Sciences Laboratory. (2013, July 2013). *firemodels.org*. Retrieved September 11, 2013, from http://www.firemodels.org/index.php/behaveplussoftware/behaveplus-downloads

Mitsopoulos, I. D., & Dimitrakopoulos, A. P. (2007). Canopy fuel characteristics and pontential crown fire behavior in Alleppo pine forests. *Annals of Forest Science, 64*, 287-299.

Morandini, F., Silvanie, X., Rossi, L., Santoni, P.-A., Simeoni, A., Balbi, J.-H., . . . Marcelli, T. (2006). Fire spread experiment across Mediterranean shrub: Influence of wind on flame front properties. *Fire Safety Journal*, 229-235.

Moreira, F., Catry, F., Rego, F., & Bacao, F. (2010, June 3). Size-dependent pattern of wildfire ignitions in Portugal: when do ignitions turn into big fires? *Landscape Ecology, 25*, 1405-1417.

Nijland, W. (2011). *Mediterranean evergreen vegetation dynamics.* Utrecht: Utrecht Studies in Earht Sciences 002.

NOAA. (2013). *Vapor Pressure*. (N. O. Administration, Producer) Retrieved June 2013, from http://www.srh.noaa.gov/images/epz/wxcalc/vaporPressure.pdf

Office of Environment and Heritage NSW. (2011, February 27). *How a fire behaves*. Retrieved March 21, 2013, from Nature Conservation NSW Government: http://www.environment.nsw.gov.au/fire/howafirebehaves.htm

Pastor, E., Zarate, L., Planas, E., & Arnaldos, J. (2003). Mathematical Models and Calculation Systems for the study of wildland fire behavior. *Progress in Energy and Combustion Science, 29*, 139-153.

Pausas, J. G. (2004). Changes in Fire and Climate in the Eastern Iberian Peninsula (Mediterranean Basin). *Climatic Change, 67*, 337 - 350.

Pausas, J. G., & Vallejo, V. R. (1999). The role of fire in European Mediterranean Ecosystems. *Remote sensing of large wildfires in the European Mediterranean basin*, 3-16.

Peel, M. C., Finlayson, B. L., & McMahon, T. A. (2007). Updated world map of the Koppen-Geiger climate classification. *Hydrology and Earth System Sciences Discussions*, 437 - 473.

Pinol, J., Terradas, J., & Lloret, F. (1998). Climate Warming, Wildfire Hazard, and Wildfire Occurence in Coastal Eastern Spain. *Climatic Change, 35*, 345-357.

Pollet, J., & Brown, A. (2007). *Fuel Moisture Sampling Guide.* Guide , Utah State Office , Bureau of Land Management, Salt lake City .

Riano, D., Chuvieco, E., Salas, J., Palacios-Orueta, A., & Bastarrika, A. (2002). Generation of fuel type maps from Landsat TM images and ancillary data in Mediterranean ecosystems. *Canadian Journal of Forest Research, 32*, 1301-1315.

Risson, M. (1995). *Incidence de la Complexité du Milieu Physique et des Lois de Comportement sur la Résponse Hydrologique d'un Bassin Versant. Modèle de Représentation et de Dynamique. Application au Bassin de la Peyne (Hérault, France).* PhD Thesis , Université Montpelllier II, Montpellier.

Rothermel, R. (1972). A mahtematical model for predicting fire spread in wildland fuels. *Research Paper INT -115*, 1-40.

Rothermel, R., Wilson, R., Morris, G. A., & Sackett, S. S. (1986). *Modeling Moisture Content of Fine Dead Wildland Fuels.* February: United States Department of Agriculture, Forest Service.

Salis, M. (2007). *Fire Behavior Simulation in Mediterranean Maquis Using Farsite.* University of Sassari.

Scarascia-Mugnozza, G., Oswald, H., Piussi, P., & Radoglou, K. (2000). Forests of the Mediterranean region: gaps in knowledge and research needs. *Forest Ecology and Management, 132*, 97 - 107.

Schelhaas, M.-J., Nabuurs, G.-J., & Schuck, A. (2003). Natural disturbances in the European forests in the 19th and 20th centuries. *Global Change Biology, 9*, 1620 - 1633.

Schmuck, G., San-Miguel-Ayanz, J., Camia, A., Durrant, T., Santos de Oliveira, S., Boca, R., . . . Giovando, G. (2011). Forest Fires in Europe, Middle East and North Africa 2011. *EU Report* .

Scott, J. (2000, December). The Pre-Quaternary history of fire. *Palaeogeography, Palaeoclimatology, Palaeoecology, 164*(1 - 4), 281-329.

Scott, J. H., & Burgan, R. E. (2005). *Standard Fire Behavior Fuel Models: A Comprehensive Set for Use with Rothermel's Surface Fire Spread Model.* United States Department of Agriculture, Forest Service. Fort Collins: USDA Forest Service.

Scott, J. H., & Reinhardt, E. D. (2001). *Assesing Crown Fire Potential by Linking Models of Surface and Crown Fire Behavior.* Forest Service , United States Department of Agriculture. Fort Collins: USDA.

Sluiter, R. (2005). *Mediterranean land cover change.* Universiteit Utrecht, Faculteit Geowetenschappen. Utrecht : Labor Grafimedia b.v. .

Smith, K. (2001). *Enivronmental Hazards: Assesing Risk and Reducinig Disaster* (Third ed.). London, Great Britain: Routledge.

Stambaugh, M. C., Dey, D. C., Guyette, R. P., He, H. S., & Marschall, J. M. (2011). Spatial patterning of fuels and fire hazard across a central U.S. deciduous forest region. *Landscape Ecology, 26*, 923-935.

State of California. (n.d.). *Govenment Code 55602.* State of California.

The Guardian. (2009, October 19). Spanish wetlands shrouded in smoke as overfarming dries out peat. . (G. Tremlett, Ed.) *The Guardian* .

Utrecht University. (2013). *PCRaster*. Retrieved September 11, 2013, from http://pcraster.geo.uu.nl/

Van de Water, K., & North, M. (2011). Stand structure, fuel loads, and fire behavior in riparian and upland forests, Sierra Nevada Mountains, USA; a comparison of current and reconstructed conditions. *Forest Ecology and Management, 262*(2), 215-228.

Van Wagner, C. E. (1976). Conditions for the start and spread of crown fire. *Canadian Journal on Forest Research, 7*, 23-34.

Van Wagner, C. E. (1987). *Development and Structure of the Canadian Forest Fire Weather Index System.* Technical Report, Canadian Forestry Service, Ottawa Ontario.

Van Wagner, C. E., Stocks, B. J., Lawson, B. D., Alexander, M. E., Lynham, T. J., & McAlpine, R. S. (1992). *Development and Structure of the Canadian Forest Fire Behavior Prediction System.* Fire Danger Group, Forestry Canada . Ottowa: Catherine Carmody.

Vasilakos, C., Kalabokidis, K., Hatzopoulos, J., & Matsinos, I. (2008). Identifying wildland fire ignition factors through sensitivity analysis of a neural network. *Natural Hazards*, 1-19.

Viegas, D. X. (1998). Forest Fire Propgation. *Philosophical Transaction of the Royal Society, 356*, 2907-2928.

Viegas, D. X. (2002). Fire behavior models: an overview. In *Forest Fires: Ecology and Control* (pp. 37-47). Padova.

Viegas, D. X., Ribeiro, L. M., Palheiro, M. P., Pita, L. P., & Afonso, C. (2004). Slope and wind effects on fire spread. *International Journal of Wildland Fire, 13*, 143-156.

Weise, D. R., & Biging, G. S. (1997). A Qualitative Comparison of Fire Spread Models Incorporationg Wind and Slope Effects . *Forest Science, 43*(2), 170-180.

Wesseling, C., Karssenberg, D., van Deursen, W., & Burrough , P. (1996). Integrating environmental models in GIS: the development of a Dynamic Modelling language. *Transactions in GIS, 1*, 40-48.

Wilson, R. (1980). *Reformulation of Forest Fire Spread Equations in SI Units.* Ogden, Utah : USDA Forest Service.

Wotton, B. M. (2009). Interpreting and using outputs from the Canadian Forest Fire Danger Rating System in research applications. *Enivronmental and Ecological Statistics, 16*, 107-131.

Wotton, B. M., & Beverly, L. J. (2007, August). Stand-specific litter moisture content calibrations for the Canadian Fine Fuel Moisture Code . *International Journal of Wildland Fire, 16*(4), 463-472.

Ziel, R., & Jolly, M. (2009). Performance of fire behavior fuel models developed for the rothermel surface fire spread model. *Fire in Eastern Oak Forests Conference* (pp. 78-87). Newton Square: Department of Agriculture .

APPENDIX A

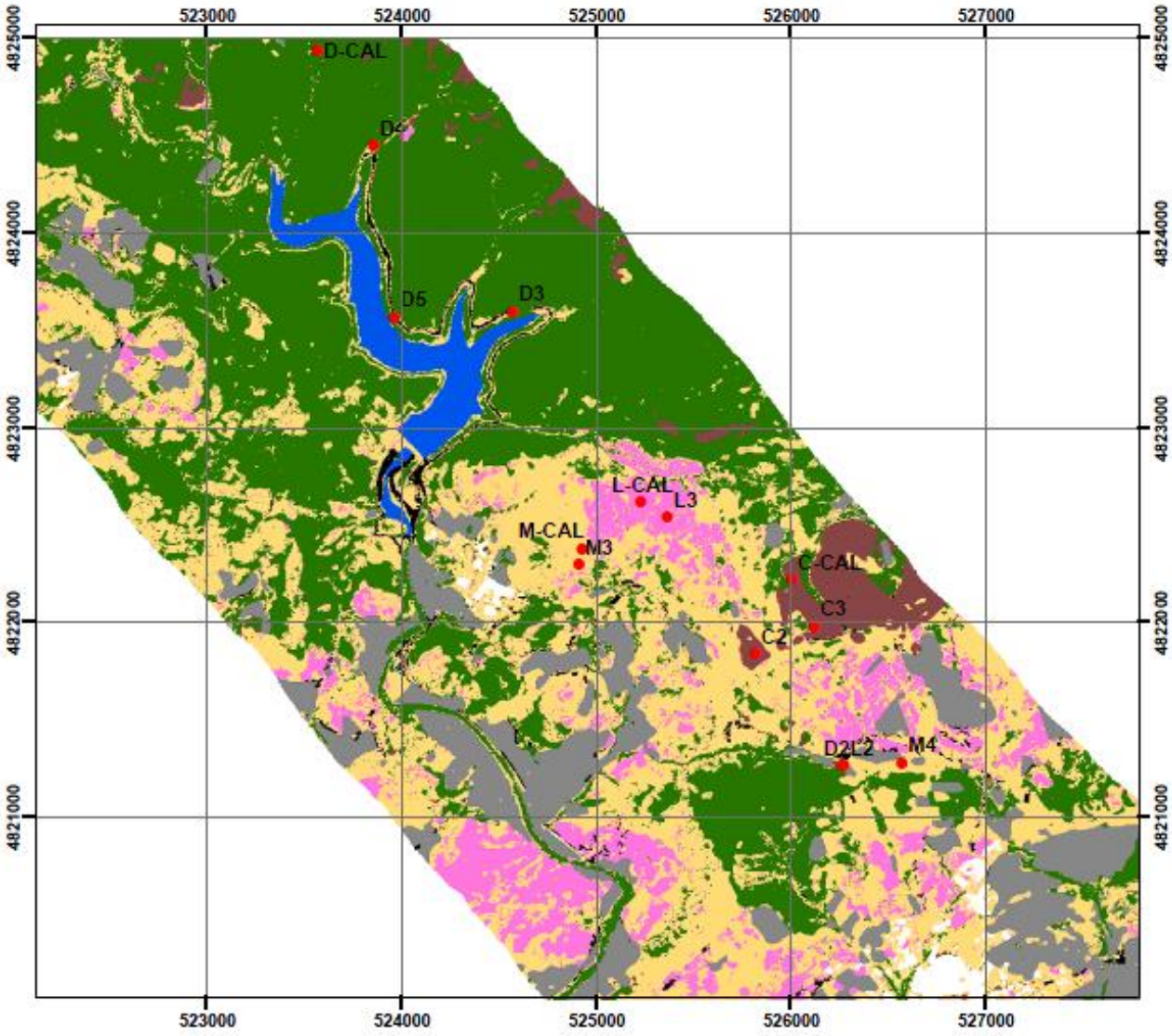

Ancillary Data Classification Model - Vegetation Map

Coordinate System: WGS 1984 UTM Zone 31N

1:30,000

Sources:

Sluiter (2005)

Made by: Niek Meijer (September 2013)

N W E S

0 0.5 1 2 Kilometers

Legend

- Sample_locations_GPS
- meteo
- Dense matorral
- Coniferous
- Middle matorral
- Low matorral
- Water
- Vineyards and other agricultural
- Roads and tracks
- Built-up

APPENDIX B

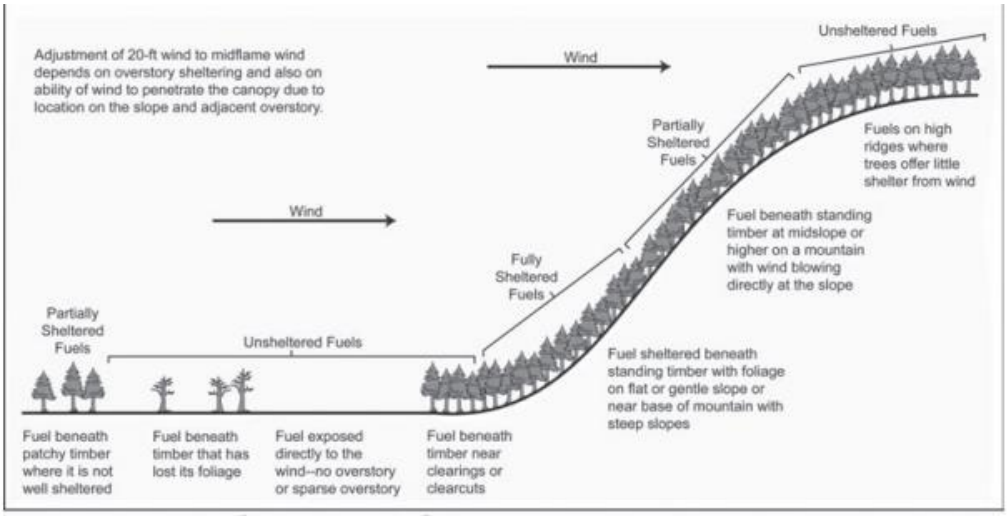

Surface fuel sheltering from the wind	Wind Adjustment Factor (WAF)	Fuel Model
Unsheltered • Surface fuels not sheltered from the wind • No overstory • Sparse overstory • Timber that has lost its foliage • Timber on high ridges where trees offer little sheltering	0.5	• 4, 13 • GR7, GR8, GR9 • SH4, SH5, SH7, SH8, SH9 (depth < 0.9 ft, < 0.3 m)
	0.4	• 1, 2, 3, 5, 6, 7, 10, 11, 12 • GR2, GR3, GR4, GR5, GR6 • GS1, GS2, GS3, GS4 • SH1, SH2, SH3, SH6 • TU2, TU3, TU5 • SB1, SB2, SB3, SB4 (depth 0.9 - 2.7 ft, 0.3 - 0.8 m)
	0.3	• 8, 9 • GR1 • TU1, TU4 • TL1, TL2, TL3, TL4, TL5, TL6, TL7, TL8, TL9 (depth > 2.7 ft, > 0.8 m)
Partially sheltered • Patchy timber • Timber at midslope or higher with wind blowing directly at the slope	0.3	• All fuel models
Fully Sheltered • Standing timber on flat or gentle slope • Standing timber near base of mountain with steep slopes	0.2	• **Open stands.** All fuel models
	0.1	• **Dense stands.** All fuel models

From the BehavePlus Wind Ajustment Factor help window. The diagram illustrates sheltering conditions described on the table. The unsheltered wind adjustment factor is based on the fuel bed depth (Rothermel, et al., 1986).

APPENDIX C

Carrier	FM #	FM Code	Fuel Model Name	1hr Load	10hr Load	100hr Load	Herb Load	Woody Load	Total Load	Dynamic	1hr SAV	Herb SAV	Woody SAV	Bed Depth	Moist Extinct	Dead Heat	Live Heat
GR	1	FB1	Short grass	0.7	0.0	0.0	0.0	0.0	0.7	static	3500	9999	9999	1.0	12	8000	8000
GR	2	FB2	Timber grass and understory	2.0	1.0	0.5	0.5	0.0	4.0	static	3000	1500	9999	1.0	15	8000	8000
GR	3	FB3	tall grass	3.0	0.0	0.0	0.0	0.0	3.0	static	1500	9999	9999	2.5	25	8000	8000
GR	101	GR1	Short, sparse dry climate grass	0.1	0.0	0.0	0.3	0.0	0.4	dynamic	2200	2000	9999	0.4	15	8000	8000
GR	102	GR2	Low load dry climate grass	0.1	0.0	0.0	1.0	0.0	1.1	dynamic	2000	1800	9999	1.0	15	8000	8000
GR	103	GR3	Low load very coarse humid climate grass	0.1	0.4	0.0	1.5	0.0	2.0	dynamic	1500	1300	9999	2.0	30	8000	8000
GR	104	GR4	Moderate load dry climate grass	0.3	0.0	0.0	1.9	0.0	2.2	dynamic	2000	1800	9999	2.0	15	8000	8000
GR	105	GR5	low load humid climate grass	0.4	0.0	0.0	2.5	0.0	2.9	dynamic	1800	1600	9999	1.5	40	8000	8000
GR	106	GR6	moderate load humid climate grass	0.1	0.0	0.0	3.4	0.0	3.5	dynamic	2200	2000	9999	1.5	40	9000	9000
GR	107	GR7	High load dry climate grass	1.0	0.0	0.0	5.4	0.0	6.4	dynamic	2000	1800	9999	3.0	15	8000	8000
GR	108	GR8	High load very coarse humid climate grass	0.5	1.0	0.0	7.3	0.0	8.8	dynamic	1500	1300	9999	4.0	30	8000	8000
GR	109	GR9	very high load humid climate grass	1.0	1.0	0.0	9.0	0.0	11.0	dynamic	1800	1600	9999	5.0	40	8000	8000
GS	121	GS1	low load dry climate grass-shrub	0.2	0.0	0.0	0.5	0.7	1.4	dynamic	2000	1800	1800	0.9	15	8000	8000
GS	122	GS2	moderate load dry climate grass-shrub	0.5	0.5	0.0	0.6	1.0	2.6	dynamic	2000	1800	1800	1.5	15	8000	8000
GS	123	GS3	moderate load humid climate grass-shrub	0.3	0.3	0.0	1.5	1.3	3.3	dynamic	1800	1600	1600	1.8	40	8000	8000
GS	124	GS4	high load humid climate grass-shrub	1.9	0.3	0.1	3.4	7.1	12.8	dynamic	1800	1600	1600	2.1	40	8000	8000
SH	4	FB4	chaparral	5.0	4.0	2.0	0.0	5.0	16.0	static	2000	9999	1500	6.0	20	8000	8000
SH	5	FB5	brush	1.0	0.5	0.0	0.0	2.0	3.5	static	2000	9999	1500	2.0	20	8000	8000
SH	6	FB6	dormant brush	1.5	2.5	2.0	0.0	0.0	6.0	static	1750	9999	9999	2.5	25	8000	8000
SH	7	FB7	southern rough	1.1	1.9	1.5	0.0	0.4	4.9	static	1750	9999	1500	2.5	40	8000	8000
SH	141	SH1	low load dry climate shrub	0.3	0.3	0.0	0.2	1.3	2.0	dynamic	2000	1800	1600	1.0	15	8000	8000
SH	142	SH2	moderate load dry climate shrub	1.4	2.4	0.8	0.0	3.9	8.4	static	2000	9999	1600	1.0	15	8000	8000
SH	143	SH3	moderate load humid climate shrub	0.5	3.0	0.0	0.0	6.2	9.7	static	1600	9999	1400	2.4	40	8000	8000
SH	144	SH4	low load humid climate timber-shrub	0.9	1.2	0.2	0.0	2.6	4.8	static	2000	1800	1600	3.0	30	8000	8000
SH	145	SH5	high load dry climate shrub	3.6	2.1	0.0	0.0	2.9	8.6	static	750	9999	1600	6.0	15	8000	8000
SH	146	SH6	low load humid climate shrub	2.9	1.5	0.0	0.0	1.4	5.8	static	750	9999	1600	2.0	30	8000	8000
SH	147	SH7	very high load dry climate shrub	3.5	5.3	2.2	0.0	3.4	14.4	static	750	9999	1600	6.0	15	8000	8000
SH	148	SH8	high load humid climate shrub	2.1	3.4	0.9	0.0	4.4	10.7	static	750	9999	1600	3.0	40	8000	8000
SH	149	SH9	very high load humid climate shrub	4.5	2.5	0.0	1.6	7.0	15.5	dynamic	750	1800	1500	4.4	40	8000	8000
TU	10	FB10	timber litter and understory	3.0	2.0	5.0	0.0	2.0	12.0	static	2000	9999	1500	1.0	25	8000	8000
TU	161	TU1	light load dry climate timber-grass-shrub	0.2	0.9	1.5	0.2	0.9	3.7	dynamic	2000	1800	1600	0.6	20	8000	8000
TU	162	TU2	moderate load humid climate timber-shrub	1.0	1.8	1.3	0.0	0.2	4.2	static	2000	9999	1600	1.0	30	8000	8000
TU	163	TU3	moderate load humid climate timber-grass-shrub	1.1	0.2	0.3	0.7	1.1	3.3	dynamic	1800	1600	1400	1.3	30	8000	8000
TU	164	TU4	dwarf conifer with understory	4.5	0.0	0.0	0.0	2.0	6.5	static	2300	9999	2000	0.5	12	8000	8000
TU	165	TU5	very high load dry climate timber-shrub	4.0	4.0	3.0	0.0	3.0	14.0	static	1500	9999	750	1.0	25	8000	8000
TL	8	FB8	compact timber litter	1.5	1.0	2.5	0.0	0.0	5.0	static	2000	9999	9999	0.2	30	8000	8000
TL	9	FB9	hardwood litter	2.9	0.4	0.2	0.0	0.0	3.5	static	2500	9999	9999	0.2	25	8000	8000
TL	181	TL1	Low load compact conifer litter	1.0	2.2	3.6	0.0	0.0	6.8	static	2000	9999	9999	0.2	30	8000	8000
TL	182	TL2	low load broadleaf litter	1.4	2.3	2.2	0.0	0.0	5.9	static	2000	9999	9999	0.2	25	8000	8000
TL	183	TL3	moderate load conifer litter	0.5	2.2	2.8	0.0	0.0	5.5	static	2000	9999	9999	0.3	20	8000	8000
TL	184	TL4	Small downed logs	0.5	1.5	4.2	0.0	0.0	6.2	static	2000	9999	9999	0.4	25	8000	8000
TL	185	TL5	high load conifer litter	1.2	2.5	4.4	0.0	0.0	8.1	static	2000	9999	1600	0.6	25	8000	8000
TL	186	TL6	moderate load broadleaf litter	2.4	1.2	1.2	0.0	0.0	4.8	static	2000	9999	9999	0.3	25	8000	8000
TL	187	TL7	Large downed logs	0.3	1.4	8.1	0.0	0.0	9.8	static	2000	9999	9999	0.4	25	8000	8000
TL	188	TL8	long-needle litter	5.8	1.4	1.1	0.0	0.0	8.3	static	1800	9999	9999	0.3	35	8000	8000
TL	189	TL9	very high load broadleaf litter	6.7	3.3	4.2	0.0	0.0	14.1	static	1800	9999	1600	0.6	35	8000	8000
SB	11	FB11	light slash	1.5	4.5	5.5	0.0	0.0	11.5	static	1500	9999	9999	1.0	15	8000	8000
SB	12	FB12	medium slash	4.0	14.0	16.5	0.0	0.0	34.6	static	1500	9999	9999	2.3	20	8000	8000
SB	13	FB13	heavy slash	7.0	23.0	28.1	0.0	0.0	58.1	static	1500	9999	9999	3.0	25	8000	8000
SB	201	SB1	low load activity fuel	1.5	3.0	11.0	0.0	0.0	15.5	static	2000	9999	9999	1.0	25	8000	8000
SB	202	SB2	moderate load activity or low load blowdown	4.5	4.3	4.0	0.0	0.0	12.8	static	2000	9999	9999	1.0	25	8000	8000
SB	203	SB3	high load activity fuel or moderate load blowdown	5.5	2.8	3.0	0.0	0.0	11.3	static	2000	9999	9999	1.2	25	8000	8000
SB	204	SB4	high load blowdown	5.3	3.5	5.3	0.0	0.0	14.0	static	2000	9999	9999	2.7	25	8000	8000

Fuel model parameters for use with the Rothermel surface fire spread model; dynamic models are shaded. All 53 fuel models and the characteristic model parameters are listed (Ziel & Jolly, 2009).

APPENDIX D

Weighting factors for calculating weighted-average dead fuel moisture content, presence of live fuel component, and wind adjustment factor (WAF) for the original 13 and new 40 fire behavior fuel models. Weighting factors assume all herbaceous load is in the 1-h class (full curing). WAF values were estimated using Albini and Baughman's (1979) model of wind reduction over exposed fuelbeds on flat terrain assuming flame height is twice fuelbed depth.

	Weighting factors			Live fuel		
Fuel model	1-h	10-h	100-h	Herb	Woody	WAF
1	1.00	0.00	0.00			0.36
2	0.98	0.02	0.00	√		0.36
3	1.00	0.00	0.00			0.44
4	0.95	0.04	0.01		√	0.55
5	0.97	0.03	0.00		√	0.42
6	0.89	0.09	0.02			0.44
7	0.89	0.09	0.02		√	0.44
8	0.94	0.03	0.02			0.28
9	0.99	0.01	0.00			0.28
10	0.94	0.03	0.02		√	0.36
11	0.77	0.17	0.06			0.36
12	0.75	0.19	0.06			0.43
13	0.76	0.18	0.06			0.46
GR1	1.00	0.00	0.00	√		0.31
GR2	1.00	0.00	0.00	√		0.36
GR3	0.98	0.02	0.00	√		0.42
GR4	1.00	0.00	0.00	√		0.42
GR5	1.00	0.00	0.00	√		0.39
GR6	1.00	0.00	0.00	√		0.39
GR7	1.00	0.00	0.00	√		0.46
GR8	0.99	0.01	0.00	√		0.49
GR9	0.99	0.01	0.00	√		0.52
GS1	1.00	0.00	0.00	√	√	0.35
GS2	0.97	0.03	0.00	√	√	0.39
GS3	0.99	0.01	0.00	√	√	0.41
GS4	1.00	0.00	0.00	√	√	0.42
SH1	0.97	0.03	0.00	√	√	0.36
SH2	0.90	0.09	0.01		√	0.36
SH3	0.69	0.31	0.00		√	0.44
SH4	0.93	0.07	0.00		√	0.46
SH5	0.92	0.08	0.00		√	0.55
SH6	0.93	0.07	0.00		√	0.42
SH7	0.80	0.18	0.02		√	0.55
SH8	0.80	0.19	0.01		√	0.46
SH9	0.96	0.04	0.00	√	√	0.50
TU1	0.84	0.11	0.05	√	√	0.33
TU2	0.89	0.09	0.02		√	0.36
TU3	0.99	0.01	0.00	√	√	0.38
TU4	1.00	0.00	0.00		√	0.32
TU5	0.92	0.07	0.01		√	0.36
TL1	0.85	0.10	0.05			0.28
TL2	0.90	0.08	0.02			0.28
TL3	0.76	0.18	0.06			0.29
TL4	0.78	0.13	0.10			0.31
TL5	0.85	0.10	0.05			0.33
TL6	0.97	0.03	0.01			0.29
TL7	0.60	0.15	0.24			0.31
TL8	0.98	0.01	0.00			0.29
TL9	0.96	0.03	0.01			0.33
SB1	0.82	0.09	0.09			0.36
SB2	0.94	0.05	0.01			0.36
SB3	0.97	0.03	0.01			0.38
SB4	0.95	0.03	0.01			0.45

APPENDIX E

Meteostation-observations at 14:00 for temperature, relative humidity, solar radiation and windspeed plus the 24-hour accumulated rainfall from June 1, 2013 until September 8, 2013. The fieldwork period (August 27, 2013 – September 6, 2013) is marked in red.

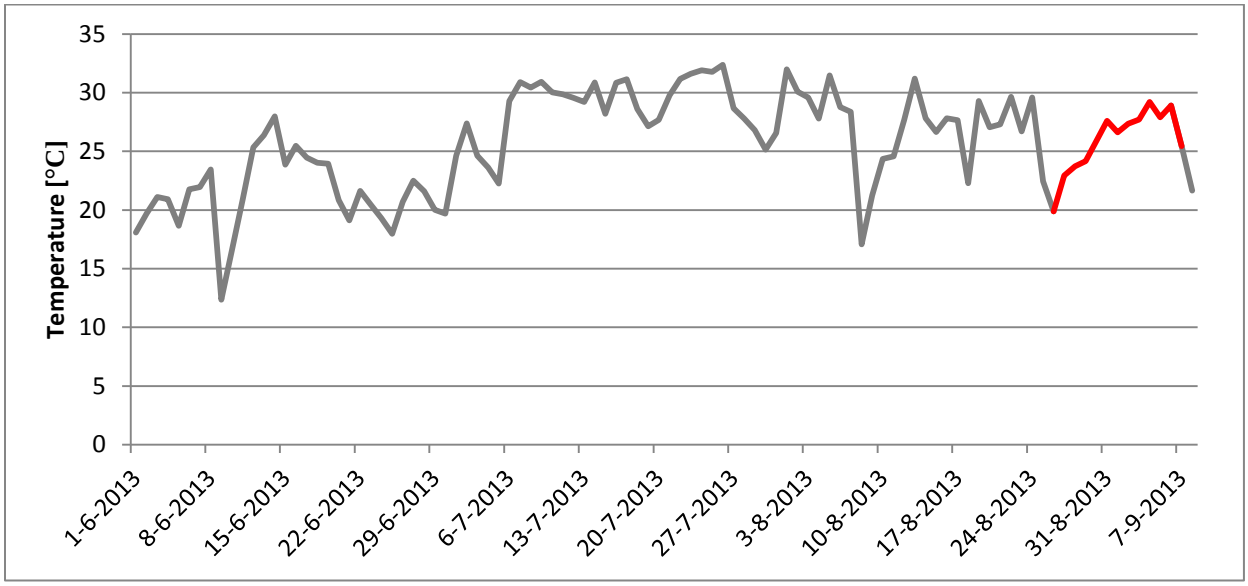

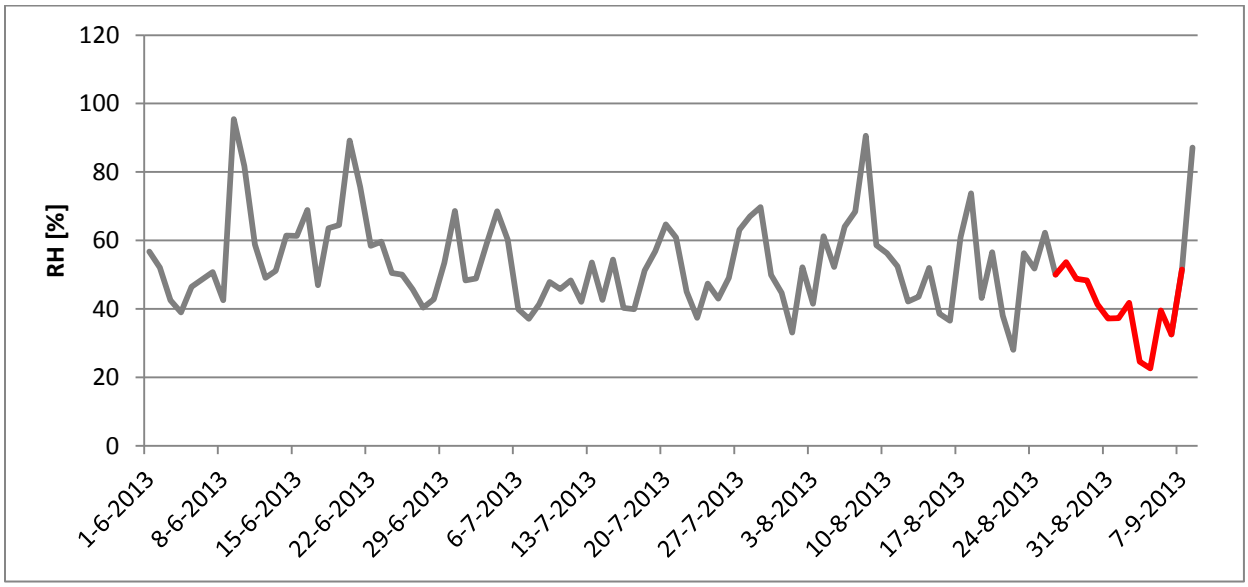

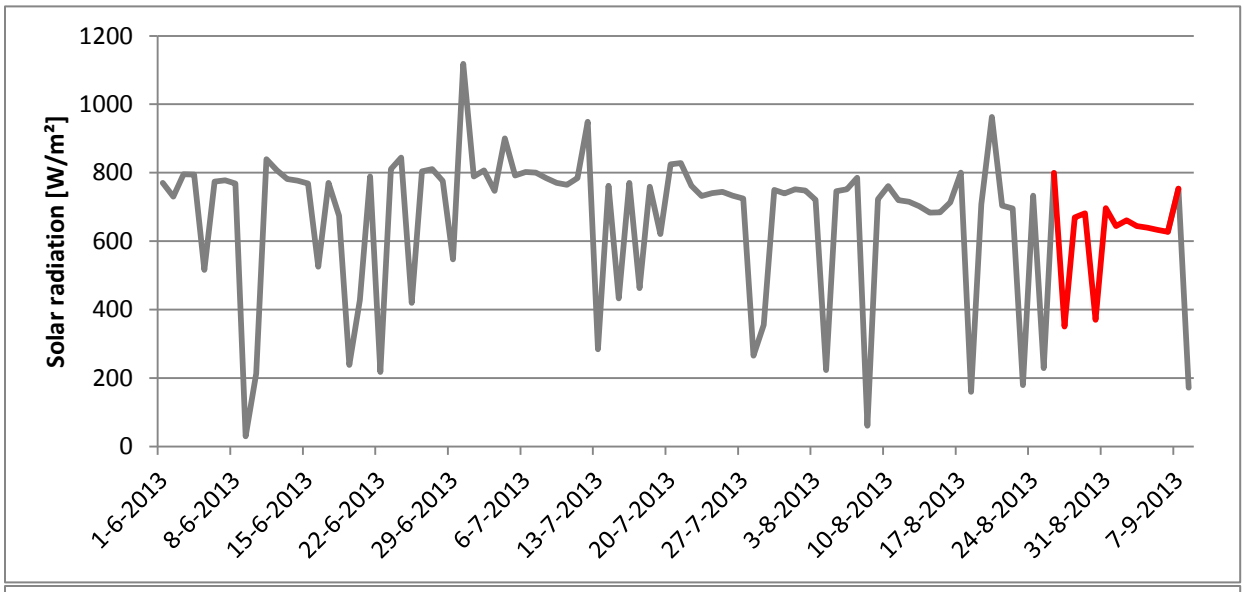
Solar radiation [W/m²]
1200
1000
800
600
400
200
0
1-6-2013
8-6-2013
15-6-2013
22-6-2013
29-6-2013
6-7-2013
13-7-2013
20-7-2013
27-7-2013
3-8-2013
10-8-2013
17-8-2013
24-8-2013
31-8-2013
7-9-2013

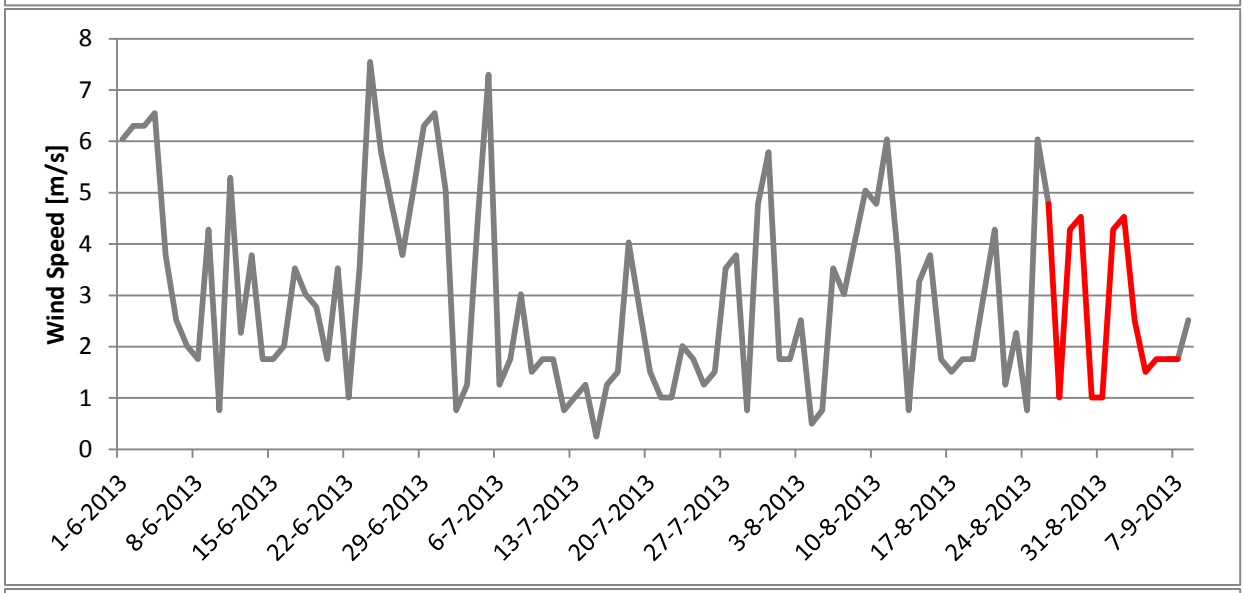
Wind Speed [m/s]
8
7
6
5
4
3
2
1
0
1-6-2013
8-6-2013
15-6-2013
22-6-2013
29-6-2013
6-7-2013
13-7-2013
20-7-2013
27-7-2013
3-8-2013
10-8-2013
17-8-2013
24-8-2013
31-8-2013
7-9-2013

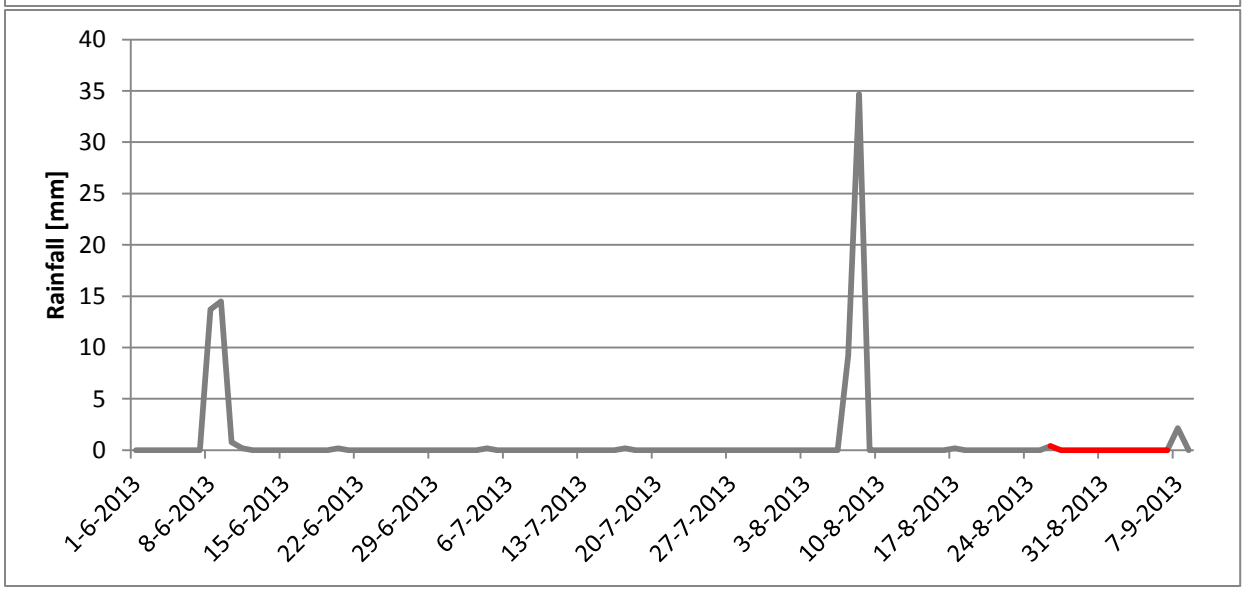
Rainfall [mm]
40
35
30
25
20
15
10
5
0
1-6-2013
8-6-2013
15-6-2013
22-6-2013
29-6-2013
6-7-2013
13-7-2013
20-7-2013
27-7-2013
3-8-2013
10-8-2013
17-8-2013
24-8-2013
31-8-2013
7-9-2013

APPENDIX F

The data acquired during the fieldwork period per plot, showing the date, time, infrared temperature of fuels in the sun (when available) and shade, the relative humidity, wet bulb temperature and related fuel moisture content.

D-Cal	Date	Time	IR sun (°C)	IR shade (°C)	RH (%)	Wet Bulb (°C)	Fuel Moisture Content (%)
	27-aug	13:15	26	23	41,5	15,9	12,80%
	28-aug	18:25		24	42,33	17,93	25,98%
	29-aug	12:40	25	24	36,02	18,58	18,03%
	30-aug	12:20	28	24	30,6	18,12	14,70%
	31-aug	12:30	30	26	33,42	17,35	12,03%
	1-sep	12:30	33	26	32,41	17,91	11,02%
	2-sep	12:30	26	23	22,67	13,95	10,28%
	3-sep						
	4-sep	15:25	43	29	32,59	19,21	10,18%
	5-sep	12:30	27	24	41,06	17,3	11,84%
	6-sep	11:35		23	58,97	18,33	12,65%
D2	**Date**	**Time**	**IR sun (°C)**	**IR shade (°C)**	**RH (%)**	**Wet Bulb (°C)**	**Fuel Moisture Content (%)**
	27-aug	18:20		24	41,75	16,08	11,58%
	28-aug	17:45		25	34,28	17,43	10,59%
	29-aug	13:25		25	31,98	17,56	11,64%
	30-aug	13:15		26	29,68	17,23	10,11%
	31-aug	13:15	33	25	27,08	17,98	10,00%
	1-sep	13:10	30	26	28,78	19,29	10,02%
	2-sep	13:40	37	26	11,49	15,73	8,99%
	3-sep						
	4-sep	14:40	39	29	31,42	18,5	8,70%
	5-sep	13:10	33	28	26,35	16,57	9,82%
	6-sep	12:40		25	48,18	19,23	10,50%
D3	**Date**	**Time**	**IR sun (°C)**	**IR shade (°C)**	**RH (%)**	**Wet Bulb (°C)**	**Fuel Moisture Content (%)**
	27-aug	14:00	29	26	35	17,74	13,38%
	28-aug	18:00	28	26	31,81	16,68	9,22%
	29-aug	13:05	29	26	33,93	17,3	7,46%
	30-aug	12:55	35	26	28,04	18,76	9,77%
	31-aug	12:55	33	28	28,53	17,7	9,52%
	1-sep	12:55	31	28	29,68	18,86	9,27%
	2-sep	13:10	37	28	14,4	15,9	7,98%
	3-sep						
	4-sep	14:55	35	29	31,61	18,97	9,55%
	5-sep	12:50	34	28	30,52	20,05	9,28%
	6-sep	12:15	35	25	46,19	19,6	10,85%

D4	Date	Time	IR sun (°C)	IR shade (°C)	RH (%)	Wet Bulb (°C)	Fuel Moisture Content (%)
	27-aug	13:30	37	25	40	17,5	11,41%
	28-aug	18:15		25	41,07	17,58	8,99%
	29-aug	12:50	36	25	34,71	19,44	11,26%
	30-aug	12:30	34	28	31,45	18,62	10,08%
	31-aug	12:40	34	28	31,31	18,26	9,31%
	1-sep	12:40	36	28	30,31	19,16	9,91%
	2-sep	12:40	30	25	22,76	15,18	8,19%
	3-sep						
	4-sep	15:15	33	28	34,02	19,06	8,09%
	5-sep	12:35	37	28	35,86	18,31	9,81%
	6-sep	11:55	30	24	55,07	29,35	10,88%
D5	Date	Time	IR sun (°C)	IR shade (°C)	RH (%)	Wet Bulb (°C)	Fuel Moisture Content (%)
	27-aug	13:40	39	24	40,3	17,38	12,05%
	28-aug	18:10	27	26	35,74	18,3	9,80%
	29-aug	13:00	29	25	33,86	18,86	11,34%
	30-aug	12:47	45	26	32,8	18,21	10,31%
	31-aug	12:45	35	26	30,27	17,61	10,64%
	1-sep	12:45	32	26	33,08	19,31	10,38%
	2-sep	12:55	36	25	22,3	15,22	9,16%
	3-sep						
	4-sep	15:10	35	29	34,23	19,31	10,27%
	5-sep	12:45	34	25	35,55	18,45	11,33%
	6-sep	12:05	26	24	49,03	19,24	11,35%
C-Cal	Date	Time	IR sun (°C)	IR shade (°C)	RH (%)	Wet Bulb (°C)	Fuel Moisture Content (%)
	27-aug	17:15		24	37,08	17,18	9,42%
	28-aug	16:58	25	24	43,37	18,66	33,19%
	29-aug	15:39		30	40	19,53	12,60%
	30-aug	15:50	40	30	20,56	19,75	7,89%
	31-aug	15:35	38	30	25,83	18,59	8,15%
	1-sep	15:30	40	32	23,2	18,87	8,43%
	2-sep	14:50	39	28	9,55	16,49	7,58%
	3-sep						
	4-sep	13:25	36	26	32,75	19,72	9,19%
	5-sep	14:45	37	28	17,59	17,54	8,74%
	6-sep	13:45		30	39,82	19,97	9,30%
C2	Date	Time	IR sun (°C)	IR shade (°C)	RH (%)	Wet Bulb (°C)	Fuel Moisture Content (%)
	27-aug	16:50	30	24	32	17,43	10,46%
	28-aug	16:36	34	29	24,01	21,61	9,03%
	29-aug	15:25		26	30,25	18,16	9,48%
	30-aug	15:37	41	29	19,36	18,51	7,23%
	31-aug	15:20	44	32	22,93	18,89	8,72%
	1-sep	15:15	48	29	22,37	19,36	9,04%
	2-sep	15:00	46	22	9,32	14,77	7,97%
	3-sep						
	4-sep	13:20	34	26	32,29	20,96	8,22%
	5-sep	14:35	35	28	16,12	18,05	8,29%
	6-sep	14:00	44	30	38,16	20,33	10,05%

C3	Date	Time	IR sun (°C)	IR shade (°C)	RH (%)	Wet Bulb (°C)	Fuel Moisture Content (%)
	27-aug	17:00	33	25	33,6	17	9,40%
	28-aug	16:52	34	28	28,76	17,98	8,41%
	29-aug	15:45	35	28	30,05	19,56	7,98%
	30-aug	16:00	44	31	23,21	17,83	7,86%
	31-aug	15:40	45	28	23,39	17,44	7,10%
	1-sep	15:40	47	29	21,87	18,14	7,63%
	2-sep	14:45	44	30	9,25	15,35	7,11%
	3-sep						
	4-sep	13:35	44	30	33,03	18,62	7,46%
	5-sep	14:50	39	29	20,25	17,99	6,58%
	6-sep	13:35	50	31	35,73	21,6	8,01%
M-Cal	Date	Time	IR sun (°C)	IR shade (°C)	RH (%)	Wet Bulb (°C)	Fuel Moisture Content (%)
	27-aug	15:15	31	24	35,3	16,7	9,78%
	28-aug	16:32	25	26	67,77	18,35	31,39%
	29-aug	14:45		28	41,71	20,07	14,19%
	30-aug	15:00	45	30	27,91	18,89	8,72%
	31-aug	14:35	48	31	26,18	18,59	7,38%
	1-sep	14:35	48	30	29,56	18,69	7,30%
	2-sep	15:40	50	30	11,35	16,72	4,40%
	3-sep						
	4-sep	12:55	39	34	24	22,17	7,05%
	5-sep	14:15	44	34	15,34	19,99	4,93%
	6-sep	15:00	46	28	31,68	20,17	6,35%
M3	Date	Time	IR sun (°C)	IR shade (°C)	RH (%)	Wet Bulb (°C)	Fuel Moisture Content (%)
	27-aug	15:50	30	25	35,3	16,8	7,42%
	28-aug	16:14	38	32	29,13	18,51	4,94%
	29-aug	14:35		32	22,64	18,68	5,95%
	30-aug	14:35	52	37	19,04	20,02	5,84%
	31-aug	14:25	58	35	15,1	20,2	5,21%
	1-sep	14:25	57	37	22,43	21,87	4,73%
	2-sep	15:31	55	35	5,87	16,14	3,29%
	3-sep						
	4-sep	12:50	45	37	31,86	20,07	5,28%
	5-sep	14:05	43	36	15,33	19,09	2,60%
	6-sep	14:45	50	36	28,38	21,67	6,22%
M4	Date	Time	IR sun (°C)	IR shade (°C)	RH (%)	Wet Bulb (°C)	Fuel Moisture Content (%)
	27-aug	18:41		24	45,15	17,78	9,05%
	28-aug	17:34	30	28	29,8	18,07	7,56%
	29-aug	13:40		28	31,43	18,56	7,61%
	30-aug	13:25	30	26	36,15	19,14	7,10%
	31-aug	13:25	35	28	24,83	17,92	6,37%
	1-sep	13:20	39	29	28,65	18,14	6,93%
	2-sep	13:45	50	30	10,55	16,04	7,31%
	3-sep						
	4-sep	14:30	48	29	39,75	20,19	7,22%
	5-sep	13:20	45	31	21,73	18,14	7,20%
	6-sep	12:45		27	40,35	21,26	7,42%

L-Cal	Date	Time	IR sun (°C)	IR shade (°C)	RH (%)	Wet Bulb (°C)	Fuel Moisture Content (%)
	27-aug	16:10	36	27	32	17,71	7,20%
	28-aug	16:04		35	28,8	19,02	6,47%
	29-aug	15:00		32	28,78	18,63	6,47%
	30-aug	15:15	40	39	16,1	19,92	6,16%
	31-aug	14:50	42	34	13,57	21,52	5,46%
	1-sep	14:50	40	32	16,07	20,51	5,76%
	2-sep	15:55	44	35	6,45	17,23	3,39%
	3-sep						
	4-sep	13:05	44	38	19,05	23,7	5,34%
	5-sep	14:20	45	36	11,84	21,42	4,76%
	6-sep	15:10	40	33	22,75	23,26	5,66%
L2	Date	Time	IR sun (°C)	IR shade (°C)	RH (%)	Wet Bulb (°C)	Fuel Moisture Content (%)
	27-aug	18:20		27	35,5	17,4	7,12%
	28-aug	17:42	29	28	27,86	18,76	5,22%
	29-aug	13:21	31	27	27,1	20,83	5,14%
	30-aug	13:10		26	24,36	18,71	5,54%
	31-aug	13:10	37	33	15,71	21,67	6,01%
	1-sep	13:05	37	32	23,51	14,12	4,87%
	2-sep	13:30	41	32	4,73	19,16	4,82%
	3-sep						
	4-sep	14:35	40	32	24,82	20,23	5,92%
	5-sep	13:05	39	34	19,7	20,66	4,93%
	6-sep	12:35		30	37,18	21,47	6,79%
L3	Date	Time	IR sun (°C)	IR shade (°C)	RH (%)	Wet Bulb (°C)	Fuel Moisture Content (%)
	27-aug	16:25	31	28	27,1	17,3	5,55%
	28-aug	15:54		36	24,04	18,76	5,64%
	29-aug	15:05		31	22,93	19,18	5,58%
	30-aug	15:25	44	31	13,08	20,35	4,65%
	31-aug	15:00	44	34	15,9	19,61	4,59%
	1-sep	14:55	44	34	17,31	20,61	3,04%
	2-sep	16:00	46	34	4,85	16,84	2,69%
	3-sep						
	4-sep	13:10	46	35	19,96	24,77	5,02%
	5-sep	14:30	50	37	11,59	21,67	3,23%
	6-sep	14:25	43	34	24,34	22,72	4,53%

APPENDIX G

The graphs below show the modeled and observed moisture values during the fieldwork period (August 27, 2013 – September 6, 2013). The calibrated FFMC model is illustrated by the continuous black line the uncalibrated FFMC model by the dotted black line. The 95% confidence interval is the gray shaded area and its width is noted in the legend. The observed values are in red.

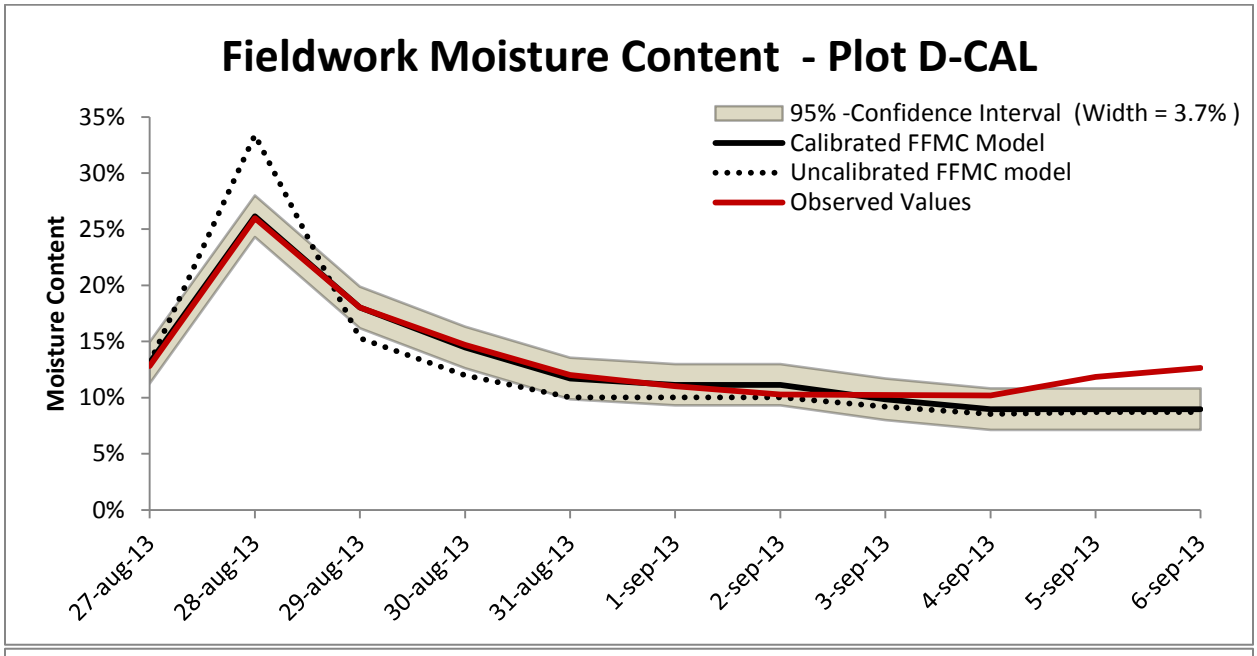

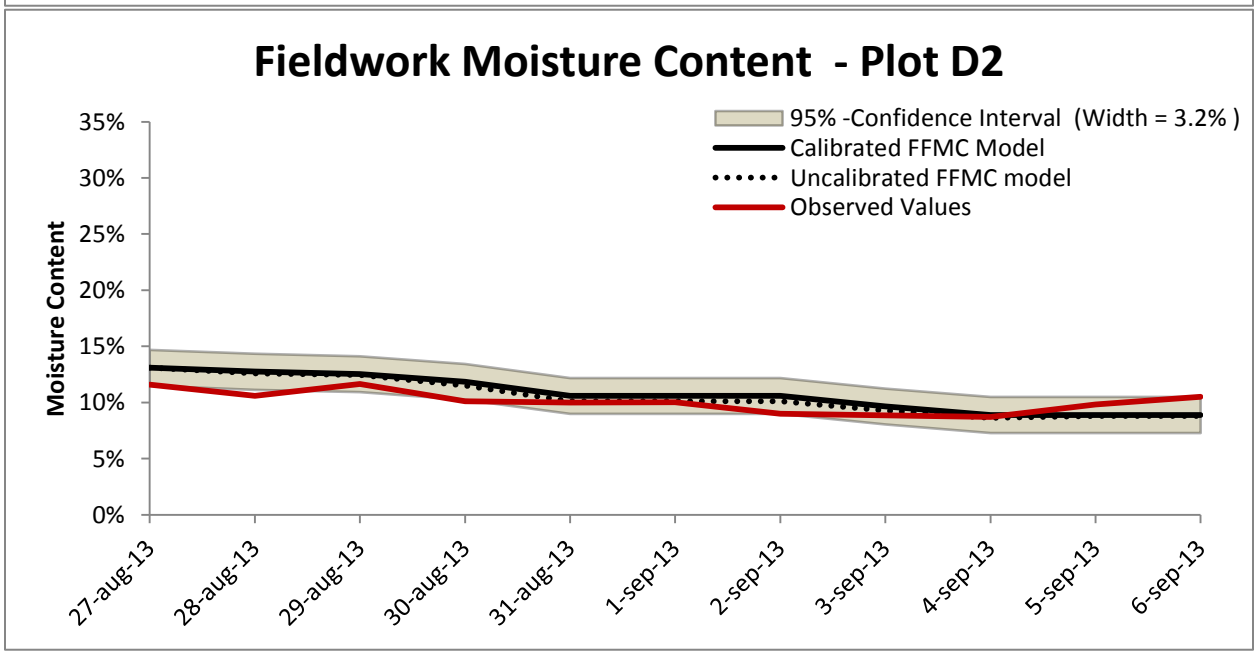

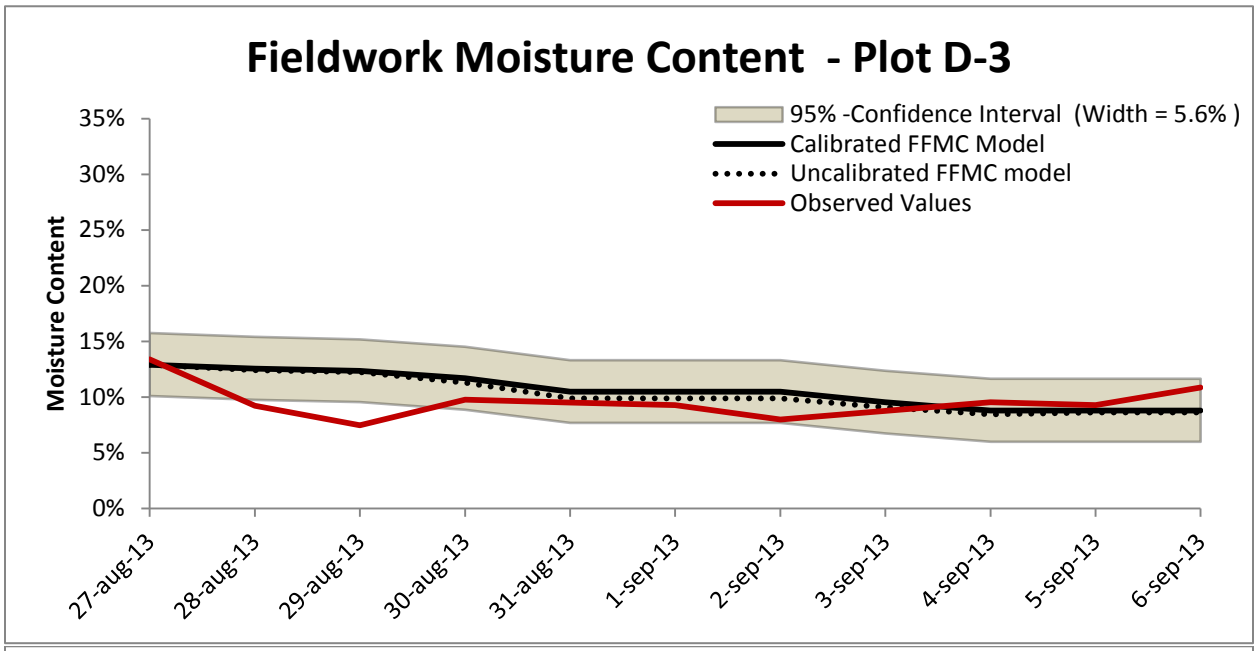
Fieldwork Moisture Content - Plot D-3
95% -Confidence Interval (Width = 5.6%)
Calibrated FFMC Model
Uncalibrated FFMC model
Observed Values
Moisture Content
35%
30%
25%
20%
15%
10%
5%
0%
27-aug-13
28-aug-13
29-aug-13
30-aug-13
31-aug-13
1-sep-13
2-sep-13
3-sep-13
4-sep-13
5-sep-13
6-sep-13

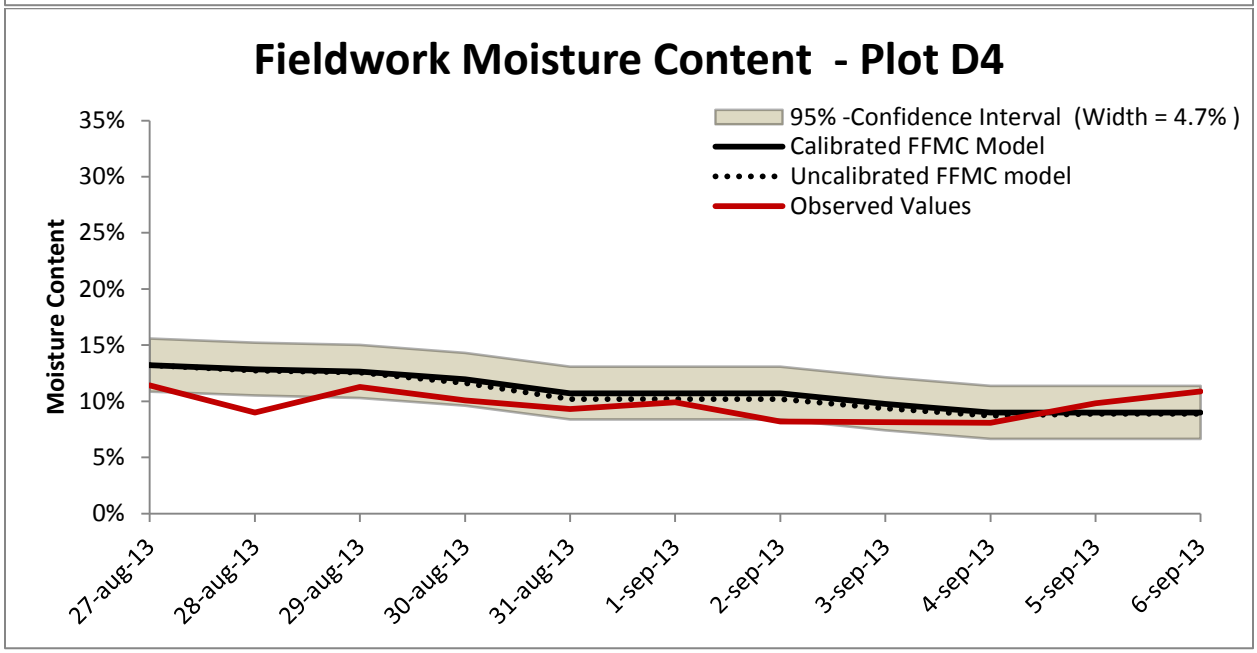
Fieldwork Moisture Content - Plot D4
95% -Confidence Interval (Width = 4.7%)
Calibrated FFMC Model
Uncalibrated FFMC model
Observed Values
Moisture Content
35%
30%
25%
20%
15%
10%
5%
0%
27-aug-13
28-aug-13
29-aug-13
30-aug-13
31-aug-13
1-sep-13
2-sep-13
3-sep-13
4-sep-13
5-sep-13
6-sep-13

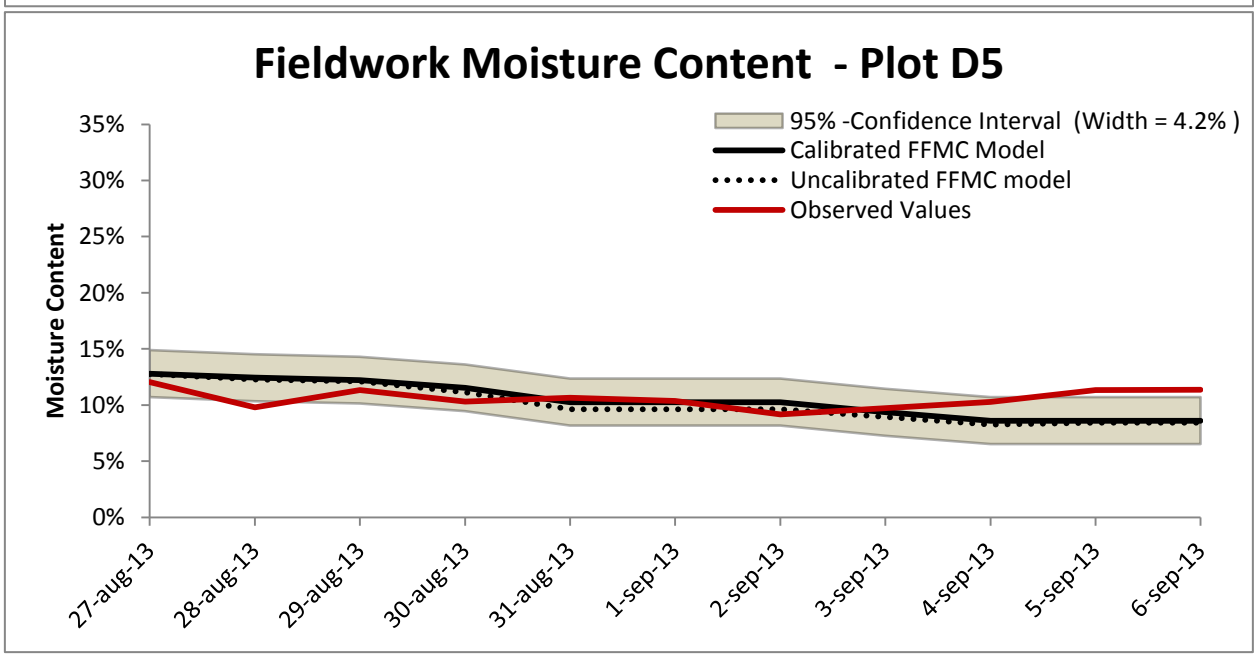
Fieldwork Moisture Content - Plot D5
95% -Confidence Interval (Width = 4.2%)
Calibrated FFMC Model
Uncalibrated FFMC model
Observed Values
Moisture Content
35%
30%
25%
20%
15%
10%
5%
0%
27-aug-13
28-aug-13
29-aug-13
30-aug-13
31-aug-13
1-sep-13
2-sep-13
3-sep-13
4-sep-13
5-sep-13
6-sep-13

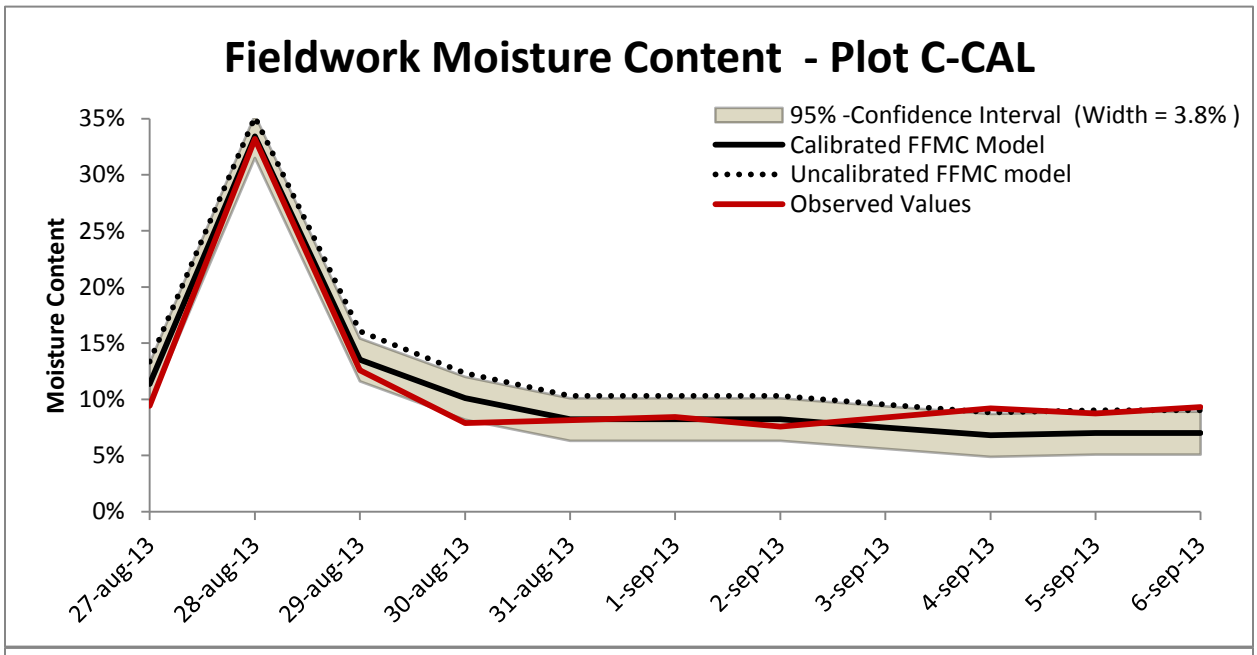
Fieldwork Moisture Content - Plot C-CAL
95% -Confidence Interval (Width = 3.8%)
Calibrated FFMC Model
Uncalibrated FFMC model
Observed Values
Moisture Content
35%
30%
25%
20%
15%
10%
5%
0%
27-aug-13
28-aug-13
29-aug-13
30-aug-13
31-aug-13
1-sep-13
2-sep-13
3-sep-13
4-sep-13
5-sep-13
6-sep-13

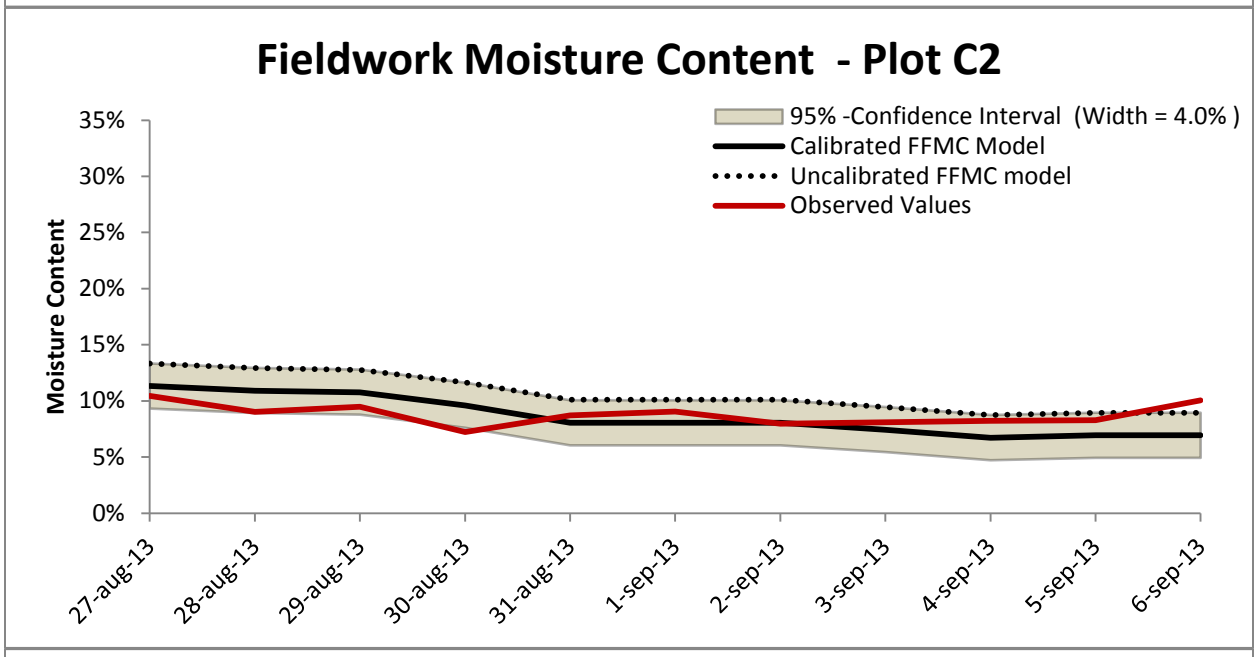
Fieldwork Moisture Content - Plot C2
95% -Confidence Interval (Width = 4.0%)
Calibrated FFMC Model
Uncalibrated FFMC model
Observed Values
Moisture Content
35%
30%
25%
20%
15%
10%
5%
0%
27-aug-13
28-aug-13
29-aug-13
30-aug-13
31-aug-13
1-sep-13
2-sep-13
3-sep-13
4-sep-13
5-sep-13
6-sep-13

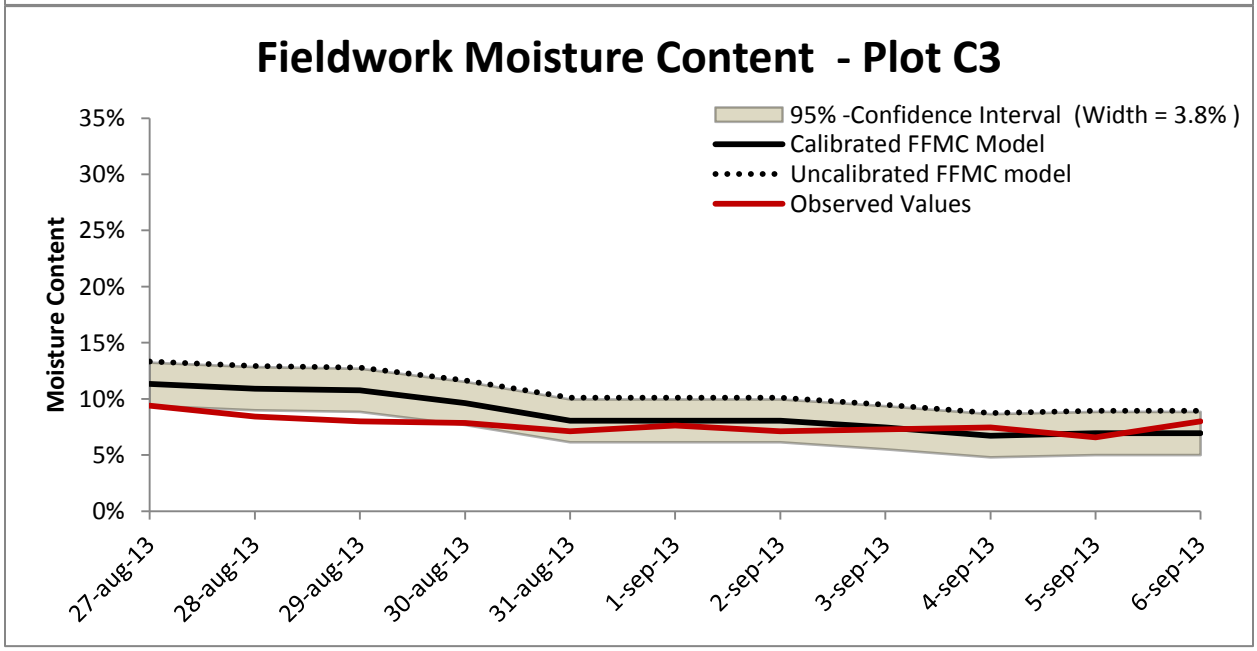
Fieldwork Moisture Content - Plot C3
95% -Confidence Interval (Width = 3.8%)
Calibrated FFMC Model
Uncalibrated FFMC model
Observed Values
Moisture Content
35%
30%
25%
20%
15%
10%
5%
0%
27-aug-13
28-aug-13
29-aug-13
30-aug-13
31-aug-13
1-sep-13
2-sep-13
3-sep-13
4-sep-13
5-sep-13
6-sep-13

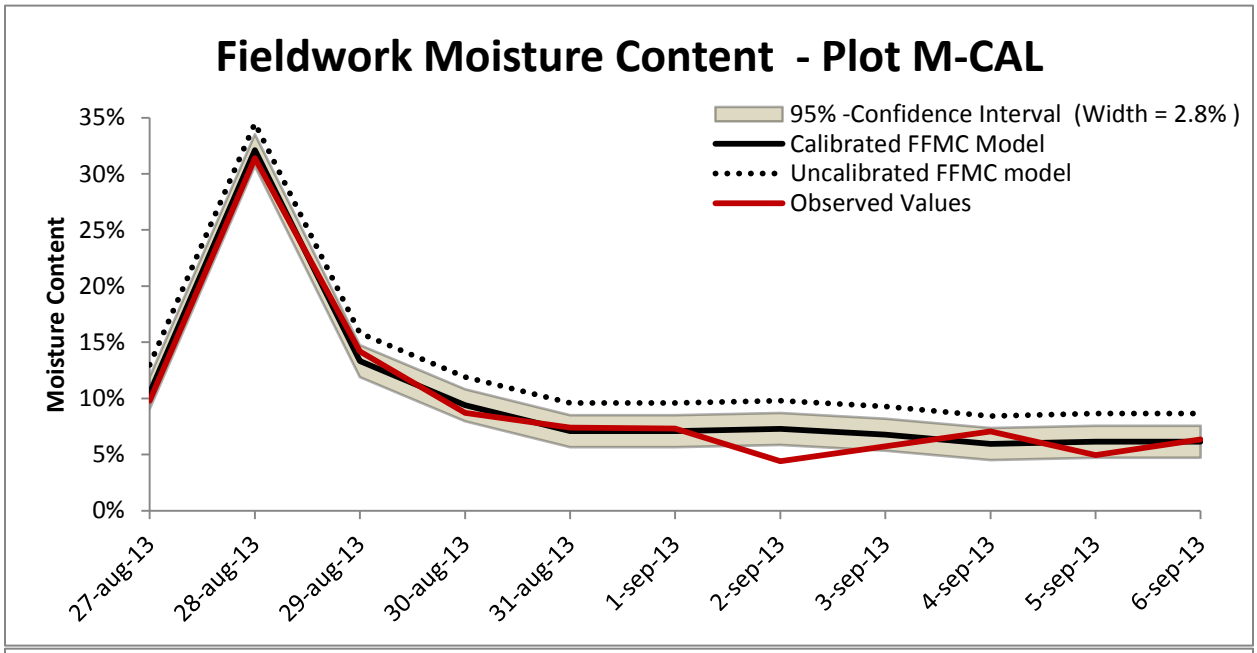
Fieldwork Moisture Content - Plot M-CAL
95% -Confidence Interval (Width = 2.8%)
Calibrated FFMC Model
Uncalibrated FFMC model
Observed Values
Moisture Content
35%
30%
25%
20%
15%
10%
5%
0%
27-aug-13
28-aug-13
29-aug-13
30-aug-13
31-aug-13
1-sep-13
2-sep-13
3-sep-13
4-sep-13
5-sep-13
6-sep-13

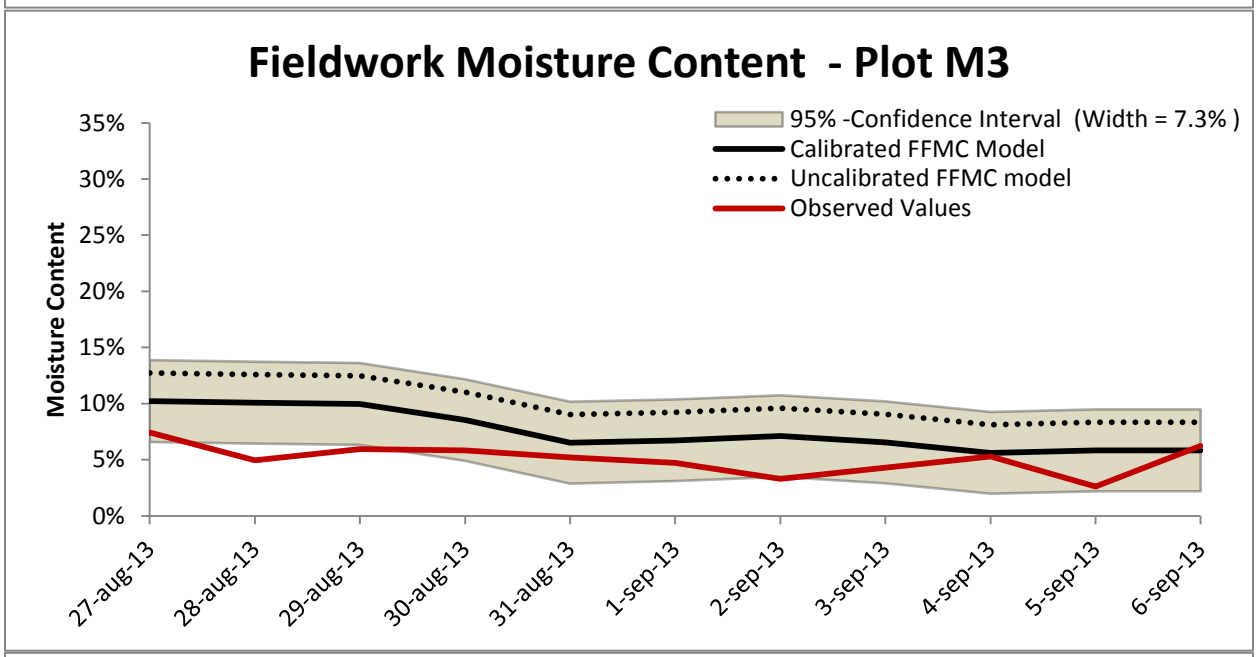
Fieldwork Moisture Content - Plot M3
95% -Confidence Interval (Width = 7.3%)
Calibrated FFMC Model
Uncalibrated FFMC model
Observed Values
Moisture Content
35%
30%
25%
20%
15%
10%
5%
0%
27-aug-13
28-aug-13
29-aug-13
30-aug-13
31-aug-13
1-sep-13
2-sep-13
3-sep-13
4-sep-13
5-sep-13
6-sep-13

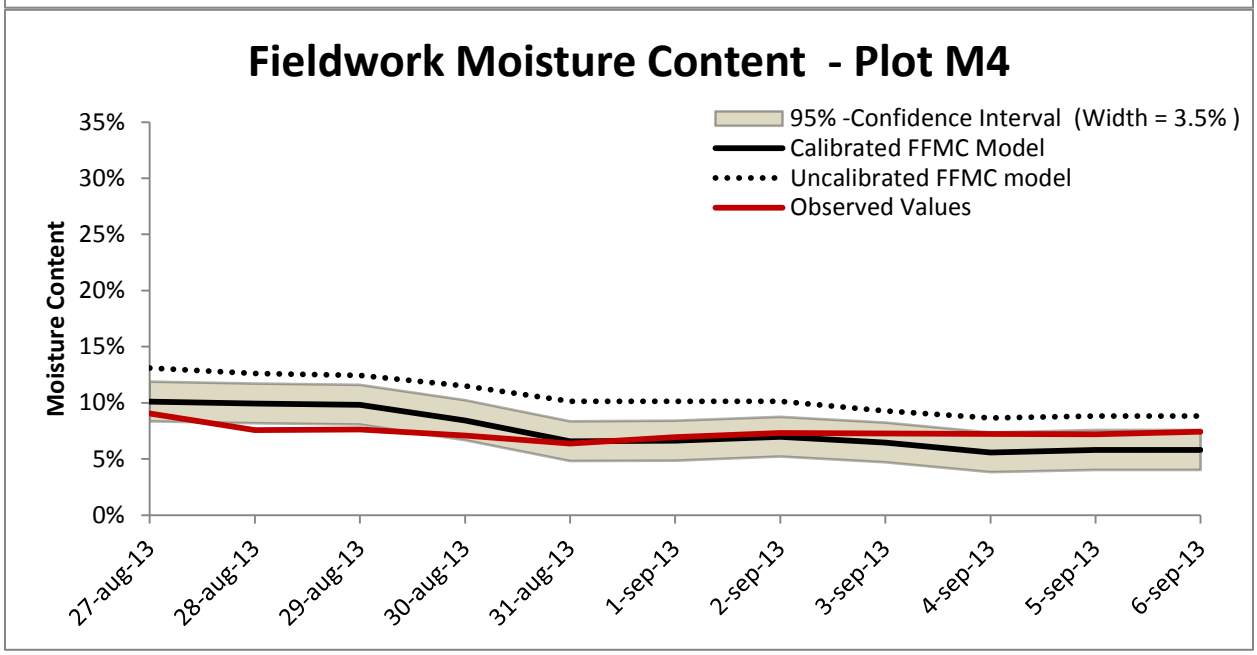
Fieldwork Moisture Content - Plot M4
95% -Confidence Interval (Width = 3.5%)
Calibrated FFMC Model
Uncalibrated FFMC model
Observed Values
Moisture Content
35%
30%
25%
20%
15%
10%
5%
0%
27-aug-13
28-aug-13
29-aug-13
30-aug-13
31-aug-13
1-sep-13
2-sep-13
3-sep-13
4-sep-13
5-sep-13
6-sep-13

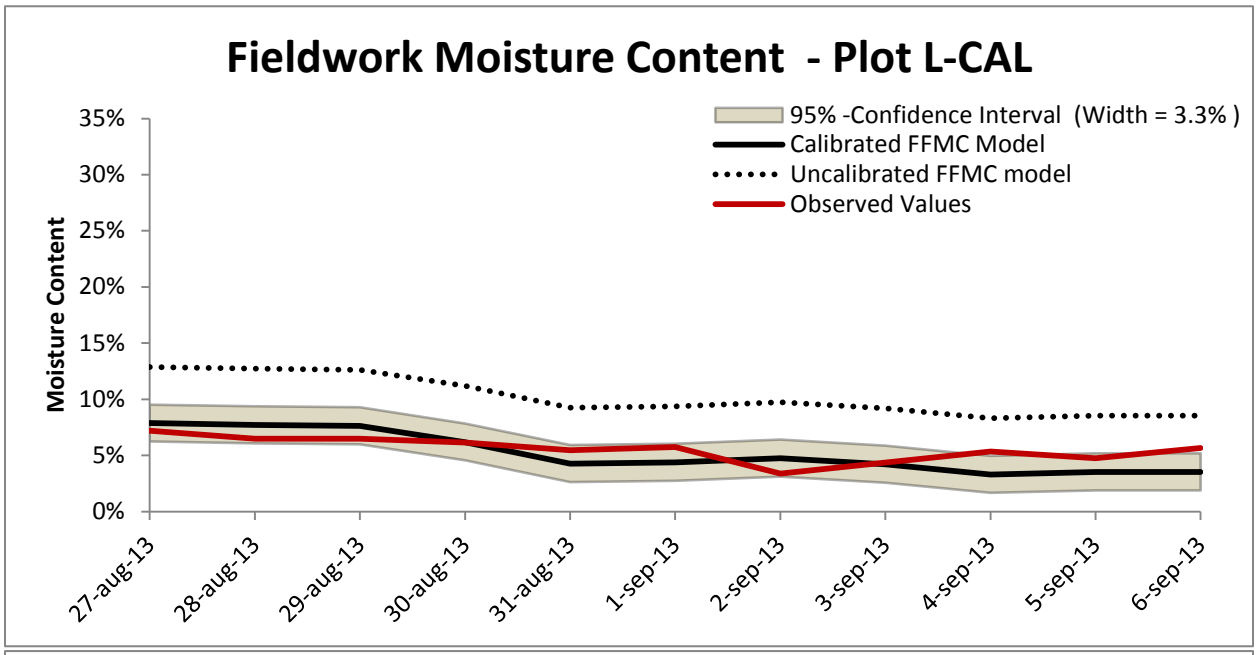
Fieldwork Moisture Content - Plot L-CAL
95% -Confidence Interval (Width = 3.3%)
Calibrated FFMC Model
Uncalibrated FFMC model
Observed Values
Moisture Content
35%
30%
25%
20%
15%
10%
5%
0%
27-aug-13
28-aug-13
29-aug-13
30-aug-13
31-aug-13
1-sep-13
2-sep-13
3-sep-13
4-sep-13
5-sep-13
6-sep-13

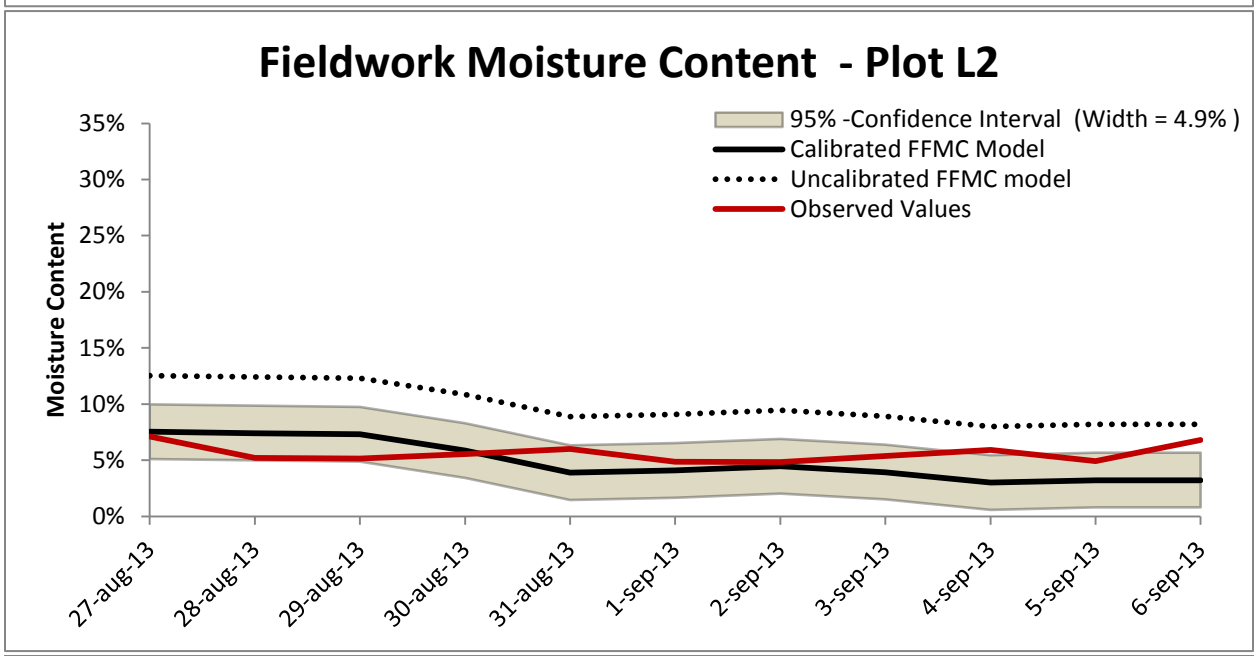
Fieldwork Moisture Content - Plot L2
95% -Confidence Interval (Width = 4.9%)
Calibrated FFMC Model
Uncalibrated FFMC model
Observed Values
Moisture Content
35%
30%
25%
20%
15%
10%
5%
0%
27-aug-13
28-aug-13
29-aug-13
30-aug-13
31-aug-13
1-sep-13
2-sep-13
3-sep-13
4-sep-13
5-sep-13
6-sep-13

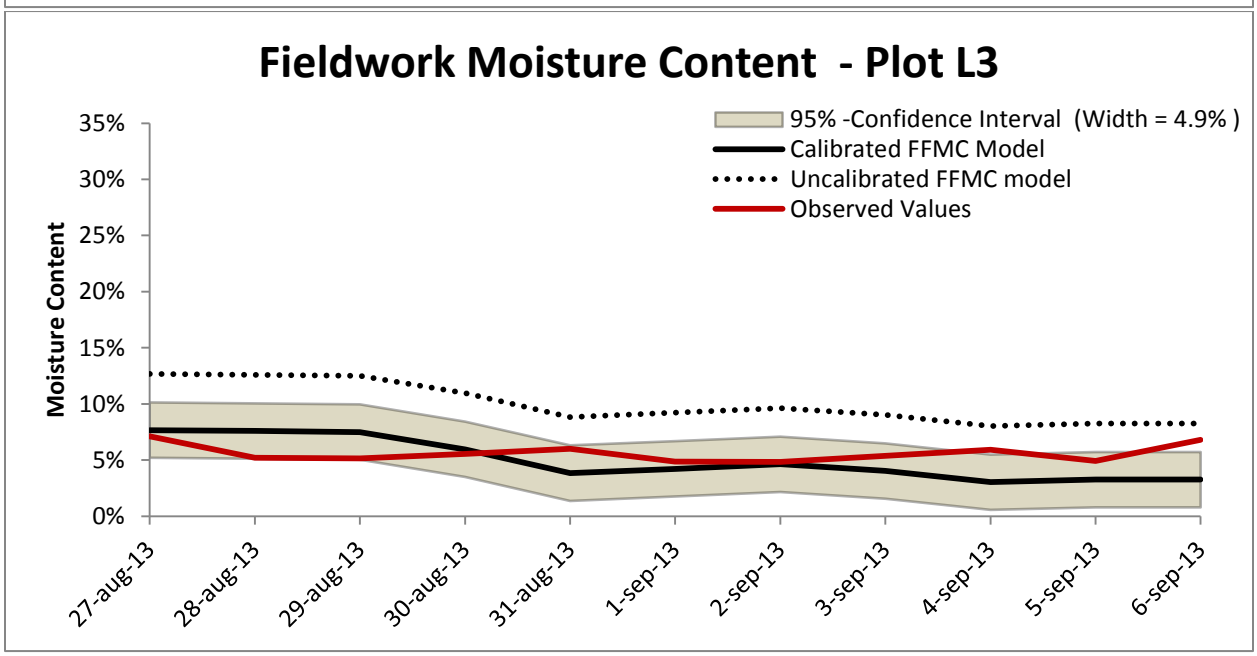
Fieldwork Moisture Content - Plot L3
95% -Confidence Interval (Width = 4.9%)
Calibrated FFMC Model
Uncalibrated FFMC model
Observed Values
Moisture Content
35%
30%
25%
20%
15%
10%
5%
0%
27-aug-13
28-aug-13
29-aug-13
30-aug-13
31-aug-13
1-sep-13
2-sep-13
3-sep-13
4-sep-13
5-sep-13
6-sep-13

APPENDIX H

The GPS-coordinates and the elevation and aspect of the plots used in this study. The projected coordinate system is WGS 1984 (UTM zone 31N). See Appendix A for the related map.

Plot	X-Coordinate	Y-Coordinate	Elevation [m]	Aspect [°]
C-CAL	526002	4822221	297	356
C2	525813	4821844	311	153
C3	526116	4821983	311	209
D-CAL	523564	4824938	254	211
D2	526258	4821265	218	323
D3	524568	4823599	176	166
D4	523852	4824452	177	281
D5	523958	4823572	180	241
M-CAL	524924	4822382	292	109
M3	524907	4822301	288	166
M4	526569	4821284	213	341
L-CAL	525226	4822620	302	41
L2	526270	4821265	216	33
L3	525363	4822546	312	287

APPENDIX I

The full PCraster-Python script including the FFMC and the Behave section.

```
from PCRaster import *
from PCRaster.Framework import *
import math

class MyFirstModel(DynamicModel):
  def __init__(self):
    DynamicModel.__init__(self)
    setclone('dem.map')



  def initial(self):
    self.dem = self.readmap('dem')     # Import Digital Elevation Model
    self.veg = self.readmap('veg')     # Import Vegetation Map

    self.slopeangle = scalar(atan(slope(self.dem)))                          # Calculate slope angle
    self.slopeangle = ifthenelse(self.slopeangle<35.0,self.slopeangle,35.0)  # Limit slope angle to avoid extreme values
    self.report(self.slopeangle,'slopeangle')


    self.altmeteo = 282.0                      #Altitude meteo station [m]
    self.lapserate = -6.49/1000                #Adiabatic lapse rate [C/1000m]
    self.dewlapserate = -2.730/1000            #Dew point lapse rate [C/1000m]

    self.fo = scalar(30.0)                     # initial value of F
    self.p0 = scalar(15.0)                     # initial value of dmc

    self.report(self.fo,'selffo')
    self.report(self.p0,'selfp0')

    self.aspect= ifthenelse(scalar(self.slopeangle)>0.001,aspect(self.dem),0.0)   # Aspect calculatie met N=0!
    self.report(self.aspect,'aspect')
    self.aspectZ0 = scalar(self.aspect)-180.0                                     # Aspect met Z=0!
    self.report(self.aspectZ0,'aspectz')


  def dynamic(self):

    #input variables

    tempmeteo = timeinputscalar('meteodata2013.tss',1)                # temp at 14:00 GMT
    RH = timeinputscalar('meteodata2013.tss',2)                       # RH [%]
    meassuredradiance = timeinputscalar('meteodata2013.tss',3)        # Radiance [w/m^2]
    meassurewindspeed = 3.6 * timeinputscalar('meteodata2013.tss',4)  # Windspeed at 20ft [km/h]
    rainfall = timeinputscalar('meteodata2013.tss',6)                 # daily rainfall [mm]
    doy = timeinputscalar('meteodata2013.tss',7)                      # Day of Year
    waf = lookupscalar('waf.txt',self.veg)                            # Wind Adjustment Factor [-]



    # WINDSPEED CORRECTION
    windspeed20 = meassurewindspeed                                   # Creating parameter copy [km/h]
    self.report(windspeed20,'wind')

    vegheight = lookupscalar('vegheight.txt',self.veg)                # Vegetation height table lookup
    self.report(vegheight,'vegh')
```

```
fuelwind = waf * windspeed20                                    # Wind at fuel level calculation
self.report(fuelwind,'fuelwind')



# TEMPERATURE CORRECTION


#Adiabatic temperature

airtemp = (self.dem - self.altmeteo)*(self.lapserate)+ tempmeteo    #Calculation of spatial airtemperature
self.report(airtemp,"airtemp")


#Solar Heating

declinationangle = 23.45 *sin((360.0/365.0)*(doy-81))               # Calculation of declination angle

hourangle = 30.0                                                    # The hour angle at 14:00

latitude = 43.557381                                                # Latitude Vailhan

coso = sin(declinationangle)*sin(latitude)*sin(self.slopeangle)-
sin(declinationangle)* cos(latitude)*sin(self.slopeangle)* cos(self.aspectZ0)+
cos(declinationangle)*cos(latitude)*cos(self.slopeangle)* cos(hourangle)+
cos(declinationangle)*sin(latitude)*sin(self.slopeangle)* cos(self.aspectZ0) * cos(hourangle)+
cos(declinationangle)*sin(self.slopeangle)*sin(self.aspectZ0)*sin(hourangle)

self.report(coso,'coso')                                        # Cosine of angle of incidence

angle = scalar(acos(coso))                                      # Angle of incidence

self.report(angle,'angle')

cosoz= cos(latitude-self.slopeangle)*cos(declinationangle)*cos(hourangle)+
sin(latitude-self.slopeangle)*sin(declinationangle)

self.report(cosoz,'cosoz')                                      # Cosine of zenith angle

rb = coso/cosoz                                                 # Ratio beam radiation on slope and horizontal

self.report(rb,'rb')


#radiation

shade = lookupscalar('shade.txt',self.veg)                          # Shading factor lookup
self.report(shade,'shade')

radiance =(1.0-shade)* meassuredradiance * ifthenelse(rb<0.0,0.0,rb)  # Radiance (assuming horizontal measurements!)
self.report(radiance,'radiance')


#fuel temp

fueltemp = max(airtemp + (radiance/((42.5 * fuelwind)+32.7)), airtemp)      # Fuel temperature calculation
self.report(fueltemp,'fueltemp')



# Relative Humidity Correction

dewpointmeteo = tempmeteo - ((100-RH)/5)                                    # Dew point at meteo station
dewpoint = (self.dem - self.altmeteo)*(self.dewlapserate) + dewpointmeteo   # Spatial dew point
self.report(dewpoint,'dewpoint')
```

```
saturatedvaporpressure = 6.11 * 10**((7.5*airtemp)/(237.7+airtemp))             # Saturated vapor pressure caculation

actualvaporpressure = 6.11 * 10**((7.5*dewpoint)/(237.7+dewpoint))              # Actual vapor pressure calculation

RH = (actualvaporpressure/saturatedvaporpressure)*100                           # Relative humidty
self.report(RH,'RH')

tempdelta = scalar(airtemp - fueltemp)                                          # Temperature difference air/fuel
self.report(tempdelta,'tempd')

RHtemp = RH * exp(0.059*(tempdelta))                                            # Fuel corrected relative humidity

self.report(RHtemp,'rhtemp')




#FFMC CALCULATION

aa = lookupscalar('aa.txt',self.veg)         # Calibration factor for log drying rate
self.report(aa,'aa')

bb = lookupscalar('bb.txt',self.veg)         # Calibration factor for EMC
self.report(bb,'bb')

cc = lookupscalar('cc.txt',self.veg)         # Calibration factor for rain input
self.report(cc,'cc')

rf=scalar(ifthenelse(rainfall>0.5,rainfall-0.5,rainfall+0.00001))     # FFMC rainfall input
self.report(rf,'rf')

mo = scalar(32.87*(101-self.fo)/(13.28+self.fo))                      # Initial moisture content (FX-scale)
self.report(mo,'mo')


mr = ifthenelse(rf>0.001,cc*ifthenelse(mo<=150.0,mo+42.5*rf*(exp((-100.0)/(251.0-mo))*(1.0-exp((-6.93)/rf))),
        mo+42.5*rf*(exp((-100.0)/(251.0-mo))*(1.0-exp(-6.93/rf)))+(0.0015*((mo-150.0)**2.0)*((rf)**0.5))),mo)
self.report(mr,'mr')                                                   # Moisture content after rain

mo = ifthenelse(mr>250.0,250.0,mr)
self.report(mo,'moo')



ed = 0.942*RHtemp**(0.679)+11.0*exp((RHtemp-100.0)/10.0)+0.18*(21.1-fueltemp)*(1.0-exp(-0.115*RHtemp))+bb

self.report(ed,'ed')

k0 = 0.424*(1.0-((RHtemp/100.0)**1.7))+0.0694*((windspeed20)**0.5)*(1.0-((RHtemp/100.0)**8.0))

self.report(k0,'k0')

kd = k0 * 0.581 * exp(0.0365*fueltemp)*aa

self.report(kd,'kd')

k1 = 0.424*(1.0-((100.0-RHtemp)/100.0)**1.7)+0.0694*((windspeed20)**0.5)*(1.0-((100.0-RHtemp)/100.0)**8.0)

self.report(k1,'k1')

kw = k1 * 0.581 * exp(0.0365*fueltemp)

self.report(kw,'kw')

ew = 0.618 * (RHtemp**0.753) + 10.0*exp((RHtemp-100.0)/10.0) + 0.18*(21.1-fueltemp)*(1.0-exp(-0.115*RHtemp))+bb
```

```
self.report(ew,'ew')

m = ifthenelse(mo>ed,ed+(mo-ed)*(10.0**(-kd)),ifthenelse(mo<ew,ew-(ew-mo)*(10.0**(-kw)),mo))

self.report(m,'m')                                          # FFMC moisture content output

F= ((-(1328.0*m-331987.0))/(100.0*m+3287.0))                #invert FX

self.fo = F

self.report(F,'f')



#BEHAVE

#input variables

TotalMineralContent = 0.0555            # [%]  Total mineral content
EffectiveMineralContent = 0.01          # [%]  Total effective mineral content

mf = m/100                              # From percentage to fraction
self,report(mf,'mf')


#table read-out

surfacearea = lookupscalar('surfacearea.txt',self.veg)                          # SAV in [cm-1]
self.report(surfacearea,'sa')

fueldepth = lookupscalar('fueldepth.txt',self.veg)                              # Depth of fuel bed in [m]
self.report(fueldepth,'depth')

fuelloading = lookupscalar('ovendry_fuel_loading.txt',self.veg)                 # Fuel loading Wo in [kg/m2]
self.report(fuelloading,'loading')

relativepackingratio = lookupscalar('relative_packing_ratio.txt',self.veg)      # b/bp [-]

mx = scalar(lookupscalar('mx.txt',self.veg))                                    # Moisture of extinction [%]
self.report(mx,'mx')

heatcontent = lookupscalar('heat_content.txt',self.veg)                         # Fuel heat content [kJ/kg]

packingratio = lookupscalar('packing_ratio.txt',self.veg)                       # Packing ratio B [-]


#********calculations********

# reaction intensity


Tmax = ifthenelse(self.veg<5,((0.0591+2.926*(surfacearea**(-1.5)))**(-1.0)),0.0)    # Maximum reaction velocity [min-1]
self.report(Tmax,'Tmax')

A = ifthenelse(self.veg<5,6.7229*(surfacearea**(0.1))-7.27,0.0)                     # [-]
self.report(A,'A')

T = ifthenelse(self.veg<5,Tmax*((relativepackingratio) * exp(1.0-(relativepackingratio)))**A,0.0)
self.report(T,'T')                                                                   # Optimum reaction velocity

wn = ifthenelse(self.veg<5,fuelloading * (1-TotalMineralContent),0.0)               # Net fuel loading [kg/m2]
self.report(wn,'wn')

ratio = (mf/mx)                                                                     # Ratio mc to moisture of extinct
self.report(ratio,'ratio')
```

```
    nm = ifthenelse(self.veg<5,ifthenelse((mf/mx)<1.0,1.0-(2.59*(mf/mx))+(5.11*((mf/mx)**2.0))-
                                          (3.52*((mf/mx)**3.0)),0.0),0.0)              # moisture damping coefficient [-]
    self.report(nm,'nm')

    ns = 0.174*(EffectiveMineralContent**(-0.19))                          # mineral damping coefficient, about 0.417  [-]



    Ir = ifthenelse(mf>mx,0.0,ifthenelse(self.veg<4.5,T*wn*heatcontent*nm*ns,0.0))      # Fire intenisty [kJ/min)/m2]
    self.report(Ir,'ir')

    Irw = Ir/60                                                                 # Fireline intensity [kW/m2]
    self.report(Irw,'irw')


    #Wind factor

    midflame = (meassurewindspeed*waf*1000.0)/60.0                              # Midflame windspeed [m/min]!

    windB = 0.15988*(surfacearea**0.54)
    windC = 7.47 * exp(-0.8711*(surfacearea**0.55))
    windE = 0.715 * exp(-0.01094*surfacearea)

    windcoefficient = ifthenelse(self.veg<5,windC*((3.281*midflame)**windB)*(relativepackingratio**(-windE)),0.0)
    self.report(windcoefficient,'windco')                                       # Wind coefficient

    #Slope factor
    tanslopeangle = tan(self.slopeangle)                                        # Tangent of the slope angle
    self.report(tanslopeangle,'tanslope')

    slopecoefficient = 5.275*(packingratio**(-0.3))*((tanslopeangle)**2.0)      # Calculation of slope-coefficient
    self.report(slopecoefficient,'slopeco')


    #Rate of Spread

    Qig = 581 + 2594 * mf                                                       # Heat of preignition [kJ/kg]
    self.report(Qig,'qig')

    EffectiveHeatingNumber= ifthenelse(self.veg<5, exp(-4.528/surfacearea),0)   # Effective Heating Number [-]
    self.report(EffectiveHeatingNumber,'effhn')

    OvendryBulkDensity = ifthenelse(self.veg<5,(fuelloading/fueldepth),0)       # Ovendry Bulk Density [-] (Pb)
    self.report(OvendryBulkDensity,'ovenbd')

    E = ifthenelse(self.veg<5,((192 + 7.9095*surfacearea)**(-1.0))*exp((0.792 +
                            3.7597*(surfacearea**(0.5)))*(packingratio+0.1)),0)  # Propagating flux ratio
    self.report(E,'E')


    R = ifthenelse(self.veg<5,((Ir*E*(1+windcoefficient+slopecoefficient))/
                             (OvendryBulkDensity*EffectiveHeatingNumber*Qig)),0)  # Rate of spread [m/min]
    self.report(R,'R')


    #Byrams intensity

    Ib = ifthenelse(self.veg<5,(Ir/60) * ((R*12.6)/scalar(surfacearea)),0)      # Fireline intensity [kW/m]
    self.report(Ib,'ib')

    #Flame length

    Lf = ifthenelse(self.veg<5,0.0775 * (Ib**0.46),0)                           # Flame length [m]
    self.report(Lf,'lf')

nrOfTimeSteps=200
myModel = MyFirstModel()
dynamicModel = DynamicFramework(myModel,nrOfTimeSteps)
dynamicModel.run()
```

APPENDIX J

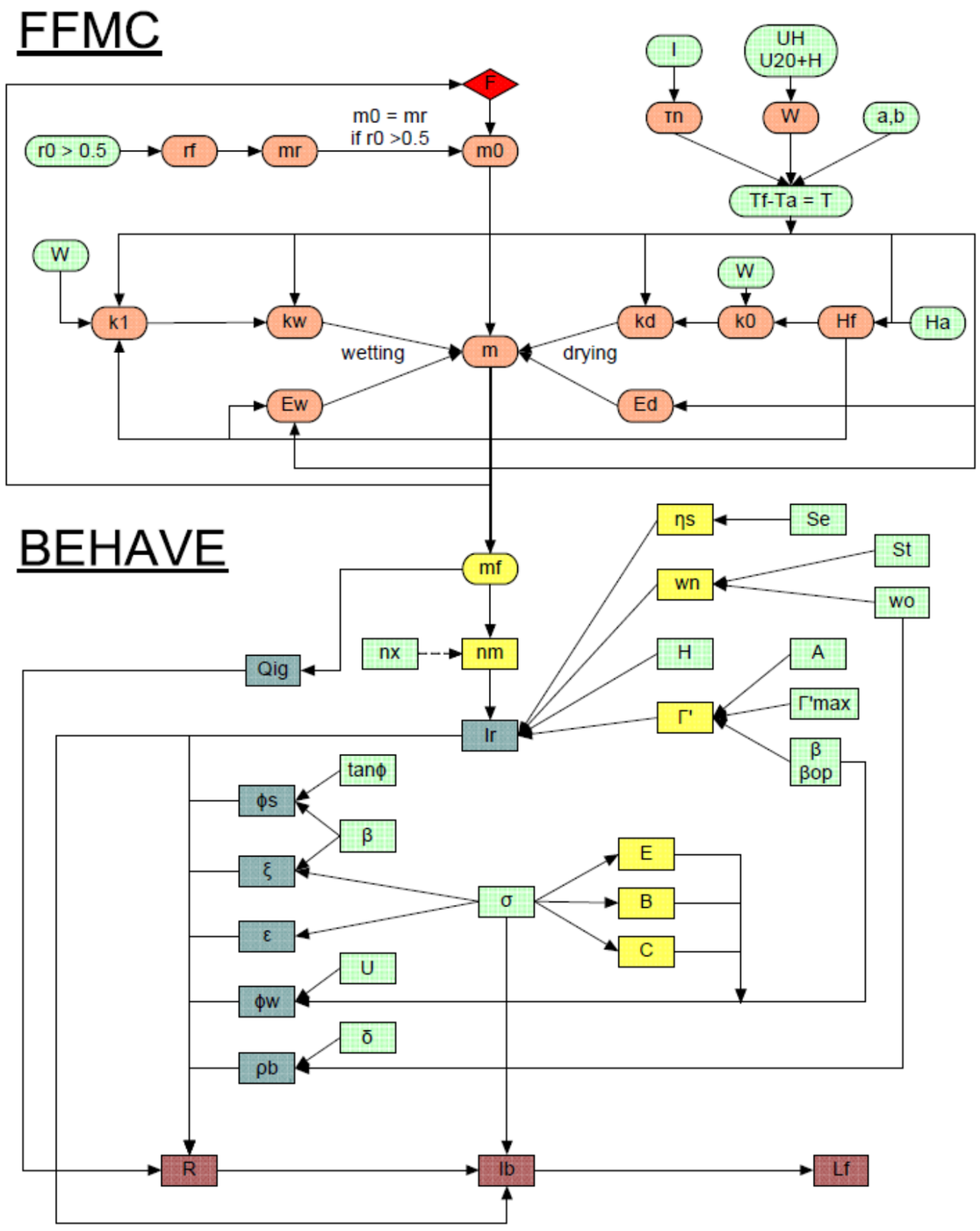

A detailed flowchartillustrating the relation between the different variables and constants of the Fine Fuel Moisture Code (FFMC, upper part) and the Behave fire behavior prediction model. All fire weather observations, geographic parameters and fuel model parameters are in green. The FFMC calulations are in orange, the seven inputs for the Rate of Spread (R) in blue and secondary calculations for the Behave model in yellow. The dark red variables are the main fire behavior outputs; the rate of spread (R), fire line intensity (Ib) and flame lenght (Lf).